STOCHASTIC OPTIMIZATION FOR POWER MANAGEMENT IN RADIAL DISTRIBUTION NETWORKS WITH RENEWABLE PHOTOVOLTAIC GENERATION

APPROVED BY SUPERVISING COMMITTEE:

Nikolaos Gatsis, Ph.D., Chair

Hariharan Krishnaswami, Ph.D.

Rolando Vega, Ph.D.

Brian Kelley, Ph.D.

Accepted:

Dean, Graduate School

DEDICATION

To my mother Samin, my little brother Alisina, and my two best friends Azima and Negar.

STOCHASTIC OPTIMIZATION FOR POWER MANAGEMENT IN RADIAL DISTRIBUTION NETWORKS WITH RENEWABLE PHOTOVOLTAIC GENERATION

by

MOHAMMADHAFEZ BAZRAFSHAN, B.S.

THESIS
Presented to the Graduate Faculty of
The University of Texas at San Antonio
in Partial Fulfillment
of the Requirements
for the Degree of

MASTER OF SCIENCE IN ELECTRICAL ENGINEERING

THE UNIVERSITY OF TEXAS AT SAN ANTONIO
College of Engineering
Department of Electrical and Computer Engineering
August 2014

ProQuest LLC.
789 East Eisenhower Parkway
P.O. Box 1346
Ann Arbor, MI 48106 - 1346

ACKNOWLEDGEMENTS

First and foremost, my deepest gratitude goes to my supervising professor, Dr. Nikolaos Gatsis for all the support he has given me. Since the very start of working with him, Dr. Gatsis has encouraged me to become the better of myself, both in research and in personality. His determination in solid work, vast knowledge, patience, enthusiasm and moral principles have made every minute I've spent with him extremely valuable.

I would also like to express my sincere thanks to Dr. Brian Kelley for his support for me over the past two years at UTSA. In addition to his academic assistance, his guidance and encouragement has motivated me through the hardest times in my graduate studies.

My appreciation also goes to Dr. Krishanswami and Dr. Vega, for accepting my invitation to be my committee members and dedicating their time to attend my thesis defense session, reviewing my writing, and providing me with their insightful suggestions.

I owe a lot to Xuan Uribe who was always there to answer my questions regarding the writing of this thesis. I am greatly indebted to Lauren Beaver for her invaluable assistance in the formatting of this document. I am also very much grateful to Dr. Daniel Pack for doing a final review of my writing and giving me useful comments.

Finally, my special thanks extends to the faculty, staff and the students of the Electrical and Computer Engineering Department at UTSA who have all contributed to the fabulous atmosphere for pursuing graduate studies here. It is an honor for me to continue my studies here in the following years with all of you.

August 2014

STOCHASTIC OPTIMIZATION FOR POWER MANAGEMENT IN RADIAL DISTRIBUTION NETWORKS WITH RENEWABLE PHOTOVOLTAIC GENERATION

Mohammadhafez Bazrafshan, M.S.
The University of Texas at San Antonio, 2014

Supervising Professor: Nikolaos Gatsis, Ph.D., Chair

The stochastic nature of solar renewable power poses challenges in distribution networks with high-penetration photovoltaic (PV) generation in terms of maintaining adequate generation to satisfy end-users as well as accomplishing voltage regulation. However, real power control of modern programmable electric loads and reactive power compensation from the power electronic interfaces of PV generators offer opportunities to overcome these challenges to eventually achieve customer satisfaction and minimize costs for the operation of distribution systems. To cope with the random and intermittent nature of solar generation, this thesis introduces a stochastic optimization model for real and reactive power management in such distribution systems with a large number of residential-scale PV generation units. Decision variables include demand response schedules of programmable loads, as well as reactive power consumption or generation by the PV inverters in a fashion adaptive to the uncertain real power generation. Voltage regulation is also addressed in the stochastic optimization framework through enforcement of suitable constraints or using principles of risk-averse optimization. A decentralized solver based on the alternating direction method of multipliers (ADMM) is also developed featuring closed-form updates per node and communication only between neighboring nodes. Numerical tests are provided to demonstrate the superior performance of applying this stochastic optimization model for power management in large distribution networks compared to other proposed schemes in the literature.

TABLE OF CONTENTS

LIST OF TABLES

LIST OF FIGURES

Chapter 1: INTRODUCTION

The increased demand of electricity makes reliable and efficient provision of electric energy by transmission and distribution system operators hard to accomplish without the risk of regional blackouts. The fossil-fueled bulk electric energy generation of today's industry will not be able to meet this soaring demand without moving towards a smarter grid capable of decentralized production of electric energy from renewable energy sources.

Integration of renewable energy such as wind, solar, or geothermal energy will help balance the environmental impact of thermal power generation. In addition to environmental benefits of renewable energy generation, the premise of distributed generation (DG) is to produce electricity close to the point where it is consumed. Therefore, deployment of DG reduces the need for investments in bulk generation and transmission, while it also bypasses the congested transmission network. Residential-scale photovoltaic (PV) generation units are prime examples of DG.

However, the stochastic nature of renewable energy, and solar PV generation in particular, presents a challenge in that it requires consumption awareness by the users so that production is guaranteed never to be less than the demand. The rapid changes in weather conditions lead to unexpected variations in electricity generation levels. Particularly for solar power generation from PV units, abrupt irradiance condition changes may lead to inadequate or at times excess generation, which eventually may result in voltage fluctuations across the distribution feeders.

To cope with these issues, introduction of end-user programmable loads in electricity distribution networks, such as smart chargers of plug-in electric vehicles that have the ability to control their power consumption, merged with capabilities of advanced metering infrastructure can help distribution system operators (DSO) communicate with customers to balance the load during peak hours. Moreover, leveraging improvements in power electronics can facilitate voltage regulation. For instance, in solar PV generation, the inverters which interface the PV units with the grid can be allowed to generate or consume reactive power. These capabilities open up significant opportunities for successful power management, voltage regulation, and thermal loss minimization in

distribution systems.

It thus becomes necessary for DSOs to assess the underlying uncertainty in solar power generation in order to be able to successfully integrate high penetration levels of PV units into their network. An attractive solution developed in this thesis is utilizing stochastic programming tools to manage real and reactive power of users in a fashion adaptive to the uncertain generation to achieve objectives such as minimization of the thermal losses and costs of operation as well as enforce voltages to remain in safety levels.

Moreover, risk-averse optimization techniques can be harnessed so that the risk of high voltage deviations in the network is guaranteed to be minimized. Specifically, to cope with the fact that voltage deviations are random variables, a stochastic optimization problem that includes a measure of risk called the conditional-value-at-risk (CV@R) of absolute voltage deviations from the nominal value, in addition to the previously described objectives, is pursued in this thesis. The decision variables of this stochastic program comprise of real power consumption of controllable loads and reactive power injection or consumption of PV inverters. The CV@R amounts to the conditional expectation of absolute voltage deviations being greater than a specific threshold.

In what follows, Section 1.1 summarizes the current literature, and Section 1.2 presents the outline of the thesis. The work in this thesis has lead to publications [1] and [2].

1.1 Prior art

Power management in governing electricity distribution networks must include the *power flow equations* which characterize the relationship between power production, consumption, thermal losses as well as the voltage variations across the network. One of the chief challenges in real and reactive power management is that the power flow equations are non-convex; see [3], [4], [5] for the canonical form of power flow equations in radial distribution systems. In recent years, convex approximations or relaxations have been pursued to render the resulting optimization problems tractable. These are presented next according to the complexity of the optimization problem class they belong to. The centralized reactive power management problem in [6] is relying on a

linear approximation of the power flow equations in radial networks called the `LinDistFlow` model. Decentralized local policies for reactive power control are pursued in [7] and [8] using the `LinDistFlow` model as well, albeit without optimality guarantees. An optimal decentralized algorithm for reactive power control has recently been the theme of [9] using the `LinDistFlow` model and the alternating-direction method of multipliers (ADMM). A decentralized algorithm for real power control is developed in [10] relying on convex envelope approximations and the ADMM. A centralized model for reactive power control and PV inverter loss minimization is formulated in [11] leveraging a second-order cone programming (SOCP) relaxation. Distributed algorithms for real and reactive power control of programmable loads are developed in [12] and [13] using SOCP relaxations and the predictor-corrector proximal method of multipliers (PCPMM). Recently, an ADMM-based decentralized algorithm leveraging SOCP relaxations was designed [14]. See [11–14] and references therein for conditions where the SOCP relaxation is exact. A distributed scheme for real and reactive power control using semidefinite programming (SDP) relaxation and a dual subgradient method is pursued in [15]. Conditions for exactness of the SDP relaxation are also developed in [15] and references therein. Control of fossil fuel fired distributed generation is tackled in [16] for three-phase unbalanced distribution systems leveraging SDP relaxations and ADMM. Sophisticated policies for real and reactive power flow control from PV inverters are designed in [17] relying on SDP relaxations and ADMM.

Risk-averse optimization tools have also been utilized in power system operation, but not for voltage regulation. Various measures of risk, including the CV@R, are reviewed in [18, Ch. 4], and applications to electricity markets are given. Moreover, optimal power flow in transmission networks with high levels of wind integration is pursued in [19] using a CV@R objective to reduce the risk of limited renewable energy availability. To accommodate uncertainty, [20] develops a chance-constrained stochastic program under a probabilistic forecast of spatio-temporal variations of renewable energy while considering forecast errors. Conservative approximations to the chance constraints using the CV@R are adopted, and adaptive policies linear in the uncertainty are pursued.

1.2 Contributions of this thesis

In this thesis, a framework for real and reactive power management in distribution systems under uncertainty of solar power generation due to fast-changing irradiance conditions is developed. This framework is in contrast to the previously mentioned research efforts [6–17], which adopt deterministic optimization models. The overall approach here leads to stochastic programming models whereby decision making happens in two stages. First-stage decisions are the real power consumptions of programmable loads, while the reactive power generated or consumed by the PV inverters comprise the second-stage decisions. The premise is that the inverter reactive power is decided in a fashion *adaptive* to the real power generated by the PV unit, which is modeled as random taking values from a set of possible scenarios. The objective is to maximize the sum-utility of the users stemming from consuming power, minus the expected value of thermal losses in the distribution system, while maintaining the voltage at every feeder node at safe levels (voltage regulation).

The voltage regulation problem is managed in two different ways. The first method imposes hard constraints at every node and for every possible generation outcome, while the second one aims to develop risk-averse formulations by introducing a measure of risk known as the CV@R [21]. Voltage regulation in this case, is achieved by minimizing a term that calculates the CV@R of absolute voltage deviations while achieving previously described objectives. The CV@R amounts to the conditional expectation of absolute voltage deviations being greater than a specific threshold. The resulting minimization problems in both cases turn out to be a quadratic program.

A decentralized algorithm based on the ADMM has also been developed to solve the resulting optimization problems on a radial distribution network, whereby only neighboring users will need to exchange information which entails limited communication overhead. The SOCP relaxation and `LinDistFlow` models are adopted to provide approximations of the power flow equations. Notice that a large number of constraints needs to be included, because a set of power flow equations for each possible scenario of solar power generation across the feeder must be incorporated. This

challenge is well handled by ADMM.

The ADMM-based algorithm is utilizing auxiliary variables similar to the ones in [9] and [14]; in this work, decomposition per node as well as per scenario is achieved. It is also worth emphasizing that the resulting ADMM-based iterations are in closed form, thus allowing the optimization of networks with large number of nodes. Finally, the programmable loads are modeled as operating at a constant power factor. The implication is that the consumed reactive power is linearly related to consumed real power, which is a different model than the box-constrained consumed reactive power—independently of real power—adopted in [12–14].

The remainder of this thesis is organized as follows. Chapter 2 describes the power flow equations in general radial distribution networks, which can be modeled by trees. User power consumption and PV generation models are also presented. In Chapter 3 modeling of uncertain solar PV generation is followed on account of the objectives to be accomplished by DSOs. The stochastic program to attain the required objectives is formulated while voltage regulation is achieved by explicitly enforcing voltage levels for every node and generation scenario. A decentralized algorithm based on ADMM to solve the problem is also developed. Numerical tests and comparisons with a local reactive power control policies are supplied to highlight the benefits of the approach. In Chapter 4, a risk-averse formulation is presented for joint voltage regulation and power management. A CV@R objective per node is incorporated to account for the risk of having high absolute voltage deviation, in addition to terms corresponding to customer dissatisfaction, power generation costs, and line thermal losses. To highlight the benefits of the approach, a risk-neutral formulation that minimizes the expected value of absolute voltage deviations—instead of evaluating the risk of having large absolute voltage deviations—is also presented. The thesis is concluded in Chapter 5 with directions to future work.

Chapter 2: NETWORK MODEL

Consider the single-phase equivalent of a radial distribution network as depicted in Fig. 2.1. A tree is an appropriate graph to model the distribution network whereby each node i in the set $\mathcal{N} = \{0, 1, 2, ..., N\}$ represents one of the $N + 1$ buses, and each link $i \in \mathcal{E} = \{1, 2, ..., N\}$ represents the power line toward node i. Node 0 corresponds to the substation, while other nodes are the electricity end-users. The real and reactive power demand for this network is provided from the power that enters from the transmission network through the substation (i.e. bus 0) into the main feeder and flows into all nodes through the corresponding lines.

In Fig. 2.1, the root of the tree corresponds to the substation, and every other node on the tree represents a bus. The substation (node 0) provides power to nodes 1 and 2 through corresponding links 1 and 2. In this case, node 0 is called the ancestor for nodes 1 and 2, and nodes 1, 2 are called the children of node 0. From the figure, it is evident that each node i except for the root (i.e., node 0) has a unique ancestor, which we denote by A_i. For instance, node 0 is the ancestor for nodes 1 and 2, thus $A_1 = 0$ and $A_2 = 0$. Nodes that do not have children are called leaves of the tree, or terminal nodes. All nodes except for the terminal ones can have several children. Let $\mathcal{C}_i$ denote the set of children corresponding to node i. In the previous example, we have that $\mathcal{C}_0 = \{1, 2\}$. If a node does not have any children then $\mathcal{C}_i = \emptyset$.

Let P_i and Q_i indicate respectively the real and reactive power flow entering node i and $\mathcal{S}_i$ represent the complex power phasor whose real and imaginary parts are P_i and Q_i. Complex voltage phasor at node i is denoted by $\mathcal{V}_i$, while $\mathcal{I}_i$ is the complex phasor representing the current flowing into node i through the corresponding link i. The magnitudes of the aforementioned phasors are denoted by V_i and I_i. These quantities are related as follows:

$$\mathcal{S}_i = P_i + jQ_i = \mathcal{V}_i \mathcal{I}_i^* \tag{2.1}$$

with $\mathcal{I}_i^*$ representing the complex conjugate of the current phasor.

A link that connects the ancestor A_i to its child node i has an impedance $r_i + jx_i$ which

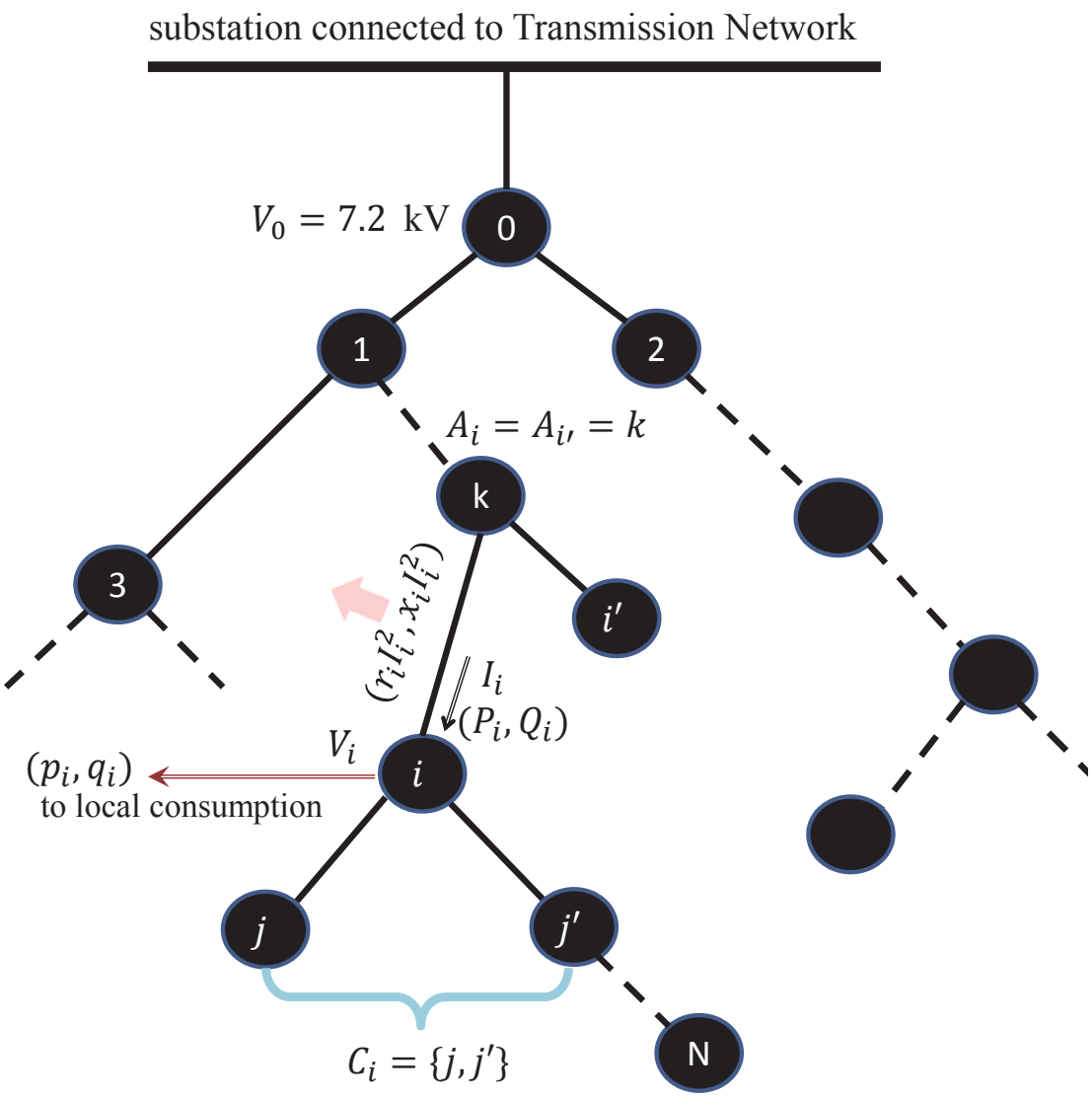

Figure 2.1: Radial distribution network with N user nodes modeled as a tree.

according to Ohm's law results in voltage drop and thermal losses on the network lines. Using KVL for node $i \in \mathcal{N}\backslash\{0\}$ and its ancestor A_i, one can derive an expression for the magnitude of voltages, currents, and power flows as follows:

$$\mathcal{V}_{A_i} = \mathcal{V}_i + (r_i + jx_i)\mathcal{I}_i \Rightarrow$$

$$V_{A_i}^2 = \big(\mathcal{V}_i + (r_i + jx_i)\mathcal{I}_i\big)\big(\mathcal{V}_i + (r_i + jx_i)\mathcal{I}_i\big)^*$$

$$
\begin{aligned}
&= \big(\mathcal{V}_i + (r_i + jx_i)\mathcal{I}_i\big)\big(\mathcal{V}_i^* + (r_i - jx_i)\mathcal{I}_i^*\big) \\
&= V_i^2 + (r_i - jx_i)\mathcal{V}_i I_i^* + (r_i + jx_i)\mathcal{V}_i^* I_i + (r_i^2 + x_i^2)I_i^2 \\
&= V_i^2 + (r_i)(\mathcal{V}_i\mathcal{I}_i^* + \mathcal{V}_i^*\mathcal{I}_i) - jx_i(\mathcal{V}_i\mathcal{I}_i^* - \mathcal{V}_i^*\mathcal{I}_i) + (r_i^2 + x_i^2)I_i^2 \\
&= V_i^2 + r_i(\mathcal{S}_i + \mathcal{S}_i^*) - jx_i(\mathcal{S}_i - \mathcal{S}_i^*) + (r_i^2 + x_i^2)I_i^2 \\
&= V_i^2 + r_i(2P_i) - jx_i(2jQ_i) + (r_i^2 + x_i^2)I_i^2 \Rightarrow \\
V_{A_i}^2 &= V_i^2 + 2(r_i P_i + x_i Q_i) + (r_i^2 + x_i^2)I_i^2. \qquad (2.2)
\end{aligned}
$$

The magnitude of voltage in the substation is a known fixed value V_0. Each node may contain electric loads which consume power, or local generators, possibly photovoltaic, which provide power. The net real power consumption for every node i, which is the total load demand minus generation, is denoted by p_i. Similarly, let q_i denote the net reactive power consumption of node i. The power flows into node i (i.e. P_i and Q_i) will supply the demand for local net consumption of bus i, as well as all the power flows to the children of bus i. Since the links connecting to the children have impedance, active and reactive losses occur in the network:

$$P_i = \sum_{j \in \mathcal{C}_i} (P_j + r_j I_j^2) + p_i, \quad i = 0, 1, \ldots, N \qquad (2.3a)$$

$$Q_i = \sum_{j \in \mathcal{C}_i} (Q_j + x_j I_j^2) + q_i, \quad i = 0, 1, \ldots, N. \qquad (2.3b)$$

In these equations, p_i and q_i can be later on be broken down to consumption minus generation in nodes capable of power generation (see Section 2.2). The terms $r_j I_j^2$ and $x_j I_j^2$ represent real and reactive power losses. Equations (2.1)–(2.3) are known as the power flow equations. The variables in these equations are $\{P_i\}_{i=0}^N$, $\{Q_i\}_{i=0}^N$, $\{V_i\}_{i=1}^N$, $\{I_i\}_{i=1}^N$, and active and reactive net consumptions $\{p_i\}_{i=0}^N$ and $\{q_i\}_{i=0}^N$. By using (2.3) in (2.2), it is evident that in addition to thermal losses on the links (i.e., $r_j I_j^2$ and $x_j I_j^2$), real and reactive consumption of users contribute to the voltage drop from ancestor node A_i to node i.

The power flow equations (2.1)-(2.3) must hold in a distribution network under any circum-

stances, hence they impose themselves as constraints in optimization problems for distribution networks. Notice that these constraints are non-convex. To render optimization problems involving power flow equations as their constraints tractable, convex approximations and relaxations of (2.1)-(2.3) have been pursued; see e.g. [8], [13], [12], [14], [6], [7], [9], [11], [3], [22], [23] and references therein. The approximations that will be utilized in this thesis are presented next using unifying notations for general tree networks.

2.1 Approximations of power flow equations

A linear approximation of power flow equations known as `LinDistFlow` is presented in Subsection 2.1.1. Next, in Subsection 2.1.2 the SOCP relaxation of the power flow equations is obtained using a suitable change of variables in (2.1).

2.1.1 `LinDistFlow` approximation

The real and reactive power losses for link $i \in \mathcal{E}$, that is, the terms $r_i I_i^2$ and $x_i I_i^2$ in equations (2.3), can be equivalently calculated upon squaring (2.1) to obtain I_i^2:

$$r_i I_i^2 = r_i \frac{P_i^2 + Q_i^2}{V_i^2} \tag{2.4}$$

$$x_i I_i^2 = x_i \frac{P_i^2 + Q_i^2}{V_i^2}. \tag{2.5}$$

In many practical cases, the loss terms in (2.4) and (2.5) are much smaller than real power flow P_i and reactive power flow Q_i:

$$r_i I_i^2 = r_i \frac{P_i^2 + Q_i^2}{V_i^2} << P_i \tag{2.6}$$

$$x_i I_i^2 = x_i \frac{P_i^2 + Q_i^2}{V_i^2} << Q_i. \tag{2.7}$$

In this case, the terms involving $r_i I_i^2$ and $x_i I_i^2$ can be dropped from (2.2) and (2.3). Upon defining $v_i = V_i^2$, the following linear power flow equations known as *simplified Dist-Flow* equations are

obtained from (2.2) and (2.3) [3], [4], [9]:

Simplified Dist-Flow:

$$P_i = \sum_{j \in \mathcal{C}_i} P_j + p_i,\ i \in \mathcal{N} \tag{2.8a}$$

$$Q_i = \sum_{j \in \mathcal{C}_i} Q_j + q_i,\ i \in \mathcal{N} \tag{2.8b}$$

$$v_{A_i} = v_i + 2(r_i P_i + x_i Q_i),\ i \in \mathcal{N} \backslash \{0\} \tag{2.8c}$$

$$v_i \geq 0,\ i \in \mathcal{N} \backslash \{0\}. \tag{2.8d}$$

Note that (2.8d) is enforced because of the definition of v_i. Since the voltage deviations from the nominal values are small [i.e. $(V_i - V_0)^2 \approx 0$] a further approximation of (2.8c) has been proposed [7], [23]. By expanding the quadratic term the following approximation holds:

$$\begin{aligned} (V_i - V_0)^2 = V_i^2 + V_0^2 - 2V_i V_0 \approx 0 \\ \Rightarrow V_i^2 \approx 2V_i V_0 - V_0^2. \end{aligned} \tag{2.9}$$

Applying equation (2.9) to nodes i and A_i yields:

$$V_{A_i}^2 = 2V_{A_i} V_0 - V_0^2 \tag{2.10}$$

$$V_i^2 = 2V_i V_0 - V_0^2. \tag{2.11}$$

Using (2.10) in (2.2) yields

$$\begin{aligned} 2V_{A_i} V_0 - V_0^2 = 2V_i V_0 - V_0^2 + 2(r_i P_i + x_i Q_i) \Rightarrow \\ V_{A_i} = V_i + \frac{r_i P_i + x_i Q_i}{V_0} \end{aligned}$$

The latter is a linear equality. Equations (2.8a)–(2.8b) are linear approximations of power flow

equations and are called `LinDistFlow`:

`LinDistFlow:`

$$P_i = \sum_{j \in \mathcal{C}_i} P_j + p_i,\ i \in \mathcal{N} \tag{2.12a}$$

$$Q_i = \sum_{j \in \mathcal{C}_i} Q_j + q_i,\ i \in \mathcal{N} \tag{2.12b}$$

$$V_{A_i} = V_i + \frac{r_i P_i + x_i Q_i}{V_0},\ i \in \mathcal{N}\backslash\{0\} \tag{2.12c}$$

$$V_i \geq 0,\ i \in \mathcal{N}\backslash\{0\}. \tag{2.12d}$$

Note that (2.12d) is enforced because V_i is a phasor magnitude.

2.1.2 SOCP relaxation

Define variables $v_i = V_i^2$ (as before), and $l_i = I_i^2$. Squaring (2.1) yields

$$P_i^2 + Q_i^2 = v_i l_i \tag{2.13}$$

Equation (2.13) is a quadratic equality constraint and hence it is not convex. The equality can be relaxed to an inequality [22], which, together with (2.3), forms the following SOCP relaxation to the power flow equations:

`SOCP Power Flows:`

$$P_i = \sum_{j \in \mathcal{C}_i} (P_j + r_j l_i) + p_i,\ i \in \mathcal{N} \tag{2.14a}$$

$$Q_i = \sum_{j \in \mathcal{C}_i} (Q_j + x_j l_i) + q_i,\ i \in \mathcal{N} \tag{2.14b}$$

$$v_{A_i} = v_i + 2(r_i P_i + x_i Q_i) + (r_i^2 + x_i^2) l_i,\ i \in \mathcal{N}\backslash\{0\} \tag{2.14c}$$

$$P_i^2 + Q_i^2 \leq v_i l_i,\ i \in \mathcal{N}\backslash\{0\} \tag{2.14d}$$

$$v_i \geq 0, l_i \geq 0,\ i \in \mathcal{N}\backslash\{0\}. \tag{2.14e}$$

Equations (2.14a)–(2.14c) are linear, while (2.14d) can be written equivalently as an SOCP constraint as follows [24, Exercise 4.2]:

$$\begin{aligned} 4(P_i^2+Q_i^2) \leq 4v_i l_i = (v_i+l_i)^2-(v_i-l_i)^2 \\ \Rightarrow 4(P_i^2+Q_i^2)+(v_i-l_i)^2 \leq (v_i+l_i)^2 \\ \Rightarrow \left\| \begin{array}{c} 2P_i \\ 2Q_i \\ l_i-v_i \end{array} \right\|_2 \leq l_i+v_i \end{aligned} \tag{2.15}$$

Note also that since $v_i = V_i^2$ and $l_i = I_i^2$, constraint (2.14e) has to be enforced.

2.2 Power injection model

In the distribution network of Fig. 2.1, nodes $i \in \mathcal{N}\backslash\{0\}$ represent users. Each user i demands electric loads with aggregated real and reactive power consumptions denoted by p_{c_i} and q_{c_i}. To include programmable loads in our model, each user i is allowed to demand that its real power consumption be within a certain range:

$$p_{c_i}^{\min} \leq p_{c_i} \leq p_{c_i}^{\max}. \tag{2.16}$$

For typical residential areas, reactive power consumption is linearly related to active power consumption with a constant known as power factor $\mathrm{PF}_i \in [0,1)$:

$$q_{c_i} = \sqrt{\frac{1}{\mathrm{PF}_i^2}-1} p_{c_i}. \tag{2.17}$$

User i may also be capable of PV generation. We will assume that for these types of users a photovoltaic inverter is installed that generates real electric power w_i by utilizing the available solar power. Generating solar power w_i at node i has an effect on the net real power consumption

p_i in equation (2.3a). Specifically, p_i can now be broken down to consumption minus generation:

$$p_i = p_{c_i} - w_i. \tag{2.18}$$

The maximum apparent power capability of the inverter for node i is denoted by s_{w_i} which is the nameplate capacity of the PV inverter. Currently, the PV inverters must operate with $\mathrm{PF} = 1$ which means that they cannot inject or consume reactive power and hence $s_{w_i} = w_i$. However, by taking note of power flow equations in (2.1)–(2.3) a possible method to overcome voltage drop in distribution networks is to generate or consume an optimized amount of reactive power.

To elaborate, consider the linear approximation of power flow equations (2.12):

$$V_{A_i} = V_i + \frac{r_i P_i + x_i Q_i}{V_0} \Rightarrow \Delta V_i = V_{A_i} - V_i = \frac{r_i P_i + x_i Q_i}{V_0}. \tag{2.19}$$

If the power flow P_i is positive such that the voltage drop is significant, one possible solution is to alter the net reactive power consumption q_i to make up for the voltage drop by providing negative Q_i in (2.8b). This strategy is called reactive power control [23]. In order to allow reactive power compensation, PV inverters will need to operate at power factors less than one. In this case, maximum apparent power s_{w_i} can be considered to be a factor k greater than the maximum real power capability of the PV unit, that is:

$$s_{w_i} = k w_i^{\max}. \tag{2.20}$$

Quantities s_{w_i}, k, and $w_i^{\max}$ are all parameters of the PV system. Deviating from operating at $\mathrm{PF} = 1$ offers the opportunity to alter q_i using the PV inverters as sinks or sources of reactive power. Assume the PV inverter at node i generates reactive power q_{w_i}, then the term q_i in equation (2.3) is broken down to:

$$q_i = q_{c_i} - q_{w_i} \tag{2.21}$$

The reactive power generation by PV inverter is a controllable variable but is limited to lie within

the following bounds [25] [6]:

$$q_{w_i} \in [q_{w_i}^{\min}, q_{w_i}^{\max}] = [-\sqrt{s_{w_i}^2 - {w_i}^2}, \sqrt{s_{w_i}^2 - w_i^2}]. \tag{2.22}$$

On a sunny day, when the irradiance conditions are optimal for PV generation, real power generation will be at its maximum, that is, $w_i = w_i^{\max}$, which limits the possible range of reactive power generation by that PV. unit.

Chapter 3: VOLTAGE-CONSTRAINED REAL AND REACTIVE POWER MANAGEMENT

Distribution networks are usually governed by distribution system operators (DSO) which commit to provide electric power to end-users. The first important objective for a DSO is to deliver the required power levels to users in order to increase customer satisfaction. The required power for the users is injected into the distribution network through the substation, which is connected to the transmission network. Achieving minimum costs in provision of this total power is a second objective for a DSO. In addition, delivering power to the users requires that current flows through the lines which incurs thermal losses. Minimization of these losses is a third objective for a DSO. Moreover, increased power demand of end-users forces voltage levels to drop significantly (see Chapter 2 for details). Maintaining voltage levels within acceptable bounds at the network buses is known as *voltage regulation* and is also among the important tasks of a DSO.

Distributed solar power generation can help reduce the thermal losses in the network, because part of customer demand is supplied by distributed generation nearby. However, solar power generation is inherently of stochastic nature due to fast changing irradiance conditions–caused by e.g., transient clouds. This uncertainty in available solar power poses difficulties for the DSO to efficiently achieve the previously mentioned objectives.

To elaborate, consider a situation in which the weather condition is such that solar power generation is so low that it does not meet the demand. To achieve customer satisfaction in this case, the DSO will need to incur a cost to provide power from the transmission network as well as sustain additional thermal losses on the distribution lines. On the other hand, unexpected increased levels of grid-connected local generation along with variation in sun irradiance conditions lead to large variations of voltage levels in the network, which is unacceptable for network-connected equipment.

Introduction of programmable loads into the smart grid opens up the possibility to modify customer's demand based on available power and hence minimize the network operating costs.

Moreover, the reactive power control capabilities of PV inverters offer an opportunity to perform voltage regulation. Based on the possibilities that these technologies offer, this chapter develops a framework for real and reactive power management in distribution networks under uncertain solar power generation. The overall approach is to model the problem as a stochastic program with two sets of decision variables. The first set is the real power consumptions of programmable loads, while the second set features the reactive power generation or consumption of PV inverter units. The goal is to optimize these decision variables in a fashion adaptive to the uncertain power generation by PV units. This uncertain solar power generation at every node is modeled as a random variable taking values from a possible set of scenarios.

In what follows, Section 3.1 describes power management in tree networks with the SOCP relaxation of the power flow equations. This includes explanation of the stochastic generation model, introduction of mathematical expressions for the previously mentioned objectives, formulation of the optimization problem and finally, the detailed derivation of a decentralized solver for that problem. Section 3.2 focuses on specialized decentralized solvers for power management in single-feeder distribution networks, which are particular cases of tree networks, relying on the `LinDistFlow` approximation. Section 3.3 provides details of computer simulations and numerical test results for typical examples of tree and single-feeder distribution networks.

3.1 Power management in tree networks with SOCP relaxation of power flow equations

3.1.1 Stochastic generation model

The real solar power generation at node i is a random variable. To specify the distribution of this random variable, the typical model is to assume that it takes values from a set of M possible scenarios, each with probability π^m for $m \in \{1, 2, ..., M\}$ [18]. In each scenario m, the corresponding generated power by the PV inverter at node i is denoted by w_i^m, which is assumed to be known.

The scenario modeling of PV generation renders the real and reactive power flows (that is,

P_i and Q_i), voltage and current magnitudes squared (v_i and l_i) to be scenario-dependent as well. However, since the customers have to be immune to the various possible scenarios, customer power consumption (p_{c_i}) is considered to be scenario-independent. Using the SOCP relaxation model described in the previous chapter, the power flow equations in scenario $m \in \{1, 2, ..., M\}$ are as follows:

$$P_i^m = \sum_{j \in \mathcal{C}_i} (P_j^m + r_j l_j^m) + p_{c_i} - w_i^m, \; i \in \mathcal{N} \tag{3.1a}$$

$$Q_i^m = \sum_{j \in \mathcal{C}_i} (Q_j^m + x_j l_j^m) + \sqrt{\frac{1}{\mathrm{PF_i}^2} - 1} p_{c_i} - q_{w_i}^m, \; i \in \mathcal{N} \tag{3.1b}$$

$$v_{A_i}^m = v_i^m + 2(r_i P_i^m + x_i Q_i^m) + (r_i^2 + x_i^2) l_i^m, \; i \in \mathcal{N} \backslash \{0\} \tag{3.1c}$$

$$(P_i^m)^2 + (Q_i^m)^2 \leq v_i^m l_i^m, \; i \in \mathcal{N} \backslash \{0\} \tag{3.1d}$$

$$v_i^m \geq 0, \; l_i^m \geq 0, \; i \in \mathcal{N} \backslash \{0\} \tag{3.1e}$$

These equations are exactly the power flows derived in (2.14a)-(2.14d), where the net real and reactive power consumption (i.e., p_i and q_i) are replaced by the equivalent consumption minus generation per scenario.

3.1.2 Objective functions

The objective function to be minimized is a linear combination of three terms: 1) negative of the utility that captures customer satisfaction, 2) the expected cost of providing real power to operate the distribution system, and 3) aggregate thermal losses across the distribution network.

It was previously mentioned that customer satisfaction can be captured by evaluating the real power delivered to each customer. The model adopted here specifies that customer i is most satisfied when $p_{c_i} = p_{c_i}^{\max}$ and is least satisfied when $p_{c_i} = p_{c_i}^{\min}$. One possible utility function is a concave quadratic $u_i(p_{c_i}) = -K_{u_i}(p_{c_i} - p_{c_i}^{\max})^2$ where $K_{u_i} \geq 0$ is a user-dependent weighting parameter. If p_{c_i} has units of kilowatts, K_{u_i} will have units of $\$/(\mathrm{kW})^2$. The negative sum of all these utility functions constitutes the first objective.

As for the second objective, the total real power that needs to be provided for the operation of the distribution network at scenario m is P_0^m. A typical cost model for P_0^m can take the following form:

$$\text{Cost}(P_0^m) = \begin{cases} K_0(P_0^m)^2 & \text{for } P_0^m \geq 0 \\ 0 & \text{for } P_0^m \leq 0 \end{cases} \tag{3.2}$$

where $K_0 \geq 0$ is a constant with units of $\$/(\text{kW})^2$. In this model, it is considered that when the required power to be provided is negative there will be no cost. The expected value of this cost over all the scenarios is considered to be the second objective.

The losses incurred in each line per scenario m may be calculated by evaluating the loss term (2.4) after replacing the current magnitude value with l_i^m. The expected value of losses is therefore: $\sum_{m=1}^{M} \pi^m \sum_{i=1}^{N} r_i(l_i^m)$, and is the third objective.

As described earlier in the chapter, an important task of the DSO is to perform voltage regulation in order to avoid large variations in voltage levels across the network buses. In this chapter, the proposed formulation handles voltage regulation through enforcing the following hard constraint for every bus $i \in \{1, \ldots, N\}$ in all scenarios $m \in \{1, 2, ..., M\}$

$$(1-\epsilon)^2 V_0^2 \leq v_i^m \leq (1+\epsilon)^2 V_0^2, \; i \in \mathcal{N} \backslash \{0\} \tag{3.3}$$

where typically a value of $\epsilon = 0.05$ could be chosen.

3.1.3 Optimization problem

Let vectors $\mathbf{p_c}, \mathbf{P_0}, \mathbf{v}, \mathbf{l}, \mathbf{P}, \mathbf{Q}, \mathbf{q_w}$ collect values per node and per scenario for corresponding variables $p_{c_i}, P_0^m, v_i^m, l_i^m, P_i^m, Q_i^m, q_{w_i}^m$ respectively. By considering the objective function and rewriting the power flow equations of SOCP relaxation per scenario, the overall optimization problem will be as follows:

$$\min_{\mathbf{p_c},\mathbf{P_0},\mathbf{v},\mathbf{l},\mathbf{P},\mathbf{Q},\mathbf{q_w}} \sum_{i\in\mathcal{N}} K_{u_i}(p_{c_i}-p_{c_i}^{\max})^2 + \sum_{m=1}^{M}\pi^m \mathrm{Cost}(P_0^m)^2 + K_{\mathrm{Loss}} \sum_{i\in\mathcal{N}\backslash\{0\}}\sum_{m=1}^{M}\pi^m r_i l_i^m \tag{3.4a}$$

subject to

$$\text{for } i\in\mathcal{N} \text{ and } m=1,2,...,M:$$

$$P_i^m = \sum_{j\in C_i}(P_j^m + r_j l_j^m) + p_{c_i} - w_i^m \tag{3.4b}$$

$$Q_i^m = \sum_{j\in C_i}(Q_j^m + x_j l_j^m) + \sqrt{\frac{1}{\mathrm{PF}_i^2}-1}p_{c_i} - q_{w_i}^m \tag{3.4c}$$

$$p_{c_i}^{\min} \le p_{c_i} \le p_{c_i}^{\max} \tag{3.4d}$$

$$q_{w_i}^{\min} \le q_{w_i}^m \le q_{w_i}^{\max} \tag{3.4e}$$

$$\text{for } i\in\mathcal{N}\backslash\{0\} \text{ and } m=1,2,...,M:$$

$$v_{A_i}^m = v_i^m + 2(r_i P_i^m + x_i Q_i^m) + (r_i^2+x_i^2) l_i^m i \tag{3.4f}$$

$$(P_i^m)^2 + (Q_i^m)^2 \le v_i^m l_i^m,\ v_i^m \ge 0, l_i^m \ge 0 \tag{3.4g}$$

$$(1-\epsilon)^2 V_0^2 \le v_i^m \le (1+\epsilon)^2 V_0^2 \tag{3.4h}$$

In the above, the function $\mathrm{Cost}(P_0^m)$ follows from (3.2), where the explicit expression with regard to P_0^m is only available by knowledge of whether P_0^m is non-negative or not. Note that P_0^m is a decision variable and hence it is not known in advance. By introducing two non-negative slack variables, namely P_{0+}^m to handle cases where P_0^m is non-negative, and P_{0-}^m to handle cases where P_0^m is non-positive, we will try to equivalently represent $\mathrm{Cost}(P_0^m)$ in (3.2) with the following form:

$$\mathrm{Cost}(P_0^m) = K_0(P_{0+}^m)^2 \tag{3.5a}$$

$$P_0^m = P_{0+}^m - P_{0-}^m \tag{3.5b}$$

$$P_{0+}^m \ge 0, P_{0-}^m \ge 0 \tag{3.5c}$$

In this representation of $\mathrm{Cost}(P_0^m)$, for cases where P_0^m is non-negative:

$$\mathrm{Cost}(P_0^m) = K_0(P_0^m)^2 = K_0(P_{0+}^m)^2.$$

This yields that $P_{0+}^m = P_0^m$ and by (3.5b) and (3.5c) $P_{0-}^m = 0$. Similarly, for cases where P_0^m is negative:

$$\mathrm{Cost}(P_0^m) = 0 = K_0(P_{0+}^m)^2.$$

This yields that $P_{0+}^m = 0$ and $P_{0-}^m = -P_0^m$. The advantage here is that, the explicit form of $\mathrm{Cost}(P_0^m)$ (i.e. (3.5a)) can be used in (3.4a), while constraints (3.5b) and (3.5b) are handled by including them along with all other constraints of optimization problem(3.4). These slack variables help to avoid the difficulty of having to deal with (3.2) directly. Let $\mathbf{P_{0+}}$ and $\mathbf{P_{0-}}$ collect P_{0+}^m and P_{0-}^m respectively for all the scenarios, the overall optimization problem amounts to the following convex quadratic program:

$$\min_{\mathbf{p_c},\mathbf{P_{0+}},\mathbf{P_{0-}},\mathbf{v},\mathbf{l},\mathbf{P},\mathbf{Q},\mathbf{q_w}} \sum_{i\in\mathcal{N}} K_{u_i}(p_{c_i} - p_{c_i}^{\max})^2 + \sum_{m=1}^{M} K_0(\pi^m)(P_{0+}^m)^2 + K_{\mathrm{Loss}} \sum_{i\in\mathcal{N}\setminus\{0\}} \sum_{m=1}^{M} \pi^m r_i l_i^m \tag{3.6a}$$

subject to

$$\text{for } i \in \mathcal{N} \text{ and } m = 1, 2, ..., M:$$

$$P_i^m = \sum_{j\in C_i} (P_j^m + r_j l_j^m) + p_{c_i} - w_i^m \tag{3.6b}$$

$$Q_i^m = \sum_{j\in C_i} (Q_j^m + x_j l_j^m) + \sqrt{\frac{1}{\mathrm{PF}_i^2} - 1}\, p_{c_i} - q_{w_i}^m \tag{3.6c}$$

$$p_{c_i}^{\min} \le p_{c_i} \le p_{c_i}^{\max} \tag{3.6d}$$

$$q_{w_i}^{\min} \leq q_{w_i}^m \leq q_{w_i}^{\max} \tag{3.6e}$$

$$P_0^m = P_{0+}^m - P_{0-}^m, P_{0+}^m \geq 0, P_{0-}^m \geq 0 \tag{3.6f}$$

$$\text{for } i \in \mathcal{N}\backslash\{0\} \text{ and } m = 1, 2, ..., M:$$

$$v_{A_i}^m = v_i^m + 2(r_i P_i^m + x_i Q_i^m) + (r_i^2 + x_i^2) l_i^m i \tag{3.6g}$$

$$(P_i^m)^2 + (Q_i^m)^2 \leq v_i^m l_i^m,\ v_i^m \geq 0, l_i^m \geq 0 \tag{3.6h}$$

$$(1-\epsilon)^2 V_0^2 \leq v_i^m \leq (1+\epsilon)^2 V_0^2 \tag{3.6i}$$

It is also not hard to prove that at the optimal point only one of the variables P_{0+}^m or P_{0-}^m is nonzero. The proof is via contradiction and is provided in appendix A.

3.1.4 Decentralized algorithm

Problem (3.6) includes variables that pertain to different parts of the distribution network. Power consumption p_{c_i}, reactive power generation $q_{w_i}^m$, and the voltages v_i^m correspond to the buses. Power flows (P_i^m, Q_i^m) and current magnitudes l_i^m pertain to every link. A centralized solution methodology, similar to the ones in today's energy management systems, requires communication of these local quantities to the DSO, which can be prohibitive once the network and/or the number of scenarios is considerably large. In addition to this communication overhead, privacy issues may arise since local information such as utility functions, real power consumption bounds, and power factors are to be communicated to a centralized DSO. Besides, in larger networks where number of the variables is high, it is preferable to break the problem into smaller subproblems allowing each node to handle their own individual problem and then talk to each other to converge to the same optimal point as the one that would have been achieved via the centralized method [26].

Since the objective (3.6a) is a sum of terms corresponding to different parts of the network, it can be readily separated per node. Moreover, constraints (3.6d) and (3.6e) are specific to user i. Constraints (3.6h) and (3.6i) can be handled on each link locally and (3.6f) only refers to the substation. The only obstacle to completely decompose the problem per node are the power flow

equations (3.6b), (3.6c) and (3.6g) which couple certain quantities of ancestor nodes to the children nodes and vice versa.

In order to write the problem in a form amenable to a decentralized solution via the ADMM (cf. Appendix B), a set of auxiliary variables must be introduced. Specifically, since any node i except for the leaves has child nodes, to bypass the need to know P_j^m,Q_j^m and l_j^m of child node $j \in \mathcal{C}_i$ at its ancestor node i, respective copies of these variables, $\hat{P}_j^m$,$\hat{Q}_j^m$,$\hat{l}_j^m$, can be introduced. The total number of these copies per scenario is N. Moreover, because all nodes except for the root have ancestors, $\hat{v}_i^m$ is ushered as the copy of ancestor voltage of node i at node i. Again, there are exactly N copies (one for every node) per scenario. An additional set of copies per scenario, namely, $\tilde{P}_i^m$, $\tilde{Q}_i^m$, $\tilde{l}_i^m$, and $\tilde{v}_i^m$ for all $n \in \mathcal{N}\backslash\{0\}$ and $\tilde{P}_{0+}^m$,$\tilde{P}_{0-}^m$ for the root (i.e., $i = 0$) is also introduced, the purpose of which will be evident shortly. Let the set of boldface variables $\{\mathbf{P}, \hat{\mathbf{P}}, \tilde{\mathbf{P}}, \mathbf{Q}, \hat{\mathbf{Q}}, \tilde{\mathbf{Q}}, \mathbf{v}, \mathbf{l}, \hat{\mathbf{l}}, \tilde{\mathbf{l}}, \hat{\mathbf{v}}, \tilde{\mathbf{v}}, \tilde{\mathbf{p}}_\mathbf{c}, \mathbf{p}_\mathbf{c}, \mathbf{q}_w, \tilde{\mathbf{q}}_w, \mathbf{P_{0+}}, \mathbf{P_{0-}}, \tilde{\mathbf{P}}_{\mathbf{0}+}, \tilde{\mathbf{P}}_{\mathbf{0}-}\}$ represent vectors collecting the corresponding values of that variable in all scenarios and nodes. The problem takes the following form:

$$\min_{\substack{\mathbf{P},\hat{\mathbf{P}},\tilde{\mathbf{P}},\\ \mathbf{Q},\hat{\mathbf{Q}},\tilde{\mathbf{Q}},\\ ,\mathbf{l},\hat{\mathbf{l}},\tilde{\mathbf{l}}\\ \mathbf{v},\hat{\mathbf{v}},\tilde{\mathbf{v}}\\ \tilde{\mathbf{p}}_\mathbf{c},\mathbf{p}_\mathbf{c},\mathbf{q}_w,\tilde{\mathbf{q}}_w\\ \mathbf{P_{0+}},\mathbf{P_{0-}},\tilde{\mathbf{P}}_{\mathbf{0}+},\tilde{\mathbf{P}}_{\mathbf{0}-}}} \quad \sum_{i\in\mathcal{N}} K_{u_i}\tilde{p}_{c_i} - p_{c_i}^{\max})^2 + \sum_{m=1}^{M} K_0\pi^m(P_{0+}^m)^2 + K_{\text{Loss}} \sum_{i\in\mathcal{N}\backslash\{0\}} \sum_{m=1}^{M} r_i l_i^m \tag{3.7a}$$

subject to:

Coupling Constraints (for $m = 1, 2, ..., M$):

$$\text{for } i \in \mathcal{N}\backslash\{0\}: \quad P_i^m = \tilde{P}_i^m \quad Q_i^m = \tilde{Q}_i^m \quad l_i^m = \tilde{l}_i^m \quad v_i^m = \tilde{v}_i^m \quad \hat{v}_j^m = \tilde{v}_{A_j}^m \tag{3.7b}$$

$$\text{for } i \in \mathcal{N},\ j \in \mathcal{C}_i: \quad \hat{P}_j^m = \tilde{P}_j^m \quad \hat{Q}_j^m = \tilde{Q}_j^m \quad \hat{l}_j^m = \tilde{l}_j^m \quad p_{c_i}^m = \tilde{p}_{c_i} \quad q_{w_i}^m = \tilde{q}_{w_i}^m \tag{3.7c}$$

$$\text{for } i = 0: \quad P_{0+}^m = \tilde{P}_{0+}^m \qquad P_{0-}^m = \tilde{P}_{0-}^m \tag{3.7d}$$

Individual Equality Constraints (for $m = 1, 2, ..., M$):

$$\text{for } i \in \mathcal{N} : P_i^m = \sum_{j \in \mathcal{C}_i} (\hat{P}_j^m + r_j \hat{l}_j^m) + p_{c_i}^m - w_i^m \tag{3.7e}$$

$$\text{for } i \in \mathcal{N} : Q_i^m = \sum_{j \in \mathcal{C}_i} (\hat{Q}_j^m + x_j \hat{l}_j^m) + \sqrt{\frac{1}{\text{PF}_i^2} - 1} p_{c_i}^m - q_{w_i}^m \tag{3.7f}$$

$$\text{for } i \in \mathcal{N} \backslash \{0\} : \quad \hat{v}_i^m = v_i^m + 2(r_i P_i^m + x_i Q_i^m) + (r_i^2 + x_i^2) l_i^m \tag{3.7g}$$

$$\text{for } i = 0 : \quad P_0^m = P_{0+}^m - P_{0-}^m \tag{3.7h}$$

Individual Inequality Constraints (for $m = 1, 2, ..., M$)

$$\text{for } i \in \mathcal{N} \backslash \{0\} : (\tilde{P}_j^m)^2 + (\tilde{Q}_j^m)^2 \leq (\tilde{v}_j^m)(\tilde{l}_j^m) \tag{3.7i}$$

$$\text{for } i \in \mathcal{N} \backslash \{0\} : (1 - \epsilon)^2 V_0^2 \leq \tilde{v}_i^m \leq (1 + \epsilon)^2 V_0^2 \tag{3.7j}$$

$$\text{for } i \in \mathcal{N} : p_{c_i}^{\min} \leq \tilde{p}_{c_i} \leq p_{c_i}^{\max} \tag{3.7k}$$

$$\text{for } i \in \mathcal{N} : -\sqrt{s_{w_i}^2 - (w_i^m)^2} \leq \tilde{q}_{w_i}^m \leq \sqrt{s_{w_i}^2 - (w_i^m)^2} \tag{3.7l}$$

$$\text{for } i = 0 : \tilde{P}_{0+}^m \geq 0, \tilde{P}_{0-}^m \geq 0 \tag{3.7m}$$

Problem (3.7) is equivalent to (3.6) with additional equality constraints yielding a suitable form for ADMM [cf. problem B.1 in Appendix B]. The $\mathbf{x}$ and $\mathbf{z}$ [corresponding to the prototype ADMM problem (B.1) in Appendix B] variables are shown in Table 3.1. The purpose of introducing the *Tilde* variables is so that the individual inequality constraints can be handled separately in the $\mathbf{z}$-update. The $\mathbf{x}$-update on the other hand turns out to be an equality constrained QP. This separation of variables are essential to finding closed-form solutions for the updates.

Updates

The Lagrange multipliers corresponding to the coupling constrains of (3.7) are listed in Table 3.2. To perform ADMM, first the augmented Lagrangian for problem (3.7) needs to be formed which turns out to be separable across variables $\mathbf{x}_i$ ($i \in \mathcal{N}$) with $\mathbf{z}$ fixed, or across variables $\mathbf{z}_i$ ($i \in \mathcal{N}$)

Table 3.1: Variables

	Nodes involved	Variables
$\mathbf{x}_0^m$	Root	$\{P_0^m, Q_0^m, P_{0+}^m, P_{0-}^m, \{\hat{P}_j^m, \hat{Q}_j^m, \hat{l}_j^m\}_{j\in\mathcal{C}_i}, p_{c_0}^m, q_{w_0}^m\}$
$\mathbf{x}_i^m$	Neither root nor leaf	$\{P_i^m, Q_i^m, v_i^m, l_i^m, \{\hat{P}_j^m, \hat{Q}_j^m, \hat{l}_j^m\}_{j\in\mathcal{C}_i}, \hat{v}_i^m, p_{c_i}^m, q_{w_i}^m\}$
$\mathbf{x}_i^m$	Leaf	$\{P_i^m, Q_i^m, v_i^m, l_i^m, \hat{v}_i^m, p_{c_i}^m, q_{w_i}^m\}$
$\mathbf{x}_i$	All nodes	$\{\mathbf{x}_i^m\}_{m=1}^M$
$\mathbf{z}_0^m$	Root	$\{\tilde{P}_{0+}^m, \tilde{P}_{0-}^m, \tilde{q}_{w_0}^m\}$
$\mathbf{z}_0$	Root	$\{\{\mathbf{z}_0^m\}_{m=1}^M, \tilde{p}_{c_0}\}$
$\mathbf{z}_i^m$	Not root	$\{\tilde{P}_i^m, \tilde{Q}_i^m, \tilde{v}_i^m, \tilde{l}_i^m, \tilde{q}_{w_i}^m\}$
$\mathbf{z}_i$	Not root	$\{\{\mathbf{z}_i^m\}_{m=1}^M, \tilde{p}_{c_i}\}$

with $\mathbf{x}_i$ fixed. For the detailed derivation of each variable update the reader is referred to Appendix C where closed-form solution for individual updates per node and per scenario are provided.

Table 3.2: Lagrange Multipliers

Equality Constraint	Lagrange Multiplier
$P_i^m = \tilde{P}_i^m$	λ_i^m
$Q_i^m = \tilde{Q}_i^m$	μ_i^m
$l_i^m = \tilde{l}_i^m$	γ_i^m
$v_i^m = \tilde{v}_i^m$	ω_i^m
$\hat{v}_j^m = \tilde{v}_{A_j}^m$	$\hat{\omega}_j^m$
$\hat{P}_j^m = \tilde{P}_{j\in\mathcal{C}_i}$	$\hat{\lambda}_j^m$
$\hat{Q}_j^m = \tilde{Q}_{j\in\mathcal{C}_i}$	$\hat{\mu}_j^m$
$\hat{l}_j^m = \tilde{l}_{j\in\mathcal{C}_i}$	$\hat{\gamma}_j^m$
$p_{c_i}^m = \tilde{p}_{c_i}$	η_i^m
$q_{w_i}^m = \tilde{q}_{w_i}^m$	θ_i^m
$P_{0+}^m = \tilde{P}_{0+}^m$	ζ_+^m
$P_{0-}^m = \tilde{P}_{0-}^m$	ζ_-^m

Decentralized implementation and communication requirements

In the implementation of this algorithm, each node $i \in \mathcal{N}$ is responsible for maintaining and updating variables $\mathbf{x}_i$, $\mathbf{z}_i$, and the corresponding Lagrange parameters.

The ADMM algorithm works as depicted in Fig. 3.1. First, $\mathbf{z}$ and the Lagrange multipliers are initialized with arbitrary numbers. In each iteration, every node i that has children receives $\tilde{P}_j^m$, $\tilde{Q}_j^m$ and $\tilde{l}_j^m$ for every $j \in \mathcal{C}_i$. Also, each node i receives $\tilde{v}_{A_i}^m$ from its ancestor. Using these

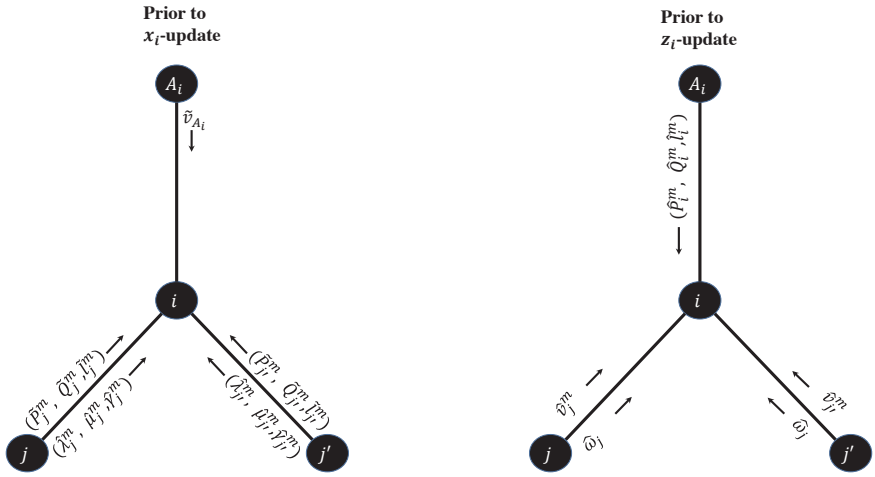

Figure 3.1: Communication requirements of the ADMM algorithm. In each iteration, prior to the $\mathbf{x}$-update, node i receives $\tilde{P}_j^m$, $\tilde{Q}_j^m$, and $\tilde{l}_j^m$ from its children nodes, and receives $\tilde{v}_{A_i}^m$ from its ancestor nodes. Prior to $\mathbf{z}$-update ancestor node A_i sends $\hat{P}_i^m$, $\hat{Q}_i^m$ and $\hat{l}_i^m$ to node i while node i receives all the $\hat{v}_j^m$ variables from its children. Note that whenever a variable is transmitted, its corresponding Lagrange multiplier is transmitted as well.

variables, $\mathbf{x}$ variable is updated according to Appendix C. Prior to the $\mathbf{z}$-update step, $\hat{P}_i^m, \hat{Q}_i^m, \hat{l}_i^m$ are sent to node i from ancestor A_i meanwhile node i collects $\{v_j^m\}_{j\in\mathcal{C}_i}$ from its children. Note that, node 0 only communicates with its children, and the leaf nodes only communicate with their ancestors. All other nodes communicate both with their children and ancestors.

Upon receiving the required information, node i performs the z-update step. Upon completion of the $\mathbf{z}$-update step, the Lagrange multipliers are updated. Therefore in this algorithm only neighbors will need to communicate. Note that whenever a variable is transferred, its corresponding Lagrange multiplier will be transferred with it. Algorithm 3.1 summarizes the specific parameters and communications in each iteration.

3.2 Power management in single-feeder networks with `LinDistFlow`

The purpose of this section is to derive a simplified version of the decentralized solver for single-feeder networks using the `LinDistFlow` equations. Consider the single-branch radial distribu-

Algorithm 3.1 Required Communications and Updates

1. Initialize $\mathbf{z}$-variables and Lagrange parameters with random numbers at every node i.
2. For every node i repeat steps 3-7 until convergence (i.e., when quantities $r(k)$ and $s(k)$ in (B.4) are smaller than an acceptable tolerance)
3. Receive $\tilde{P}_j^m$, $\tilde{Q}_j^m$, $\tilde{l}_j^m$, $\hat{\lambda}_j^m$, $\hat{\mu}_j^m$, and $\hat{\gamma}_j^m$ from all $j \in \mathcal{C}_i$ and for $m = 0, 1, 2, .., M$. Also receive $\tilde{v}_{A_i}^m$ from node A_i and $m = 0, 1, 2, .., M$.
4. Perform $\mathbf{x}$-update
5. Receive the updated $\mathbf{x}$-variables $\hat{P}_i^m$, $\hat{Q}_i^m$ and $\hat{l}_i^m$ for $m = 0, 1, 2, .., M$ from A_i. Also receive $\hat{v}_j^m$ and $\hat{\omega}_j^m$ from all nodes $j \in \mathcal{C}_i$ and $m = 0, 1, 2, ..., M$.
6. Perform $\mathbf{z}$-update
7. Update the Lagrange parameters

tion feeder depicted in Fig. 3.2. Node 0 represents the substation, while nodes $1, \ldots, N$ correspond to users. User $i = 1, \ldots, N$ will have programmable loads, and possibly PV generation. The single-feeder network is a special case of the tree network.

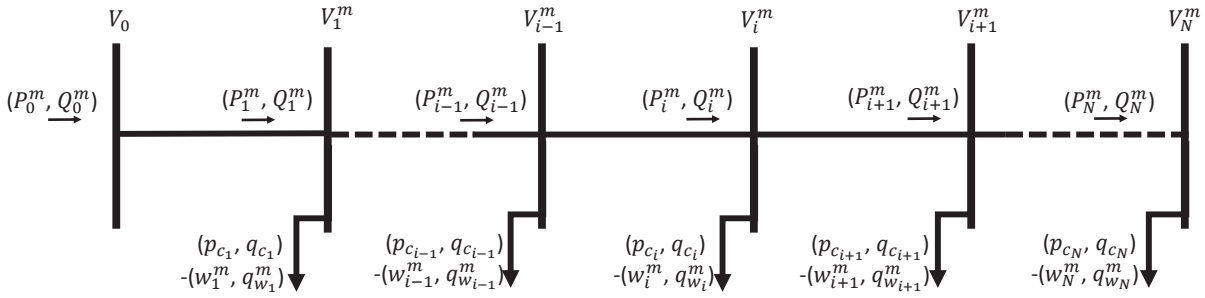

Figure 3.2: Single-branch radial distribution network with N user nodes.

Since in a single-feeder network all nodes except for the root have exactly one ancestor, and all nodes except for the leaves have exactly one child, the index j in the previous equations renders unnecessary, so that $A_i = i - 1$ and $\mathcal{C}_i = \{i + 1\}$. Concretely, let P_i^m and Q_i^m respectively be the real and reactive power flow going into node i per scenario m; and V_i^m the magnitude of the voltage phasor at node i per scenario m. Also assume that the voltages, power flows over lines, and power injections at the nodes are related through the approximation `LinDistFlow` equations

with $i \in \{0, 1, 2, ..., N-1\}$ and $m \in \{1, 2, ..., M\}$ [cf. (2.12)][1].

$$P_i^m = P_{i+1}^m + p_{c_i} - w_i^m \tag{3.8a}$$

$$Q_i^m = Q_{i+1}^m + \sqrt{\frac{1}{\mathrm{PF}_i^2} - 1} p_{c_i} - q_{w_i}^m \tag{3.8b}$$

$$V_{i+1}^m = V_i^m - \frac{r_{i+1} P_{i+1}^m + x_{i+1} Q_{i+1}^m}{1000 V_0^2} \tag{3.8c}$$

and also the terminal conditions

$$P_N^m = p_{c_N} - w_N^m \tag{3.8d}$$

$$Q_N^m = \sqrt{\frac{1}{\mathrm{PF}_N^2} - 1} p_{c_N} - q_{w_N}^m \tag{3.8e}$$

$$V_0^m = 1. \tag{3.8f}$$

In the previous equations, V_0 is the magnitude of the voltage phasor at the substation, and is a known constant measured in kilovolts. Also known constants are r_i and x_i, which respectively denote the resistance and reactance of the line connecting node i to $i+1$, and have units of Ohms. Real powers (P_i^m, p_{c_i}, $p_{g_i}^m$) are in kilowatts, while reactive powers (Q_i^m, q_{c_i}, $q_{w_i}^m$) have units of kVars. The quantities V_i^j are expressed per unit (p.u.), where the normalization is with respect to V_0.

Finally, it is evident from (3.8c) that voltage values across the network may vary significantly depending on the values of power flows. To apply voltage regulation, we can enforce

$$1 - \epsilon \leq V_i^m \leq (1 + \epsilon). \tag{3.9}$$

[1]To have a consistent notation in this section and section 3.1, for demonstration purposes, power flows are considered to be flowing into a node, for example P_0^m denotes real power going into node 0. Another model could be to consider power flows going out of the node, in which case P_0^m will be considered going out of node 0. By considering power flows going out of the node the `LinDistFlow` equations will have a slightly different form and terminal conditions which are mentioned in Appendix F along with the derivation of the ADMM algorithm. Throughout this thesis, the simulation results for single-feeder networks with `LinDistFlow` follow the latter model which is explicitly mentioned in Appendix F. The difference between the two models is merely on two conventions and the models are equivalent.

3.2.1 Objective function

The only difference in objective functions compared to Section 3.1.2 will be in the evaluation of losses. The losses across the network at scenario m can be approximated by $\sum_{i=0}^{N-1} r_i \frac{(P_i^m)^2+(Q_i^m)^2}{V_0^2}$ [6, 7].

With the aforementioned models in mind, the optimization problem to be solved stands as follows.

$$\min_{\substack{\mathbf{P},\mathbf{Q},\mathbf{v},\mathbf{p_c} \\ \mathbf{q}_w,\mathbf{P_{0+}},\mathbf{P_{0-}}}} \sum_{i=1}^{N} \left[K_{u_i}(p_{c_i} - p_{c_i}^{\max})^2\right] + \sum_{m=1}^{M} \pi^m K_0 (P_{0+}^m)^2 + \sum_{i=0}^{N-1}\sum_{m=1}^{M} K_{\text{Cost}} \pi^m r_i \frac{(P_i^m)^2 + (Q_i^m)^2}{V_0^2} \tag{3.10}$$

subject to (3.8a)-(3.9) and (3.6d)-(3.6f)

3.2.2 Equivalent problem

With $\mathbf{x}$ and $\mathbf{z}$ stacking all $\mathbf{x}_i$ and $\mathbf{z}_i$ per node and per scenario according to Table 3.1 disregarding variables $l_i^m, \hat{l}_i^m, \tilde{l}_i^m$, problem (3.10) is equivalently formulated as follows:

$$\min_{\mathbf{x},\mathbf{z}} \sum_{i=1}^{N} \left[K_{u_i}(\widetilde{p}_{c_i} - p_{c_i}^{Max})^2\right] + \sum_{m=1}^{M} \pi^m K_0 (P_{0+}^m)^2 + K_{\text{Loss}} \sum_{i=0}^{N-1}\sum_{m=1}^{M} \pi^m r_i \frac{(P_i^m)^2 + (Q_i^m)^2}{V_0^2} \tag{3.11a}$$

subject to

Coupling Constraints (for $m = 1, 2, \ldots, M$):

$$\widetilde{P}_i^m = P_i^m, \widetilde{P}_i^m = \hat{P}_i^m \quad (i \in \{0, ..., N-1\}) \tag{3.11b}$$

$$\widetilde{Q}_i^m = Q_i^m, \widetilde{Q}_i^m = \hat{Q}_i^m \quad (i \in \{0, ..., N-1\}) \tag{3.11c}$$

$$\widetilde{V}_i^m = V_i^m, \widetilde{V}_i^m = \hat{V}_i^m \quad (i \in \{1, ..., N\}) \tag{3.11d}$$

$$\widetilde{p}_{c_i} = p_{c_i}^m, \widetilde{q}_{w_i}^m = q_{w_i}^m \quad (i \in \{1, ..., N\}) \tag{3.11e}$$

$$\widetilde{P}_{0+}^m = P_{0+}^m, \widetilde{P}_{0-}^m = P_{0-}^m \tag{3.11f}$$

Individual Constraints (for $m = 1, 2, \ldots, M$):

$$P_i^m = \hat{P}_{i+1}^m + p_{c_i}^m - w_i^m \quad (i \in \{0, ..., N-1\}) \tag{3.11g}$$

$$Q_i^m = \hat{Q}_{i+1}^m + \sqrt{\frac{1}{\mathrm{PF}_i^2} - 1} p_{c_i}^m - q_{w_i}^m \quad (i \in \{1, ..., N\}) \tag{3.11h}$$

$$\hat{V}_i^m = V_i^m + \frac{r_i P_i^m + x_i Q_i^m}{1000 V_0^2} \quad (i \in \{0, ..., N-1\}) \tag{3.11i}$$

$$p_{c_i}^{\min} \leq \widetilde{p}_{c_i} \leq p_{c_i}^{\max} \quad (i \in \{1, ..., N\}) \tag{3.11j}$$

$$-\sqrt{s_{w_i}^2 - (w_i^m)^2} \leq \widetilde{q}_{w_i}^m \leq \sqrt{s_{w_i}^2 - (w_i^m)^2} (i \in \{1, ..., N\}) \tag{3.11k}$$

$$1 - \epsilon \leq \widetilde{V}_i^m \leq 1 + \epsilon \quad (i \in \{1, ..., N\}) \tag{3.11l}$$

$$P_0^m = P_{0+}^m - P_{0-}^m \tag{3.11m}$$

$$\widetilde{P}_{0+}^m \geq 0, \widetilde{P}_{0-}^m \geq 0 \tag{3.11n}$$

$$P_N^m = p_{c_N} - w_N^m \tag{3.11o}$$

$$Q_N^m = \sqrt{\frac{1}{\mathrm{PF}_N^2} - 1} p_{c_N} - q_{w_n}^m \tag{3.11p}$$

$$V_0^m = 1 \tag{3.11q}$$

In (F.1e), $\hat{v}_i$ may be interpreted as node i's estimate of the voltage in node $i+1$. Similarly, in (F.1f) and (F.1g), $\hat{P}_{i+1}^m$ and $\hat{Q}_{i+1}^m$ are interpreted as node i's estimates of the real and reactive power flow from node $i+1$, respectively. The optimization variables $\mathbf{x} := \{\mathbf{x}_0, \mathbf{x}_1, ..., \mathbf{x}_N\}$ and $\mathbf{z} := \{\mathbf{z}_0, \mathbf{z}_1, ..., \mathbf{z}_N\}$ of the previous problem are defined in (F.2). In the following lists, the boldface variables on the right-hand sides represent vectors of length M collecting the corresponding values

of that variable in all scenarios.

$$\mathbf{x}_0 := \{\mathbf{P}_0, \mathbf{Q}_0, \mathbf{v}_0, \mathbf{P}_{0+}, \mathbf{P}_{0-}\} \tag{3.12a}$$

$$\mathbf{x}_N := \left\{\mathbf{P}_N, \mathbf{Q}_N, \mathbf{v}_N, \mathbf{p}_{c_N}, \mathbf{q}_{w_N}, \hat{\mathbf{P}}_N, \hat{\mathbf{Q}}_N\right\} \tag{3.12b}$$

$$\mathbf{z}_0 := \left\{\widetilde{\mathbf{P}}_0, \widetilde{\mathbf{Q}}_0, \widetilde{\mathbf{v}}_0, \widetilde{\mathbf{P}}_{0+}, \widetilde{\mathbf{Q}}_{0+}\right\} \tag{3.12c}$$

$$\mathbf{z}_N = \{\widetilde{\mathbf{v}}_N, \widetilde{p}_{c_N}, \widetilde{\mathbf{q}}_{w_N}\} \tag{3.12d}$$

and for $i \in \{1, 2, ..., N-1\}$,

$$\mathbf{x}_i := \left\{\mathbf{P}_i, \mathbf{Q}_i, \mathbf{v}_i, \mathbf{p}_{c_i}, \mathbf{q}_{w_i}, \hat{\mathbf{P}}_i, \hat{\mathbf{Q}}_i, \hat{\mathbf{v}}_i\right\} \tag{3.12e}$$

$$\mathbf{z}_i := \left\{\widetilde{\mathbf{P}}_i, \widetilde{\mathbf{Q}}_i, \widetilde{\mathbf{v}}_i, \widetilde{p}_{c_i}, \widetilde{\mathbf{q}}_{w_i}\right\}. \tag{3.12f}$$

Note here that only $\tilde{p}_{c_i}$ is not boldfaced which means that in all the scenarios it has the same value.

Updates

The Lagrange multipliers corresponding to the coupling constrains of (F.1) are listed in Table 3.3. After forming the augmented Lagrangian for problem (F.1), it turns out that it is separable across variables $\mathbf{x}_i$ ($i \in \{0, 1, ..., N\}$) with $\mathbf{z}$ fixed, or across variables $\mathbf{z}_i$ ($i \in \{0, 1, ..., N\}$) with $\mathbf{x}$ fixed. For the detailed derivation of each variable update the reader is referred to Appendix F.

Table 3.3: Coupling Constraints & Associated Lagrange Multipliers

$\widetilde{P}_i^m = P_i^m$	$\widetilde{P}_i = \hat{P}_i^m$	$\widetilde{Q}_i^m = Q_i^m$	$\widetilde{Q}_i = \hat{Q}_i^m$	$\widetilde{q}_{w_i}^m = q_{w_i}^m$
λ_i^m	$\hat{\lambda}_i^m$	μ_i^m	$\hat{\mu}_i^m$	θ_i^m
$\widetilde{v}_i^m = v_i^m$	$\widetilde{v}_i^m = \hat{v}_i^m$	$\widetilde{p}_{c_i} = p_{c_i}^m$	$\widetilde{P}_{0+}^m = P_{0+}^m$	$\widetilde{P}_{0-}^m = P_{0-}^m$
ω_i^m	$\hat{\omega}_i^m$	η_i^m	ξ_+^m	ξ_-^m

Communication requirements

The ADMM algorithm works as depicted in Fig. 3.3. First, $\mathbf{z}$ and the Lagrange multipliers are initialized with arbitrary numbers. In each iteration, prior to $\mathbf{x}$-update, node i receives $\tilde{P}_{i+1}^m$, $\tilde{Q}_{i+1}^m$, $\hat{\lambda}_{i+1}^m$ and $\hat{\mu}_{i+1}^m$ from node $i+1$. Node i also requires reception of $\tilde{v}_{i-1}^m$ from node $i-1$ before completing the $\mathbf{x}_i$-update. Prior to the $\mathbf{z}_i$-update step, $\hat{P}_i^m$ and $\hat{Q}_i^m$ are sent from node $i-1$ to i. In this case, node 0 only sends these variables, and node N only receives them. Moreover, node $i+1$ sends $\hat{v}_{i+1}^m$ to node i. In this case, node 0 is only a receiver and node N is only a sender. Upon receiving the required information, node i performs the $\mathbf{z}_i$-update step. Upon completion of the $\mathbf{z}_i$-update step, the Lagrange multipliers are updated. These steps are summarized in Algorithm 3.2.

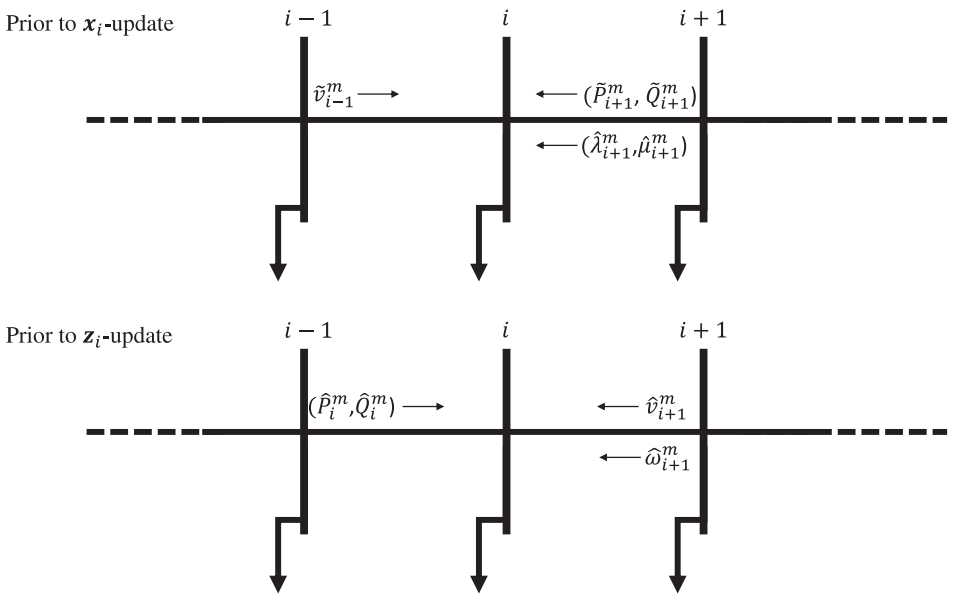

Figure 3.3: Communication requirements of the ADMM algorithm. Prior to the $\mathbf{x}_i$-update node i receives $\tilde{v}_{i-1}^m$ from node $i-1$ and receives $\tilde{P}_{i+1}^m$, $\tilde{Q}_{i+1}^m$,$\hat{\lambda}_{i+1}^m$,$\hat{\mu}_{i+1}^m$ from node $i+1$. Prior to the $\mathbf{z}$-update, node i receives $\hat{P}_i^m$ and $\hat{Q}_i^m$ from node $i-1$ while it receives $\hat{v}_{i+1}^m$ from node $i+1$.

Algorithm 3.2 Required Communications and Updates For Single-Feeder

1. Initialize $\mathbf{z}$-variables and Lagrange parameters with random numbers at every node i.
2. For every node i repeat steps 3-7 until convergence:
3. Receive $\tilde{P}^m_{i+1}$, $\tilde{Q}^m_{i+1}$, $\hat{\lambda}^m_{i+1}$ and $\hat{\mu}^m_{i+1}$ from node $i+1$ and for $m = 0, 1, 2, .., M$. Also receive $\tilde{v}^m_{i-1}$ from node $i-1$ for $m = 0, 1, 2, .., M$.
4. Perform $\mathbf{x}$-update
5. Receive the updated $\mathbf{x}$-variables $\hat{P}^m_i$, $\hat{Q}^m_i$ for $m = 0, 1, 2, .., M$ from node $i-1$. Also receive $\hat{v}^m_{i+1}$ and $\hat{\omega}^m_{i+1}$ from node $i+1$ for $m = 0, 1, 2, ..., M$.
6. Perform $\mathbf{z}$-update
7. Update the lagrange parameters

3.3 Numerical tests

In this section numerical experiments are conducted to evaluate the effectiveness of the previously formulated stochastic optimization programs and the decentralized solvers. To acquire intuitive understanding, specific examples of a single-feeder network of Fig. 3.2 which is a special case of a tree network are considered here. Tests on a general tree network are left to be covered in Chapter 4. Here, the algorithm of Section 3.2 is studied first with `LinDistFlow` in Subsection 3.3.1. The more complicated algorithm of Section 3.1 is then put to test on a single-feeder with SOCP relaxation model in Subsection 3.3.2.

3.3.1 Numerical test with `LinDistFlow` approximation

The algorithm of Section 3.2 is tested here. The single-feeder network considered is representative of a sparsely-loaded rural distribution network and resembles the test circuits in [7] and [8]. The nominal substation voltage is $V_0 = 7.2kV$, and line impedance is $(0.33 + j0.38)\Omega/km$. There are $N = 250$ user nodes. The distances between neighboring nodes are drawn from a uniform distribution between $0.2km$ to $0.3km$, unless otherwise stated. For the voltage regulation constraint in (3.3), $\epsilon = 0.03$ is selected. The real power consumption at each user node is constrained in

$[1kW, 3.5kW]$, and the corresponding power factor is considered to be 0.944 for all users. The constants in the objective function are set to $K_{u_i} = 1$ and $K_0 = N$. For the PV enabled nodes, the maximum apparent power capability is set to $s_w^{\max} = 1.1kW$, and is 10% greater than the maximum real power generation capacity of PV enabled nodes, i.e., $s_{w_i} = s_w^{\max} = 1.1w_i^{\max}$. Furthermore, four types of weather conditions are considered, namely, sunny, partly cloudy, cloudy, and intermittently changing, each corresponding to a different distribution from which w_i^m is drawn. For each of these weather types, w_i^m is selected randomly from a uniform distribution with lower and upper limits that span the designated intervals in Table. 3.4 in M scenarios. It is also assumed that the scenarios are equally probable with $\pi^m = \frac{1}{M}$.

Table 3.4: w_i^m Sample Space Based on the Weather Condition

Weather Condition	w_i^m sample space
Sunny	$[0.75w_i^{\max}, w_i^{\max}]$
Partly Cloudy	$[0.25w_i^{\max}, w_i^{\max}]$
Cloudy	$[0, 0.25w_i^{\max}]$
Intermittently Changing	$[0, w_i^{\max}]$

The effect of the number of scenarios on the solution is studied first. Specifically, Table 3.5 shows the objective value for different number of scenarios and for each type of weather. In these simulations, all the nodes are capable of PV generation (PV penetration level is 100 %), and the distances between nodes are constant and set to $0.2km$ to restrict randomness exclusively to weather. The table shows that roughly $M = 100$ scenarios are sufficient to achieve a stabilized objective value.

Next, the effect of the weather type and the penetration level (defined as the fraction of nodes having PV generation) on the total real power provided by the substation is investigated. The bar graph in Fig. 3.4 shows the expected value of P_0—that is, $\frac{1}{M}\sum_{m=1}^{M} P_0^m$—averaged over 10 simulation runs. For the case of 20% penetration, the nodes are randomly selected. The figure illustrates that

Table 3.5: Objective Value for Different Number of Scenarios in Four Types of Weather

Weather \ M	50	100	150	200
Sunny ($\times 10^7$)	0.0325	0.0327	0.0328	0.0325
Partly Cloudy($\times 10^7$)	0.4214	0.4224	0.4241	0.4211
Cloudy ($\times 10^7$)	1.2004	1.2022	1.2070	1.2064
Changing($\times 10^7$)	0.3846	0.3874	0.3901	0.3912

for a high level of PV penetration, less power is provided by the substation, and this effect is significantly more pronounced for sunny weather.

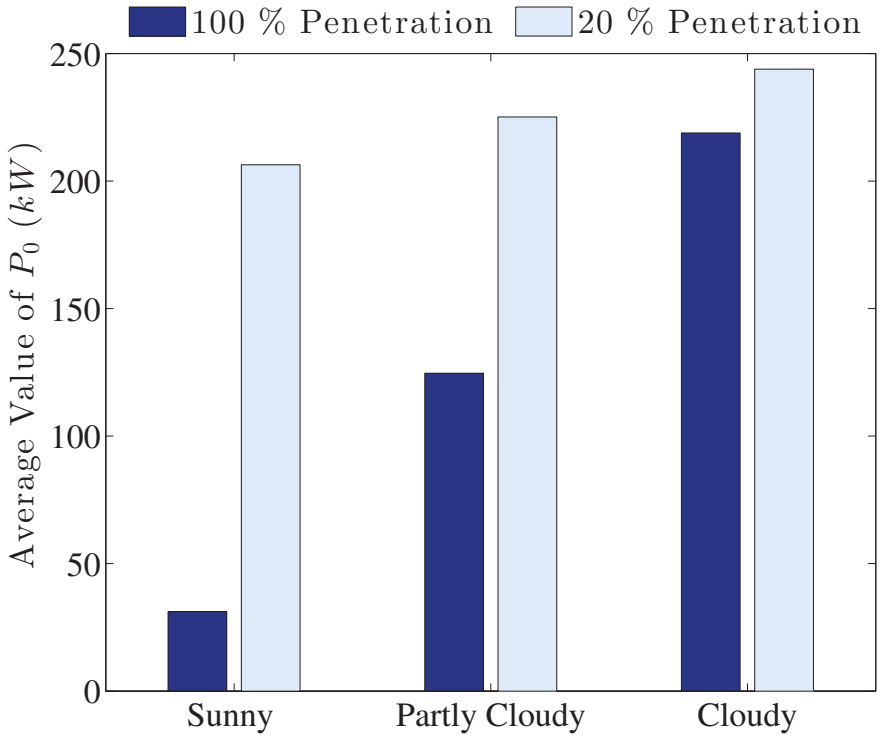

Figure 3.4: Value of $(1/M)\sum_{m=1}^{M} P_0^m$ (kW) averaged over 10 simulation runs, with $N = 100$ and $M = 200$, for three different weather types and two penetration levels.

The proposed stochastic programming approach is also compared to a local reactive power control scheme proposed in [7]. The scheme is local in the sense that it only relies on local variables w_i^m, p_{c_i}, and q_{c_i} to set $q_{w_i}^m = F_i(w_i^m, p_{c_i}, q_{c_i})$, where

$$F_i(w_i^m, p_{c_i}, q_{c_i}) = \text{Constr}_i \left[\text{K} F_i^{(L)} + (1 - \text{K}) F_i^{(V)} \right] \tag{3.13}$$

Table 3.6: Objective Values, Max Voltage Deviation and Average Voltage Deviation

Method	objective ($\times 10^7$)	$\max_{i,m} \frac{\lvert V_i^m - V0\rvert}{V0}$
Stoch. Progr.	1.0628	0.0300
$K = -5$	1.0645	0.0513
$K = -4$	1.0645	0.0513
$K = -3$	1.0645	0.0513
$K = -2$	1.0645	0.0513
$K = -1$	1.0646	0.0514
$K = 0$	1.0646	0.0514
$K = 1$	1.0646	0.0539
$K = 2$	1.0646	0.0572
$K = 3$	1.0646	0.0605
$K = 4$	1.0646	0.0638
$K = 5$	1.0646	0.0660

$$\mathrm{Constr}_i[q^m] = \begin{cases} q^m, & |q^m| \leq \sqrt{s_{w_i}^2 - (w_i^m)^2} \\ \frac{q^j}{|q^j|}\sqrt{s_{w_i}^2 - (w_i^m)^2}, & \text{otherwise} \end{cases}$$

$$F_i^{(L)} = \mathrm{Constr}_i(q_{c_i}), F_i^{(V)} = \mathrm{Constr}_i\left[q_{c_i} + \frac{x_i(p_{c_i} - w_i^m)}{r_i}\right]$$

Note that the previous control policy does not optimize p_{c_i} or q_{c_i}, but considers them given, while it depends on the parameter K [cf. (3.13)]. Upon setting $q_{w_i}^m$, the power flows P_i^m and Q_i^m as well as the voltages V_i^m can be found recursively using the `LinDistFlow` equations.

In order to compare with the previous control algorithm, first problem (F.1) is solved with

$N = 250$, $M = 100$, and PV penetration level of 20 %. This yields p_{c_i} and q_{c_i} values that can be used as inputs to the local control policy (3.13). Table 3.6 lists the objective value [cf. (3.10)] and maximum absolute voltage deviation achieved by the stochastic programming approach as well as by the local control policy for different values of K, averaged over 10 simulation runs.

The table reveals that the local control policy performs well in terms of the achieved objective value—which is largely due to the fact that the inputs to (3.13) are the optimal real power consumptions. The local control policy on the other hand performs poorly in terms of voltage regulation, which is depicted also in Fig. 3.5.

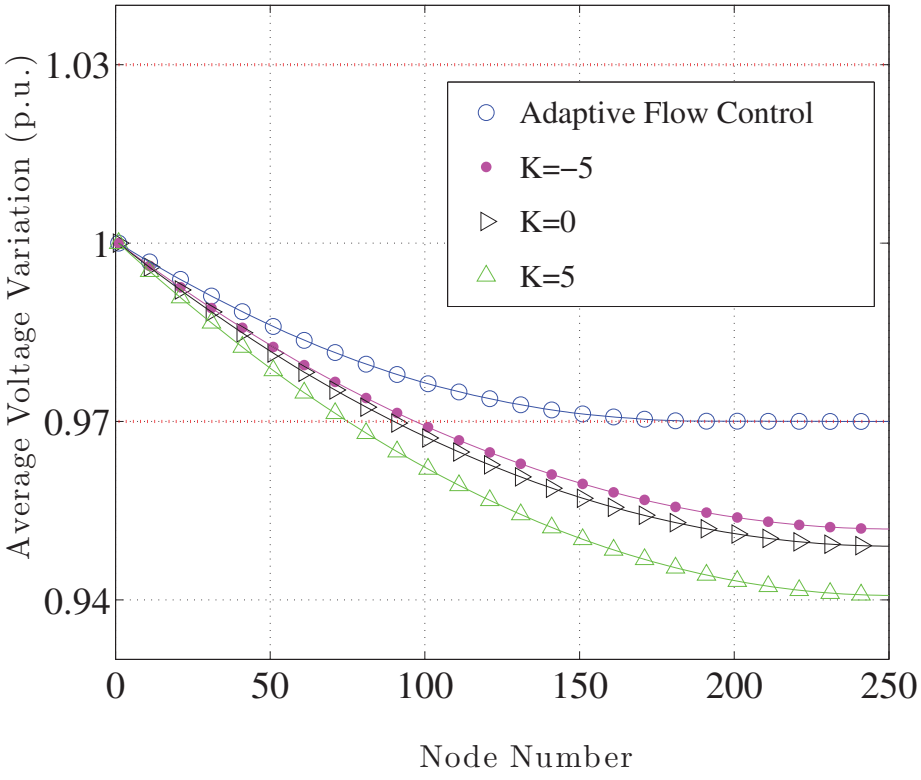

Figure 3.5: Average node voltages (i.e., $\frac{1}{M}\sum_{m=1}^{M} V_i^m$) averaged over 10 simulation runs, across $N = 250$ nodes for sunny weather type and with PV penetration level of 20 %.

3.3.2 Numerical tests with SOCP relaxation

The test circuit here is once again a single-feeder network similar to the one in the previous Subsection. The nominal substation voltage is $V_0 = 7.2$ (kV), and line impedance is $(0.33 + j0.38)\Omega/\mathrm{km}$. There are $N = 100$ user nodes and the distances between neighboring nodes is set to $d = 0.2$ (km). The maximum allowable voltage deviation from the nominal value at user nodes is set to $\epsilon = 0.05$ (p.u). Each user i requires a real power p_{c_i} that lies between the bounds shown in Fig. 3.6. Select nodes $\{5, 15, ..., 95\}$ are considered as the PV enabled nodes with real power generated following a uniform distribution from the intervals depicted also Fig. 3.6. The maximum apparent power capacity in this section is assigned to be $s_{w_i} = 40$ (kVA) which is relatively large compared to the maximum demand of each customer (i.e., $p_{c_i}^{\max}$). The intention here is to study the effect of large PV installations in select nodes on a typical distribution network.

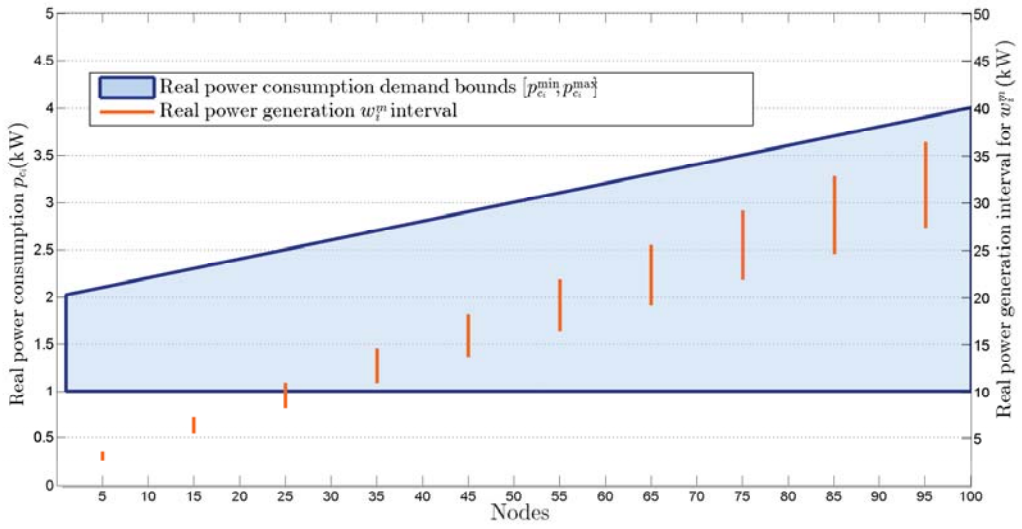

Figure 3.6: Power demand bounds $[p_{c_i}^{\min}, p_{c_i}^{\max}]$ by user nodes, and the intervals for real power generation by PV-enabled nodes

By implementing the algorithm outlined in Section 3.1 the optimal power consumption is determined and plotted for all the nodes in Fig. 3.7. It is observed that in the nodes closer to the substation where the PV generation capacity is low, the DSO optimally allocates minimum required power consumption $p_{c_i} = 1$(kW) to the users, however towards the terminal nodes, as the

generation level rises, the DSO manages to provide more satisfaction to the customer demands.

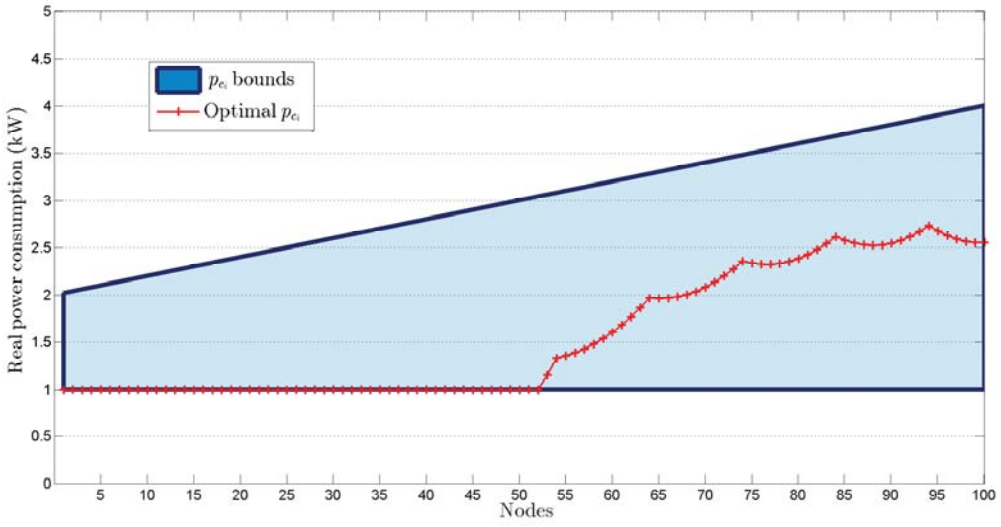

Figure 3.7: Optimal allocated power consumption p_{c_i} to the user nodes

Voltage variations across the network are also studied. Fig. 3.8 provides three plots for maximum voltage, minimum voltage and average voltages for all the scenarios across the user nodes. From the figure, it is observed that nodes close to PV generation are prone to voltage rise, whereas nodes far from PV generation are more likely to suffer from voltage drops.

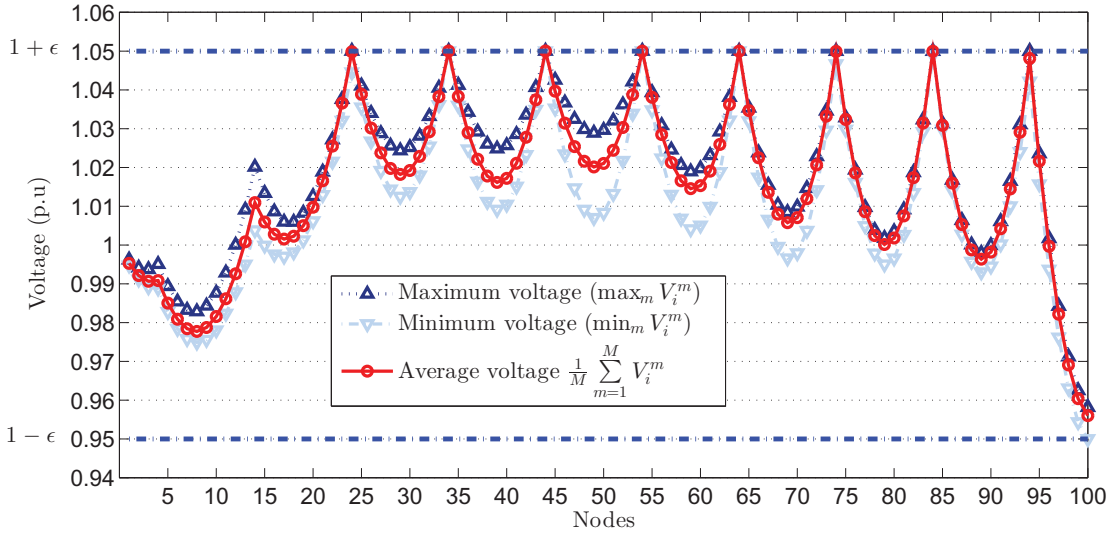

Figure 3.8: Maximum, minimum, and average voltage profile

Chapter 4: RISK-AVERSE VOLTAGE REGULATION AND POWER MANAGEMENT

4.1 Introduction

In the previous chapter, it was observed that local photovoltaic (PV) generation in electricity distribution networks imposes significant unforeseen variations on voltage levels thereby maintaining voltages close to their nominal values becomes a challenge. In an attempt to attain voltage regulation, PV inverters were permitted to inject or consume reactive power and end-user programmable loads with demand response capabilities allowed control of their real power consumption. However, voltage regulation was successfully obtained by *enforcing* voltage levels to be within an acceptable bound. The main drawback of performing voltage regulation through the use of strict constraints is that under certain circumstances the problem will turn out to be infeasible and thus there will be no option other than increasing the allowable margin prior to scheduling. The downside with the previously mentioned approach is that it will be exigent to find a margin suitable for a range of PV generation scenarios. An alternative attractive approach to voltage regulation could be to solve an optimization problem which incorporates an objective that in a way penalizes voltage deviations from the nominal value.

Due to the randomness in solar power generation and its effects on voltage levels, any objective function introduced for voltage regulation will need to account for the underlying uncertainty in voltage deviations. This chapter introduces one such objective. In particular, this chapter focuses on achieving voltage regulation through solving a stochastic program which penalizes a measure of risk known as the conditional-value-at-risk(CV@R) [21]. The CV@R is a conditional expectation of absolute voltage deviations being greater than a specific threshold.

By employing the CV@R of voltage deviations, the primary goal of this chapter is then to propose a risk-averse formulation for voltage regulation that performs real and reactive power management under uncertainty of PV power generation in radial distribution networks. Concretely,

in addition to the objectives in the previous chapter such as minimizing customer dissatisfaction, power generation costs, and power losses, the CV@R objective is included to evaluate the risk of having high values of absolute voltage deviations. The uncertainty in PV power generation is once again modeled with finite number of scenarios and a stochastic optimization program is formulated. The resulting minimization problem is a quadratic program with scenario-dependent decision variables which pertain to reactive power of PV inverters, and scenario-independent decisions variables which amount to the real power consumption in each node. To highlight the benefits of the approach, we also include a risk-neutral formulation which minimizes the expected value of absolute deviations instead of accounting for the risk of having high voltage variations.

4.2 Risk-averse voltage regulation

In the previous chapter, the objective considered minimization of the linear combination of three terms: thermal losses, the cost of providing power to the distribution system [i.e., $\mathrm{Cost}(P_0)$], as well as providing customer satisfaction. Voltage regulation was handled by enforcing constraint (3.6i). In this section, instead of enforcing such constraint, a fourth optimization goal is introduced which aims to reduce the voltage variation across the network.

Fluctuations in renewable energy generation by PV inverters (w_i) will cause random fluctuations on node voltages [see (3.8a)-(3.8c)]. The random variable capturing this voltage deviation for every node i from its nominal value is $|v_i - v_0|$. One natural objective for voltage regulation in node i can be to minimize the expected value of that random variable –that is, $E[|v_i - v_0|]$. In a distribution network, some voltage deviation from the nominal value may be tolerated; however, significant deviations from the nominal value should not occur often. A disadvantage of using the expected value as an objective for regulating voltage at node i is that in some unfavorable scenarios, it may allow significant deviations from the nominal value, only to make up for this in other scenarios which yield lower absolute deviation.

It would be interesting to have a formulation that can minimize a threshold so that for most cases the voltage deviation will be guaranteed to be less than that threshold. This formulation will

allow some deviations from the nominal value, however, it does not allow significant deviations to occur as often. In other words, a new objective can be used to measure the risk of having high voltage deviations and the new formulation can aim to minimize that risk.

4.2.1 Risk measures

For every user node i and its corresponding voltage level V_i, the α-V@R for voltage deviation is the minimum value of the absolute deviation of V_i from its nominal values V_0 such that the probability of the deviation being lower than or equal to this value is at least α.

$$e_\alpha := \min\{e \in \mathrm{R} : \mathrm{Prob}(|V_i - V_0| \leq e) \geq \alpha\}. \tag{4.1}$$

Typical values considered for α are 0.9, 0.95 and 0.99. Note that, if $v_i = V_i^2$ is used, such as in the SOCP formulation, then α-V@R will take the form :

$$e_\alpha := \min\{e \in \mathrm{R} : \mathrm{Prob}(|v_i - V_0^2| \leq e) \geq \alpha\}. \tag{4.2}$$

The conditional expectation of absolute voltage deviation the α-V@R is defined as the α-CV@R

$$\phi_\alpha(|V_i - V_0|) = E\big[|V_i - V_0| \mid |V_i - V_0| > e_\alpha\big] \tag{4.3}$$

and likewise for $v_i = V_i^2$

$$\phi_\alpha(|v_i - v_0|) = E\big[|v_i - v_0| \mid |v_i - v_0| > e_\alpha\big]. \tag{4.4}$$

In order to reduce the risk of high voltage deviations, initially one can choose to minimize the V@R which will ensure that for most scenarios the absolute voltage deviation is at its minimum. However, V@R lacks convexity which makes it a difficult objective to work with. On the other hand, CV@R can be shown to be convex, and the definitions guarantee that α-CV@R is always greater than or equal to α-V@R [21]; therefore, minimizing the α-CV@R ultimately results in

having low α-V@R's for voltage deviation as well. Since samples of random variable w_i (i.e. w_i^m) are known, by [21, Theorem 1], random variable $|V_i - V_0|$ or $|v_i - v_0|$ can be represented by its corresponding samples and α-CV@R can be approximated as:

$$\phi_\alpha(|V_i - V_0|) = \inf_{e_i}\{e_i + \frac{1}{1-\alpha}\sum_{m=1}^{M}\pi^m\big[|V_i^m - V_0| - e\big]^+\} \tag{4.5}$$

or

$$\phi_\alpha(|v_i - v_0|) = \inf_{e_i}\{e_i + \frac{1}{1-\alpha}\sum_{m=1}^{M}\pi^m\big[|v_i^m - v_0| - e\big]^+\} \tag{4.6}$$

where $[t]^+ = \max\{0, t\}$.

Equations (4.3) and (4.5) [or (4.4) and (4.6)] hold when the cumulative distribution function of $|V_i - V_0|$ (respectively of $|v_i - v_0|$) is continuous. In order to avoid mathematical complication, we assume that this is the case. (Even if this assumption does not hold, (4.5) is taken as the definition of CV@R, but the interpretation as conditional expectation needs to be modified [27, Sec. 6.2].)

In the next section, tree networks with SOCP relaxation and the the α-CV@R of v_i as an objective are considered first. A decentralized algorithm is also developed. A single-feeder network with the `LinDistFlow` approximations and the α-CV@R of V_i as objective are considered in Section 4.4. Numerical tests for tree networks and single-feeder networks, along with a comparison with a risk-neutral formulation are provided in Section 4.5.

4.3 Voltage regulation in tree networks with SOCP power flow equations

The problem at hand bears similarities to the one solved in the previous chapter, however the goal here is to minimize the linear combination of the previous objectives introduced in section 3.1.2 and the CV@R term (4.6). Minimizing the CV@R can be done by performing a joint minimization over v_i^m and e_i [21, Theorem 2]:

$$\min_{\mathbf{p_c},\mathbf{P_{0+}},\mathbf{P_{0-}},\mathbf{v},\mathbf{l},\mathbf{P},\mathbf{Q},\mathbf{q_w}} \sum_{i\in\mathcal{N}} K_{u_i}(p_{c_i}-p_{c_i}^{\max})^2 + \sum_{m=1}^{M} K_0(\pi^m)(P_{0+}^m)^2$$
$$+ K_{\text{Loss}} \sum_{i\in\mathcal{N}\setminus\{0\}} \sum_{m=1}^{M} \pi^m r_i l_i^m + \sum_{i\in\mathcal{N}\setminus\{0\}} \kappa_i\big(e_i + \frac{1}{1-\alpha_i}\sum_{m=1}^{M}\pi^m\big[|v_i^m - V_0^2| - e_i\big]^+\big) \quad (4.7)$$

subject to (3.6b)-(3.6h), (3.6d)-(3.6f) where $\kappa_i \geq 0$ is a weight.

By introducing an auxiliary decision variable f_i^m that upper bounds the term $|v_i^m - V_0^2| - e_i$ in the objective of (4.8a), we can write the *risk-averse* formulation as a quadratic program:

$$\min_{\mathbf{p_c},\mathbf{P_{0+}},\mathbf{P_{0-}},\mathbf{v},\mathbf{l},\mathbf{P},\mathbf{Q},\mathbf{q_w}} \sum_{i\in\mathcal{N}} K_{u_i}(p_{c_i}-p_{c_i}^{\max})^2 + \sum_{m=1}^{M} K_0(\pi^m)(P_{0+}^m)^2$$
$$+ K_{\text{Loss}} \sum_{i\in\mathcal{N}\setminus\{0\}} \sum_{m=1}^{M} \pi^m r_i l_i^m + \sum_{i\in\mathcal{N}\setminus\{0\}} \kappa_i\big(e_i(1-\alpha_i) + \sum_{m=1}^{M}\pi^m f_i^m\big) \quad (4.8a)$$

subject to

for $i \in \mathcal{N}$ and $m = 1, 2, ..., M$

$$P_i^m = \sum_{j\in C_i}(P_j^m + r_j l_j^m) + p_{c_i} - w_i^m \quad (4.8b)$$

$$Q_i^m = \sum_{j\in C_i}(Q_j^m + x_j l_j^m) + \sqrt{\frac{1}{\text{PF}_i^2} - 1}\, p_{c_i} - q_{w_i}^m \quad (4.8c)$$

$$p_{c_i}^{\min} \leq p_{c_i} \leq p_{c_i}^{\max} \quad (4.8d)$$

$$q_{w_i}^{\min} \leq q_{w_i}^m \leq q_{w_i}^{\max} \quad (4.8e)$$

$$P_0^m = P_{0+}^m - P_{0-}^m, P_{0+}^m \geq 0, P_{0-}^m \geq 0 \quad (4.8f)$$

for $i \in \mathcal{N}\setminus\{0\}$ and $m = 1, 2, ..., M$

$$v_{A_i}^m = v_i^m + 2(r_i P_i^m + x_i Q_i^m) + (r_i^2 + x_i^2) l_i^m i \quad (4.8g)$$

$$(P_i^m)^2 + (Q_i^m)^2 \leq v_i^m l_i^m,\ v_i^m \geq 0, l_i^m \geq 0 \quad (4.8h)$$

$$-e_i - f_i^m \leq v_i^m - V_0^2 \leq e_i + f_i^m, f_i^m \geq 0 \tag{4.8i}$$

Furthermore, in this formulation, the numerical instability of (4.7) due to the division by a small number $\big($i.e. $(1-\alpha_i)\big)$ is mitigated by multiplying the CV@R term in (4.8a) with $(1-\alpha_i)$ [21].

4.3.1 Decentralized algorithm

With variables similar to the ones explained in the previous chapter we can develop a decentralized algorithm based on the ADMM. To handle the two inequalities in (4.8i) which couple the variables v_i^m, f_i^m and e_i we introduce auxiliary variables $f_i^m, e_i^m, g_i^m, h_i^m$,$\tilde{f}_i^m, \tilde{e}_i, \tilde{g}_i^m, \tilde{h}_i^m$ and the following additional constraints:

$$f_i^m + e_i^m + v_i^m - V_0^2 - g_i^m = 0 \tag{4.9}$$

$$f_i^m + e_i^m - v_i^m + V_0^2 - h_i^m = 0 \tag{4.10}$$

$$\tilde{f}_i^m \geq 0, \tilde{e}_i \geq 0, \tilde{g}_i^m \geq 0, \tilde{h}_i^m \geq= 0 \tag{4.11}$$

$$f_i^m = \tilde{f}_i^m \tag{4.12}$$

$$e_i^m = \tilde{e}_i \tag{4.13}$$

$$g_i^m = \tilde{g}_i^m \tag{4.14}$$

$$h_i^m = \tilde{h}_i^m \tag{4.15}$$

Using these auxiliary variables and the ones provided in Chapter 3, the equivalent optimization problem can be formulated:

$$\min_{\substack{\mathbf{P},\hat{\mathbf{P}},\tilde{\mathbf{P}},\\ \mathbf{Q},\hat{\mathbf{Q}},\tilde{\mathbf{Q}},\\ \mathbf{v},\hat{\mathbf{v}},\tilde{\mathbf{v}}\\ \tilde{\mathbf{p}}_\mathbf{c},\mathbf{p_c},\mathbf{q}_w,\tilde{\mathbf{q}}_w\\ \mathbf{P_{0+}},\mathbf{P_{0-}},,\tilde{\mathbf{P}}_{\mathbf{0}+},\tilde{\mathbf{P}}_{0-}}} \sum_{i\in\mathcal{N}} K_{u_i}(\tilde{p}_{c_i} - p_{c_i}^{\max})^2 + \sum_{m=1}^{M} K_0(\pi^m)(P_{0+}^m)^2 + K_{\text{Loss}} \sum_{i\in\mathcal{N}\setminus\{0\}} \sum_{m=1}^{M} r_i l_i^m$$

$$+ \sum_{i\in\mathcal{N}\setminus\{0\}} \kappa_i\big(\tilde{e}_i(1-\alpha_i) + \sum_{m=1}^{M} \pi^m f_i^m\big) \tag{4.16a}$$

subject to

Coupling Constraints ($m = 1, 2, ..., M$):

$$\text{for } i \in \mathcal{N}\backslash\{0\}: \quad P_i^m = \tilde{P}_i^m \quad Q_i^m = \tilde{Q}_i^m \quad l_i^m = \tilde{l}_i^m \quad v_i^m = \tilde{v}_i^m \quad \hat{v}_j^m = \tilde{v}_{A_j}^m \tag{4.16b}$$

$$\text{for } i \in \mathcal{N}\backslash\{0\}: \quad e_i^m = \tilde{e}_i \quad f_i^m = \tilde{f}_i^m \quad g_i^m = \tilde{g}_i^m \quad h_i^m = \tilde{h}_i^m \tag{4.16c}$$

$$\text{for } i \in \mathcal{N},\ j \in \mathcal{C}_i: \quad \hat{P}_j^m = \tilde{P}_j^m \quad \hat{Q}_j^m = \tilde{Q}_j^m \quad \hat{l}_j^m = \tilde{l}_j^m \quad p_{c_i}^m = \tilde{p}_{c_i} \quad q_{w_i}^m = \tilde{q}_{w_i}^m \tag{4.16d}$$

$$\text{for } i = 0: \quad P_{0+}^m = \tilde{P}_{0+}^m \qquad P_{0-}^m = \tilde{P}_{0-}^m \tag{4.16e}$$

Individual Equality Constraints ($m = 1, 2, ..., M$):

$$\text{for } i \in \mathcal{N}: \quad P_i^m = \sum_{j \in \mathcal{C}_i} (\hat{P}_j^m + r_j \hat{l}_j^m) + p_{c_i}^m - w_i^m \tag{4.16f}$$

$$\text{for } i \in \mathcal{N}: \quad Q_i^m = \sum_{j \in \mathcal{C}_i} (\hat{Q}_j^m + x_j \hat{l}_j^m) + \sqrt{\frac{1}{\mathrm{PF}_i^2} - 1} p_{c_i}^m - q_{w_i}^m \tag{4.16g}$$

$$\text{for } i \in \mathcal{N}\backslash\{0\}: \quad \hat{v}_i = v_i^m + 2(r_i P_i^m + x_i Q_i^m) + (r_i^2 + x_i^2) l_i^m \tag{4.16h}$$

$$\text{for } i \in \mathcal{N}\backslash\{0\}: \quad f_i^m + e_i^m + v_i^m - V_0^2 - g_i^m = 0 \tag{4.16i}$$

$$\text{for } i \in \mathcal{N}\backslash\{0\}: \quad f_i^m + e_i^m - v_i^m + V_0^2 - h_i^m = 0 \tag{4.16j}$$

$$\text{for } i = 0: \quad P_0^m = P_{0+}^m - P_{0-}^m \tag{4.16k}$$

Individual Inequality Constraints ($m = 1, 2, ..., M$)

$$\text{for } i \in \mathcal{N}\backslash\{0\}: \quad (\tilde{P}_j^m)^2 + (\tilde{Q}_j^m)^2 \leq (\tilde{v}_j^m)(\tilde{l}_j^m) \quad \tilde{v}_i^m \geq 0, \tilde{l}_i^m \geq 0 \tag{4.16l}$$

$$\text{for } i \in \mathcal{N}\backslash\{0\}: \quad \tilde{e}_i \geq 0 \quad \tilde{f}_i^m \geq 0 \quad \tilde{g}_i^m \geq 0 \quad \tilde{h}_i^m \geq 0 \tag{4.16m}$$

$$\text{for } i \in \mathcal{N}: \quad p_{c_i}^{\min} \leq \tilde{p}_{c_i} \leq p_{c_i}^{\max} \tag{4.16n}$$

$$\text{for } i \in \mathcal{N}: \quad -\sqrt{s_{w_i}^2 - (w_i^m)^2} \leq \tilde{q}_{w_i}^m \leq \sqrt{s_{w_i}^2 - (w_i^m)^2} \tag{4.16o}$$

$$\text{for } i = 0: \quad \tilde{P}_{0+}^m \geq 0, \tilde{P}_{0-}^m \geq 0 \tag{4.16p}$$

The problem (4.16) is equivalent to (4.8) however it has the advantage of being in the form of problem (B.1) in Appendix B and can be solved via the ADMM. The purpose of introducing $\hat{P}_j^m$,$\hat{Q}_j^m$,$\hat{l}_j^m$ is to bypass the need to know P_j^m,Q_j^m and l_j^m of child node $j \in \mathcal{C}_i$ on its ancestor node i. The total number of these copies per scenario is N. Variable $\hat{v}_i^m$ is also introduced to represent the copy of voltage node A_i on node i. Again, since only the root does not have an ancestor, there are exactly N copies of this variable per scenario. The *Tilde* variables, $\tilde{P}_i^m$, $\tilde{Q}_i^m$, $\tilde{l}_i^m$, and $\tilde{v}_i^m$ for all $n \in \mathcal{N}$ and $m \in \{1, 2, ..., M\}$ provide the opportunity to handle equality constraints separate from the inequality constraints, yielding closed-form updates (the same role as in problem (3.7))

Table 4.1: Variables

	Nodes involved	Variables
$\mathbf{x}_0^m$	Root and its children $j \in \mathcal{C}_0$	$\{P_0^m, Q_0^m, P_{0+}^m, P_{0-}^m, \hat{P}_j^m, \hat{Q}_j^m, \hat{l}_j^m, p_{c_0}^m, q_{w_0}^m\}$
$\mathbf{x}_i^m$	Neither root nor leaf	$\{P_i^m, Q_i^m, v_i^m, l_i^m, \hat{P}_j^m, \hat{Q}_j^m, \hat{v}_i^m, p_{c_i}^m, q_{w_i}^m, f_i^m, e_i^m, g_i^m, h_i^m\}$
$\mathbf{x}_i^m$	Leaf	$\{P_i^m, Q_i^m, v_i^m, l_i^m, \hat{v}_i^m, p_{c_i}^m, q_{w_i}^m, f_i^m, e_i^m, g_i^m, h_i^m\}$
$\mathbf{x}_i$	All nodes	$\{\mathbf{x}_i^m\}_{m=1}^M$
$\mathbf{z}_0^m$	Root	$\{\tilde{P}_{0+}^m, \tilde{P}_{0-}^m, \tilde{q}_{w_0}^m\}$
$\mathbf{z}_0$	Root	$\{\{\mathbf{z}_0^m\}_{m=1}^M, \tilde{p}_{c_0}\}$
$\mathbf{z}_i^m$	Not root	$\{\tilde{P}_i^m, \tilde{Q}_i^m, \tilde{v}_i^m, \tilde{l}_i^m, \tilde{q}_{w_i}^m, \tilde{f}_i^m, \tilde{g}_i^m, \tilde{h}_i^m\}$
$\mathbf{z}_i$	Not root	$\{\{\mathbf{z}_i^m\}_{m=1}^M, \tilde{p}_{c_i}, \tilde{e}_i\}$

4.3.2 Algorithm and communication requirements

The augmented Lagrangian and the derivation of closed-form updates for every variable per node and per scenario is similar to the algorithm described in the previous chapter with steps that follow the same routine detailed in Appendix C. Furthermore, since the newly introduced variables in this formulation (i.e., $f_i^m, e_i^m, g_i^m, h_i^m, \tilde{f}_i^m, \tilde{e}_i, \tilde{g}_i^m$ and $\tilde{h}_i^m$) are all local, the communication requirements of this algorithm is exactly the same as the one described in Chapter 3.

4.4 Voltage regulation in single-feeder networks with `LinDistFlow`

Considering the single-feeder network of Fig. 3.2, the goal is to minimize the linear combination of the objectives introduced in Sec. 3.2.1 and the CV@R in (4.5). Once again, as per [21, Th. 2],

Table 4.2: Lagrange Multipliers

Equality Constraint	Lagrange Multiplier
$P_i^m = \tilde{P}_i^m$	λ_i^m
$Q_i^m = \tilde{Q}_i^m$	μ_i^m
$l_i^m = \tilde{l}_i^m$	γ_i^m
$v_i^m = \tilde{v}_i^m$	ω_i^m
$\hat{v}_j^m = \tilde{v}_{A_j}^m$	$\hat{\omega}_j^m$
$e_i^m = \tilde{e}_i$	$\omega_{e_i}^m$
$f_i^m = \tilde{f}_i^m$	$\omega_{f_i}^m$
$g_i^m = \tilde{g}_i^m$	$\omega_{g_i}^m$
$h_i^m = \tilde{h}_i^m$	$\omega_{h_i}^m$
$\hat{P}_j^m = \tilde{P}_{j\in\mathcal{C}_i}$	$\hat{\lambda}_j^m$
$\hat{Q}_j^m = \tilde{Q}_{j\in\mathcal{C}_i}$	$\hat{\mu}_j^m$
$\hat{l}_j^m = \tilde{l}_{j\in\mathcal{C}_i}$	$\hat{\gamma}_j^m$
$p_{c_i}^m = \tilde{p}_{c_i}$	η_i^m
$q_{w_i}^m = \tilde{q}_{w_i}^m$	θ_i^m
$P_{0+}^m = \tilde{P}_{0+} i^m$	ζ_+^m
$P_{0-}^m = \tilde{P}_{0-} i^m$	ζ_-^m

minimizing the CV@R can be done by performing a joint minimization over V_i^m and e_i [cf. (4.5)]; putting everything together, the real and reactive power management problem with risk-averse voltage regulation is

$$\begin{aligned}\min_{\mathbf{p}_c,\mathbf{q}_c,\mathbf{q}_w,\mathbf{P},\mathbf{Q},\mathbf{v},\mathbf{e}} \quad & \sum_{i=1}^{N} K_{u_i}(p_{c_i} - p_{c_i}^{\max})^2 + \sum_{m=1}^{M} \pi^m \mathrm{Cost}(\mathrm{P}_0^{\mathrm{m}}) \\ & + \sum_{i=1}^{N} K_{\mathrm{Loss}} r_i \sum_{m=1}^{M} \pi^m \frac{(P_i^m)^2 + (Q_i^m)^2}{V_0^2} \\ & + \sum_{i=1}^{N} \kappa_i \left(e_i + \frac{1}{1-\alpha_i} \sum_{m=1}^{M} \pi^m \left[|V_i^m - V_0| - e \right]^+ \right) \end{aligned} \tag{4.17}$$

subject to (3.8a)-(3.8f), where vectors $\mathbf{p}_c, \mathbf{q}_c, \mathbf{q}_w, \mathbf{P}, \mathbf{Q}, \mathbf{V}, \mathbf{e}$ collect respectively p_{c_i}, q_{c_i}, $q_{w_i}^m$, P_i^m, Q_i^m, V_i^m, and e_i for all i and m, and $\kappa_i \geq 0$ are weights.

Upon introducing an auxiliary decision variable f_i^m that upper bounds the term $[|V_i^m - V_0| - e_i]^+$

in (4.17), the problem can be written as a convex quadratic program:

$$\text{Risk} - \text{Averse Formulation}$$

$$\begin{aligned}\min_{\mathbf{p}_c,\mathbf{q}_c,\mathbf{q}_w,\mathbf{P},\mathbf{Q},\mathbf{v},\mathbf{e},\mathbf{f},\mathbf{P}_{0+},\mathbf{P}_{0-}} & \sum_{i=1}^{N} K_{u_i}(p_{c_i} - p_{c_i}^{\max})^2 + \sum_{m=1}^{M} \pi^m K_0 (P_{0+}^m)^2 \\ & + \sum_{i=1}^{N} K_{\text{Loss}} r_i \sum_{m=1}^{M} \pi^m \frac{(P_i^m)^2 + (Q_i^m)^2}{V_0^2} \\ & + \sum_{i=1}^{N} \kappa_i \left(e_i + \frac{1}{1-\alpha_i} \sum_{m=1}^{M} \pi^m f_i^m \right) \end{aligned} \tag{4.18a}$$

subject to

for $i \in \{0, 1, 2, ..., N-1\}$:

$$P_i^m = P_{i+1}^m + p_{c_i} - w_i^m \tag{4.18b}$$

$$Q_i^m = Q_{i+1}^m + \sqrt{\frac{1}{\text{PF}_i^2} - 1} p_{c_i} - q_{w_i}^m \tag{4.18c}$$

$$V_{i+1}^m = V_i^m - \frac{r_{i+1} P_{i+1}^m + x_{i+1} Q_{i+1}^m}{1000 V_0^2} \tag{4.18d}$$

for $i \in \{1, 2, ..., N\}$:

$$-e_i - f_i^m \leq v_i^m - v_0 \leq e_i + f_i^m,\ f_i^m \geq 0; \tag{4.18e}$$

and also the terminal conditions:

$$P_N^m = p_{c_N} - w_N^m \tag{4.18f}$$

$$Q_N^m = \sqrt{\frac{1}{\text{PF}_N^2} - 1} p_{c_N} - q_{w_N}^m \tag{4.18g}$$

$$V_0^m = 1. \tag{4.18h}$$

$$P_0^m = P_{0+}^m - P_{0-}^m,\ P_{0+}^m \geq 0,\ P_{0-}^m \geq 0, \tag{4.18i}$$

Formulation (4.18) has the property that the optimal α_i-V@R of $|V_i - V_0|$ is given by the optimal e_i^*,

while the optimal α_i-CV@R emerges as the optimal value of the last term in parenthesis in (4.18a). That is,

$$E\big[|V_i - V_0| \,\big|\, |V_i - V_0| > e_i^*\big] = e_i^* + \frac{1}{1-\alpha_i}\sum_{m=1}^{M} \pi^m f_i^{m*} \tag{4.19}$$

$$\text{Prob}[|V_i - V_0| \leq e_i^*] \geq \alpha. \tag{4.20}$$

In the numerical tests, the empirical counterparts of the left-hand sides of (4.19) and (4.20) (obtained using optimal solution $\{V_i^{m*}\}_{m=1}^{M}$) are found to match their theoretical values.

For comparison, the problem with the objective of minimizing the average absolute deviations is also considered. This problem is referred to as risk-neutral formulation and is stated as

$$\begin{aligned}
&\text{Risk} - \text{Neutral Formulation} \\
&\min_{\mathbf{p}_c,\mathbf{q}_c,\mathbf{q}_w,\mathbf{P},\mathbf{Q},\mathbf{v},\mathbf{P}_{0+},\mathbf{P}_{0-}} \sum_{i=1}^{N} K_{u_i}(p_{c_i} - p_{c_i}^{\max})^2 + \sum_{m=1}^{M} K_0 \pi^m (P_{0+}^m)^2 \\
&\qquad + \sum_{i=0}^{N-1} K_{\text{loss}} r_i \sum_{m=1}^{M} \pi^m \frac{(P_i^m)^2 + (Q_i^m)^2}{V_0^2} \\
&\qquad + \sum_{i=1}^{N} \kappa_i \sum_{m=1}^{M} \pi^m |V_i^m - V_0| \qquad (4.21) \\
&\text{subject to (4.18b)– (4.18i)}
\end{aligned}$$

and is also a quadratic optimization problem.

4.5 Numerical tests

4.5.1 Tree network with SOCP approximation

In this section numerical experiments are conducted on a residential scale distribution network with a tree configuration and $N = 250$ user nodes, as depicted in Fig. 4.1. Nodes $1, 2, ..., 100$ form the main branch and the two laterals branch off from nodes 74 and 75 respectively. Each nodes'

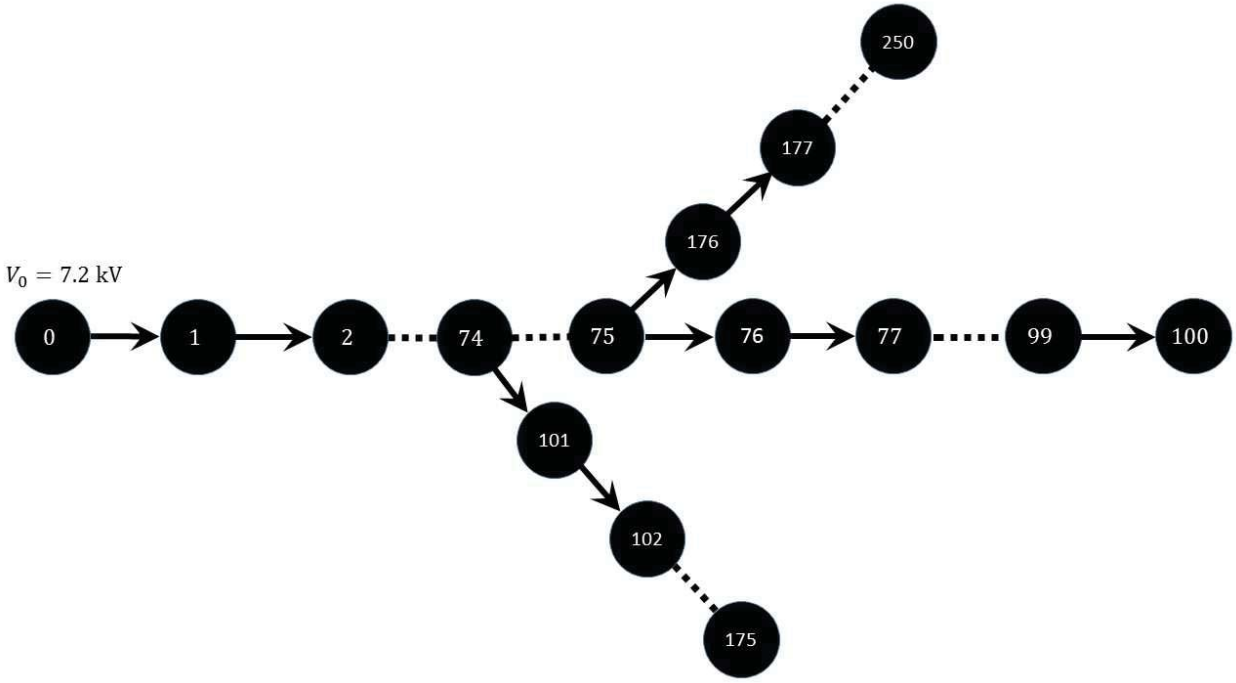

Figure 4.1: A tree network with one main branch and two laterals

load demand p_{c_i} is constrained by the interval $[p_{c_i}^{\min}, p_{c_i}^{\max}] = [1, 4]$ (kW) with PF $= 0.944$. Nodes $i \in \{0, 10, ..., 240\}$ are selected to be capable of PV generation which yields the penetration level of 10 %. For these PV-enabled nodes $s_{w_i} = 50$ (kW) and $w_i^{\max} = \frac{s_{w_i}}{1.1}$. There are $M = 100$ equally probable scenarios considered, and w_i^m which is the real power actually generated by the PV units is sampled from a uniform distribution in the interval $[0.75w_i^{\max}, w_i^{\max}]$ corresponding to a sunny day (see Table. 3.4). The nominal voltage at the substation is $V_0 = 7.2$ (kV), and the lines have impedance $r + jx = (0.33 + j0.38) \times d$ where $d = 200$(m) is considered fixed to ensure that randomness is only due to the renewable power generation. For this network, optimization problem(4.8) is solved with the decentralized algorithm described in section 4.3.1, with weight parameters $K_{u_i} = 1$,$K_0 = M$,$K_{\text{Loss}} = 1$ and $\kappa_i = 10$ for all nodes. The quantities α_i is considered to be 0.9–which means that after solving the problem, we should expect approximately that 90 % of the determined squared voltage deviations $|v_i^m - v_0|$ are less than or equal to the determined optimal e_i^* which is the 0.9-V@R[1]

[1]The ADMM algorithm converges once the primal and dual residuals go below an acceptable tolerance level [cf. (B.4)]. The greatest relative tolerance in these simulations was considered to be 0.01. This means that the optimal e_i^*

According to (4.2), the minimum margin for which the probability of $|v_i - v_0|$ being smaller than margin is 90% is equal to the 90%-V@R. The 90%-V@R is the optimal e_i^* which is determined by the algorithm. Fig. 4.2 shows the empirical probability that $\text{Prob}(|v_i - v_0| \leq e_i)$, calculated as number of scenarios for which the inequality $|v_i^m - v_0| \leq e_i$ holds divided by M. Four different values of e_i, namely $e_i = e_i^* + 0.002$,$e_i = e_i^* + 0.001$,$e_i = e_i^*$ and $e_i = e_i^* - 0.01$ are considered. The figure experimentally proves that for e_i^*, $\text{Prob}(|v_i - v_0| \leq e_i^*) \approx \alpha_i = 0.9$

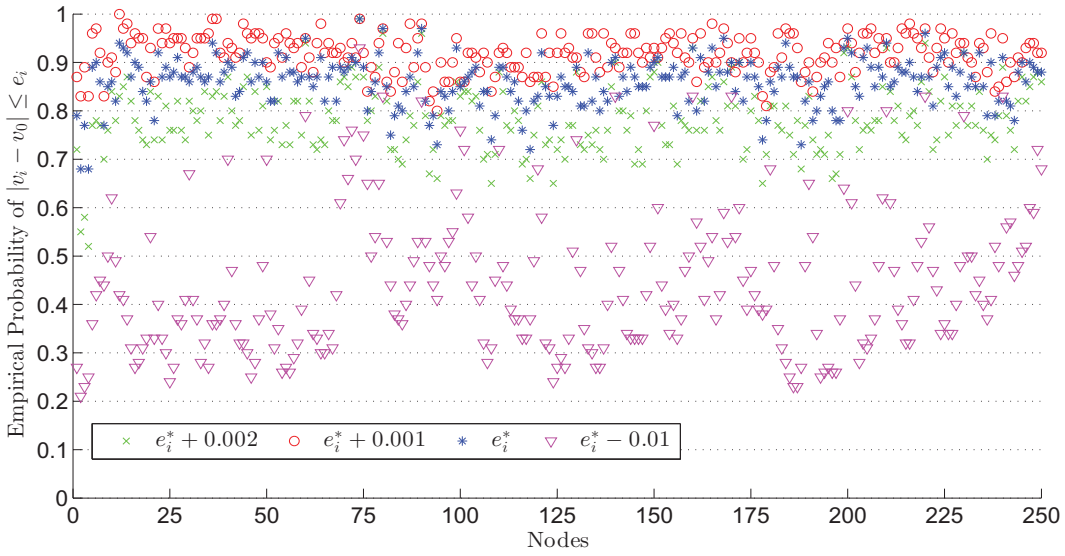

Figure 4.2: Empirical probability calculated as the number of scenarios for which $|v_i^m - v_0| \leq e_i$ divided by M. Four values of e_i, namely $e_i = e_i^* + 0.002$, $e_i = e_i^* + 0.001$, $e_i = e_i^*$, and $e_i = e_i^* - 0.01$ are considered for $\alpha_i = 0.9$ and for all nodes. Notice for $e_i \to e_i^{*+}$, almost 90% of node voltages are within the e_i-margin

Voltage variation across the nodes is also depicted in Fig. 4.3. In this setup, it turns out that the network experiences high voltage drop in many nodes. An interesting fact observed is that the branching nodes (i.e, nodes 74 and 75) are susceptible to large voltage drops implying the huge consumption burdened on these nodes due to the laterals. Notice though that the formulation only guarantees to provide a threshold such that in 90 % of cases node voltages are expected to fall

determined by the algorithm may be slightly different from the actual optimal e_i^*. Therefore, in addition to e_i^* found by the algorithm, two additional values of e_i namely, $e_i^* + 0.001$ and $e_i^* + 0.002$ were considered as possible candidates. In the simulations, the minimum calculated e_i^* was 2.53. Therefore even if we consider $e_i^* + 0.002$, the relative accuracy would be $\frac{0.002}{2.53} \approx 7.9e-4$ which is much lower than the relative tolerance of 0.01 for the simulations.

within that margin.

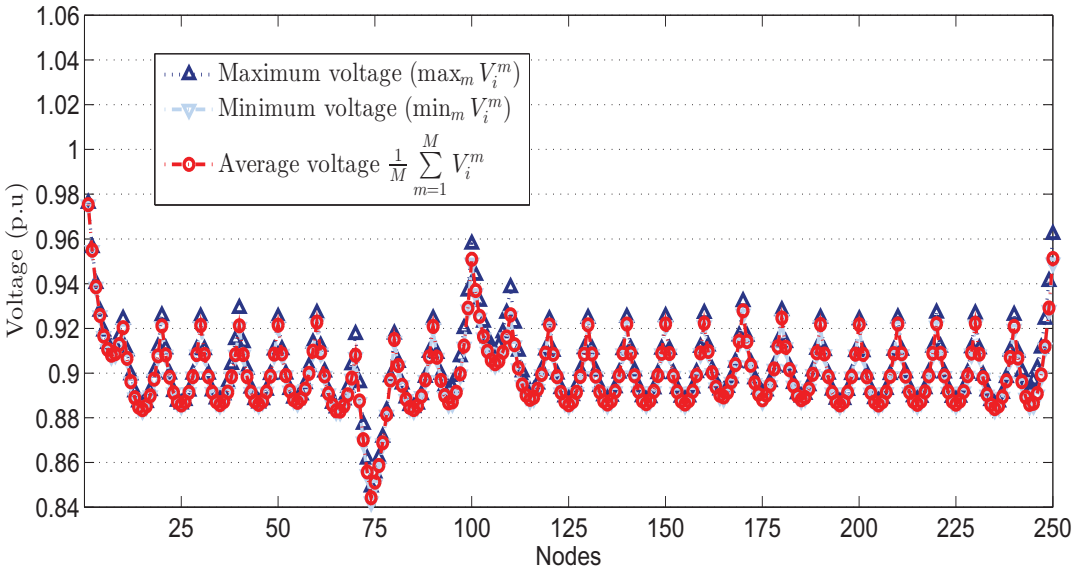

Figure 4.3: Maximum, minimum and average voltage profile

4.5.2 Single-feeder network with `LinDistFlow`

Numerical experiments are conducted on a residential distribution network as the one in Fig. 3.2 with $N = 100$ users connected to the main feeder. Each user demands load $p_{c_i} \in [p_c^{\min}, p_c^{\max}] = [10, 40]$ (kW) with $\mathrm{PF}_i = 0.944$. For user nodes capable of PV generation, the maximum apparent power generation capacity s_{w_i} is set to the same value for all i (given shortly). The maximum real power generation capacity ${w_i}^{\max}$ are related to s_{w_i} through ${w_i}^{\max} = s_{w_i}/1.1$, following [7]. If a user node does not have PV generation, then $s_{w_i} = 0$ and $w_i^{\max} = 0$. For buses with PV inverters, $M = 100$ scenarios are considered; and in scenario m, w_i^m is sampled from a uniform distribution in the interval $[0.75 w_i^{\max}, w_i^{\max}]$ to represent a relatively sunny day. The nominal voltage at the substation is $V_0 = 7.2$ (kV), while $r + jx = (0.33 + j0.38) \times d$ where d is the distance between nodes. This distance is set to $d = 200(\mathrm{m})$ to ensure that randomness is only due to renewable power generation. The scenarios are considered to be equally probable, that is, $\pi^m = \frac{1}{M}$. Throughout the simulations, the quantities α_i and weights κ_i are selected to be equal for all nodes. In the objective function, $K_{u_i} = 0.001$, $K_0 = 0.01$ and $K_{\mathrm{Loss}} = 0.01$. All optimization problems are solved using

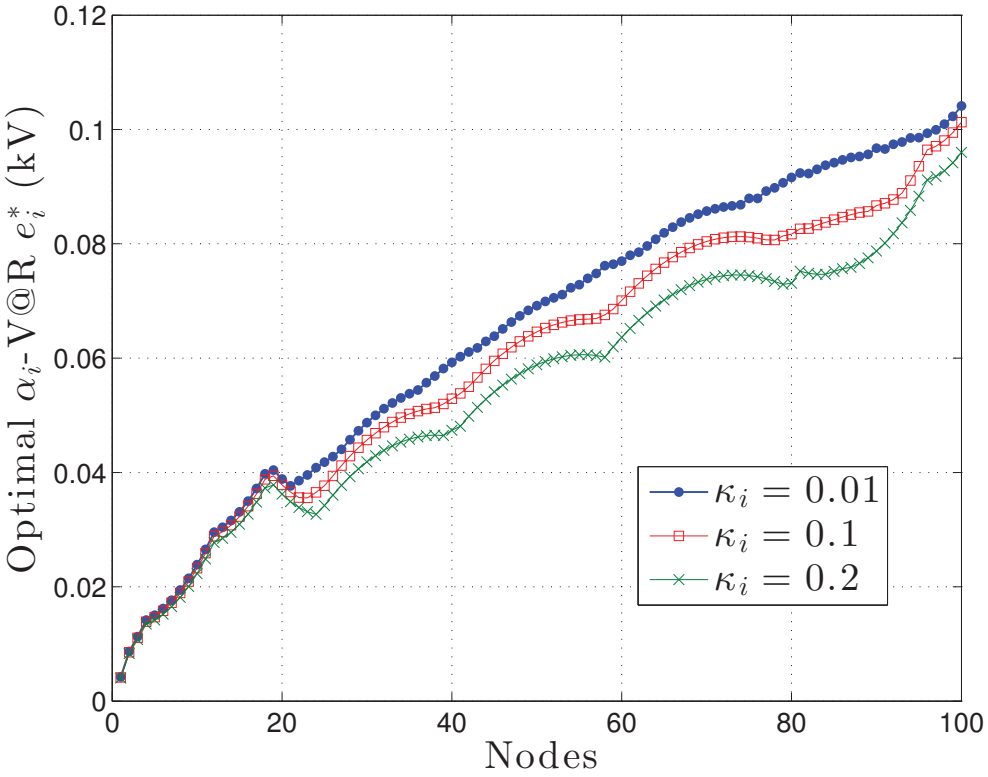

Figure 4.4: Optimal α-V@R for different κ_i.

the CVX toolbox in Matlab with solver SDPT3 [28, 29].

The risk-averse formulation is investigated first. In this set of simulations, only 10 % of user nodes (randomly selected) are capable of PV generation with $s_{w_i} = 250$ (kVA), while α_i=0.9 is selected. Fig. 4.4 shows α-V@R—which is the optimal e_i^* in (4.18)—for different values of κ_i.

Fig. 4.5 depicts the α-CV@R evaluated as sample conditional expectation [cf. (4.19)], that is, the sample average of $|V_i^{m*} - V_0|$ accounting only those scenarios that satisfy $|V_i^{m*} - V_0| > e_i^*$. The absolute difference between the left- and right-hand sides of (4.19) was found to be less than 0.3% of V_0 for all values of κ_i. It is seen from Fig. 4.4 and 4.5 that increasing κ_i puts emphasis on decreasing the corresponding α-V@R and α-CV@R. Fig. 4.6 shows the empirical probability that the absolute voltage deviation is at most α-V@R, calculated as the number of scenarios for which $|V_i^{m*} - V_0| \leq e_i^*$, divided by M. This probability matches the selected $\alpha = 0.9$.

Comparison of results obtained with the risk-averse and risk-neutral formulations is presented next. For these simulations, the number of nodes with PV generation is increased from 10 % to

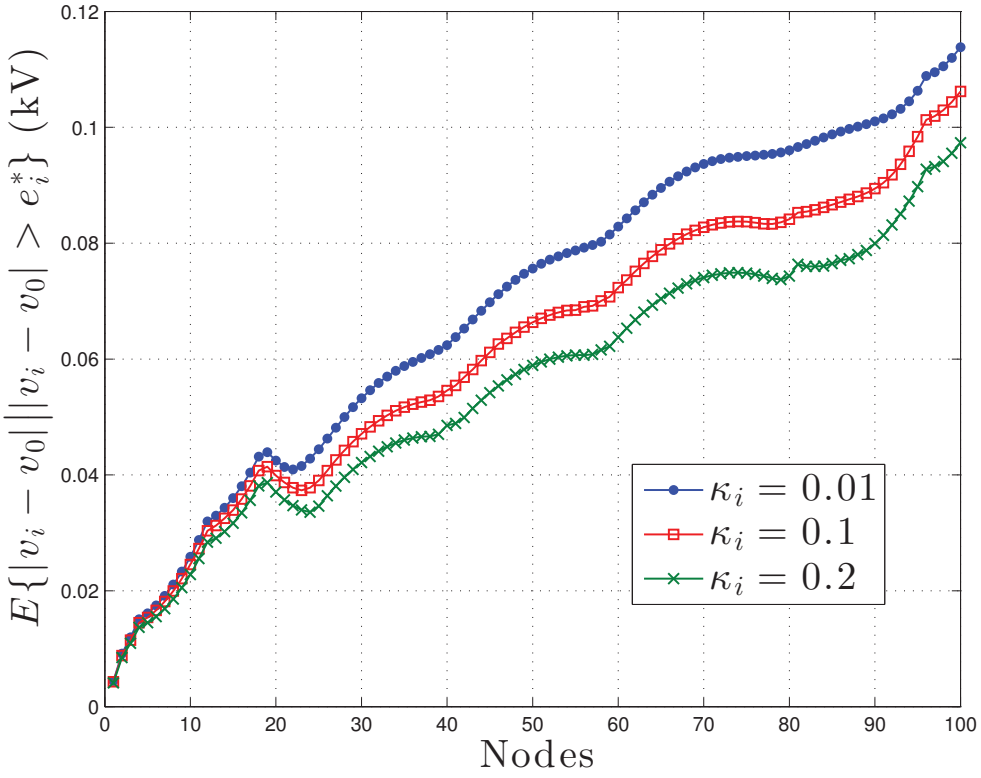

Figure 4.5: α-CV@R for different κ_i obtained using $\{V_i^{m*}\}_{m=1}^{M}$.

50 %, however maximum apparent power is reduced to $s_{w_i} = 50$ (kVA), while $\kappa_i = 1$ in both problems, and $\alpha_i = 0.8$ for the risk-averse problem. Optimal values for both problems are listed in Table 4.3.

It can be observed that the risk-neutral formulation achieves lower cost terms for the system. However, this superior performance comes at the cost of poor voltage regulation. Specifically, Fig. 4.7 and 4.8 respectively show the expected value and standard deviation of the absolute voltage deviation normalized by the nominal voltage V_0. These measures are smaller under the the risk-averse formulation as compared to the corresponding ones of the risk-neutral formulation.

Table 4.3: Objective Values of Risk-Averse and Risk-Neutral Problems

Problem / Obj	CV@R	Risk Neutral
Utility $\times K_i$	51.0936	51.0397
$K_0 \times$ Cost(P_0)	2.8681	2.6748
$K_{\text{loss}} \times$Line Losses	17.0770	15.9992

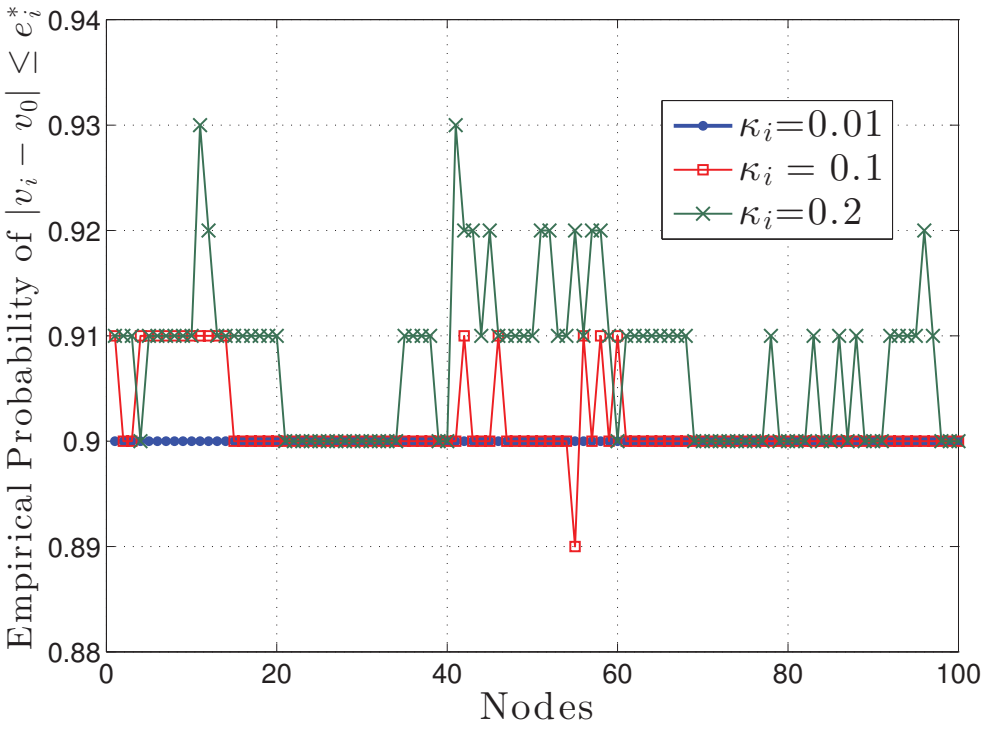

Figure 4.6: Empirical probability calculated as the number of scenarios for which $|V_i^{m*} - V_0| \leq e_i^*$ divided by M for different κ_i.

To further illustrate the effect of the CV@R objective in shaping the distribution of $|V_i - V_0|$, Fig. 4.9 shows the empirical cumulative distribution function of $|V_N - V_0|$ (obtained from the optimal voltages $\{V_N^{m*}\}_{m=1}^M$ at the terminal node). The CV@R objective guarantees that for $\alpha = 80\%$ of the scenarios the deviation of the terminal node voltage from the nominal value is below the optimal α-V@R. For all scenarios, the deviation of the terminal node voltage from V_0 is below $0.01V_0$. On the other hand, the risk-neutral formulation provides no such guarantee, and the absolute deviation of V_N from V_0 can be greater than $0.01V_0$ for many scenarios.

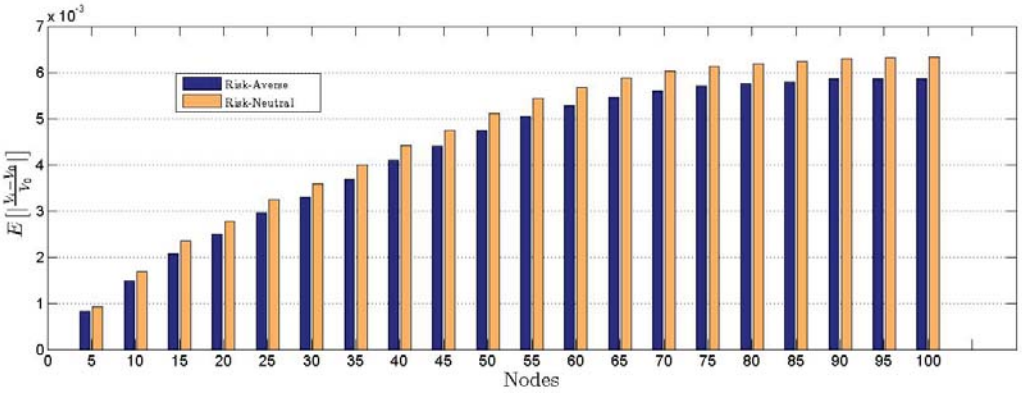

Figure 4.7: Optimal expected value of absolute voltage deviation in risk-averse and risk-neutral problems obtained using $\{V_i^{m*}\}_{m=1}^{M}$.

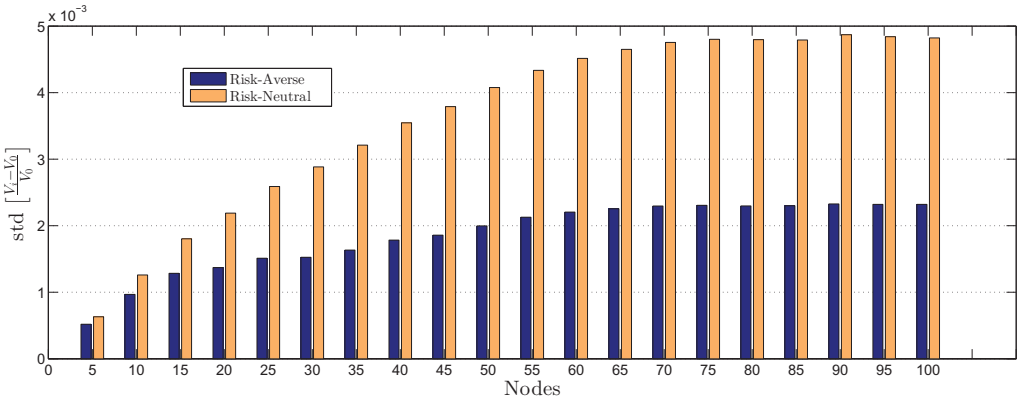

Figure 4.8: Optimal standard deviation of absolute voltage deviation in risk-averse and risk-neutral problems obtained using $\{V_i^{m*}\}_{m=1}^{M}$.

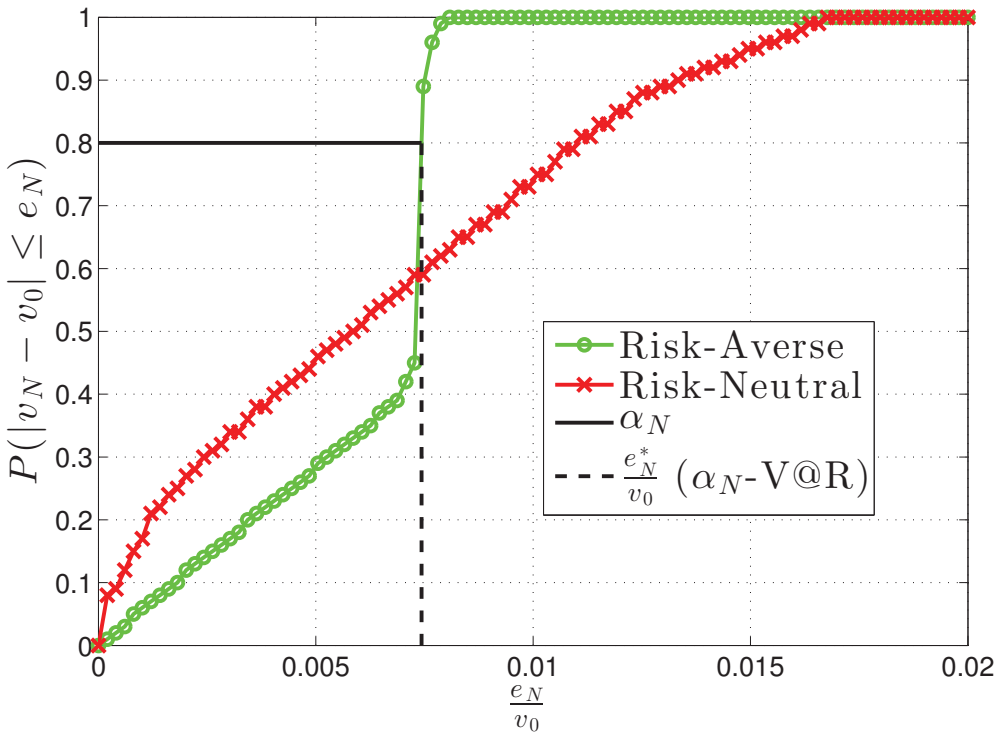

Figure 4.9: Empirical cumulative distribution function of terminal node voltage in risk-averse and risk-neutral problems obtained from samples $|V_N^{m*} - V_0| \leq e_i$ divided by M

Chapter 5: SUMMARY AND FUTURE DIRECTIONS

This thesis focused on leveraging stochastic programming tools for power management in distribution networks featuring high penetration of renewable solar photovoltaic generation and controllable loads. The introduction of PV generation in distribution networks offers production of green electric energy and lessens transmission thermal losses by reducing the distance between the place of generation and consumers. There are two chief challenges in integrating distributed PV generation into current residential distribution networks. First, due to the unpredictable patterns in weather conditions yielding unforeseen shortfalls in electricity production levels from these sources throughout the day, there is a risk of inadequate generation with respect to customer demand. Second, uncertainty in PV generation results in alteration of voltage levels across the network, rendering voltage regulation a daunting task.

Recently, demand response has been made possible by programmable loads which can adjust their real power consumption. This technology blended with advancements in power electronics which have enabled PV inverters to generate or consume reactive power offers an opportunity to overcome the two challenges previously mentioned. Demand response amounts to adjusting customer demand while there are generation fluctuations and reactive power control aids in reducing thermal losses and maintaining voltage constraints.

In this thesis, after reviewing power flow equations in tree distribution networks, and introducing models for programmable loads and PV injection, a stochastic program was formulated with the aim of minimizing customer dissatisfaction, cost of power provision, and thermal losses. The decision variables in this optimization problem were the real power consumption of programmable loads and reactive power portion of PV inverters. The uncertainty inherent in PV generation was modeled by a finite number of scenarios in each of which the value of generation was assumed to be known. Accounting for uncertainty rendered the power flow equations to be scenario dependent. Real power consumption of consumers were scenario independent, while reactive power injection or consumption of PV inverters depended on the solar generation scenario.

Voltage regulation, which is the task of maintaining voltages across the distribution network close to the nominal value of the substation voltage, was accomplished in two ways. The first method enforces every node voltage in the system to be within a specific region for every possible generation scenario and was the theme of Chapter 3. The second approach entails minimizing the CV@R of voltage deviations from the nominal value in Chapter 4. The proposed models were tested on single-feeder distribution networks to show the advantages of this formulations as opposed to the suggested alternatives.

Another focus of this thesis was to develop decentralized algorithms for solving the previously mentioned stochastic optimization problems. In distribution networks with large number of nodes, a centralized approach requires communicating all parameters and variables to a central agent, which entails large overhead and can be prone to errors in case of communication failures.The decentralized algorithm developed in this thesis has the desirable attribute that only neighbors need to exchange information, thereby reducing the communication overhead. The algorithm was based the alternating direction method of multipliers. In order to utilize ADMM, appropriate reformulations of the stochastic optimization problems with judiciously selected auxiliary variables were developed. The upshot was that, in each update of the ADMM, the minimization problems were solvable in closed form, and decomposition was achieved both per node and per scenario for scenario dependent variables.

The work in this thesis can be extended in several directions, which are listed next:

- **Exact power flow equations:** In Chapter 2, the power flow equations were detailed. These equations were non-convex, and linear and SOCP approximations were pursued in this thesis. One direction of research is to develop decentralized algorithms that utilize exact power flow equations without any approximations.

- **Inverter sizing:** In Chapter 2, while introducing the PV inverter model, it was assumed that the inverters have a nameplate capacity s_{w_i}. The research issue here is to determine appropriate inverter sizes that can yield reduced distribution system costs for different distribution

functions of irradiance.

- **Capacitor placement and sizing:** Reactive power compensation in distribution network has traditionally been accomplished through capacitor banks. In this thesis, the only source of reactive power was the inverters of PV enabled nodes. Optimally determining capacitor sizes and placement in distribution networks within the framework of optimization under uncertainty in solar generation remains a challenge.

- **Real time adjustment of real power consumption:** In the move to a smarter power grid, scheduling of energy requires not only coordinated generation but organized consumption. The programmable load model described in Chapter 2 is only a basic model accounting for the bounds of power consumption. The consumption in residential areas can be monitored by utility companies through the use of smart meters in an hourly manner. The real-time adjustment of real power consumption of devices depending on the customer preferences and the prices at a given time of day is an exciting area of research.

- **Distributed storage:** The premise here is that end-users can use batteries to store energy at certain times and utilize this energy at a later time. These storage devices may also be allowed to sell certain energy back to the network, or participate in voltage regulation. Integrating distributed storage capabilities into the power management framework is an enticing task.

Appendix A: PROOF THAT ONLY ONE OF THE TWO VARIABLES P_{0+} OR P_{0-} IS NONZERO AT THE OPTIMAL POINT

In this section we will prove that at the optimal point of problem (3.6), only one of the two decision variables P_{0+}^m and P_{0-}^m is nonzero:

Suppose that this is not the case, meaning that both P_{0+}^m and P_{0-}^m are nonzero. Following (3.6f), $P_0^m = P_{0+}^m - P_{0-}^m$. First assume that $P_0^m \geq 0$ and define two new variables $P_{0+_2}^m = P_0^m$ and $P_{0-_2}^m = 0$. Constraint (3.6f) holds for $P_{0+_2}^m$ and $P_{0-_2}^m$. Moreover, $P_{0+_2}^m = P_0^m = P_{0+}^m - P_{0-}^m$. Since P_{0-}^m is nonzero, it must be positive and hence $P_{0+_2}^m < P_{0+}^m$. Since $P_{0+_2}^m$ and P_{0+}^m are both positive:

$$P_{0+_2}^m < P_{0+}^m \Rightarrow K_0(P_{0+_2}^m)^2 < K_0(P_{0+_2}^m)^2 \tag{A.1}$$

Result (A.1) means that the cost in (3.6a) is smaller for the new set of variables $P_{0+_2}^m$ and $P_{0-_2}^m$. Since P_{0+}^m and P_{0-}^m were considered to be the optimal points, this is a contradiction and hence P_{0+}^m and P_{0-}^m cannot be both positive at the optimal point.

Next, assume that $P_0^m \leq 0$. Define two new variables $P_{0+_2}^m = 0$ and $P_{0-_2}^m = -P_0^m$. Constraint (3.6f) holds for $P_{0+_2}^m$ and $P_{0-_2}^m$. Notice that:

$$P_{0+_2}^m = 0 < P_{0+}^m \Rightarrow K_0(P_{0+_2}^m)^2 = 0 < K_0(P_{0+}^m)^2 \tag{A.2}$$

Therefore once again, the cost in (3.6a) is smaller for the new set of variables $P_{0+_2}^m$ and $P_{0-_2}^m$ and that P_{0+}^m and P_{0-}^m cannot be both positive at the optimal point.

Appendix B: OVERVIEW OF ADMM

ADMM is an algorithm that aims to solve the problems of the form

$$\min_{\mathbf{x},\mathbf{z}} f(\mathbf{x}) + g(\mathbf{z}) \tag{B.1a}$$

subject to

$$A\mathbf{x} + B\mathbf{z} = \mathbf{c} \tag{B.1b}$$

$$\mathbf{x} \in \mathcal{X}, \mathbf{z} \in \mathcal{Z} \tag{B.1c}$$

where $\mathcal{X} \subseteq \mathrm{R}^n$, and $\mathcal{Z} \subseteq \mathrm{R}^m$ are convex sets and (B.1b) is a linear equality between the $\mathbf{x}$ and $\mathbf{z}$ variables. Defining the augmented Lagrangian with parameter $\rho > 0$ as:

$$L_\rho(\mathbf{x}, \mathbf{z}, \mathbf{y}) = f(\mathbf{x}) + g(\mathbf{y}) + \mathbf{y}^T(A\mathbf{x} + B\mathbf{z} - c) + \frac{\rho}{2}||A\mathbf{x} + B\mathbf{z} - c||_2^2 \tag{B.2}$$

where $\mathbf{y}$ is the vector of Lagrange multipliers for the linear constraint (B.1b). The ADMM solves the problem by primal and dual iterations. The primal variables $\mathbf{x}$ and $\mathbf{z}$ updates are achieved successively by solving the following problems in each iteration:

$$\mathbf{x}(k+1) = \arg\min_{x \in \mathcal{X}} L_\rho\left(\mathbf{x}, \mathbf{z}(k), \mathbf{y}(k)\right) \tag{B.3a}$$

$$\mathbf{z}(k+1) = \arg\min_{z \in \mathcal{Z}} L_\rho\left(\mathbf{x}(k+1), \mathbf{z}, \mathbf{y}(k)\right) \tag{B.3b}$$

$$\mathbf{y}(k+1) = \mathbf{y}(k) + \rho\left(A\mathbf{x}(k+1) + B\mathbf{z}(k+1) - c\right) \tag{B.3c}$$

Let

$$r(k) := ||A\mathbf{x}(k) + B\mathbf{z}(k) - c|| \tag{B.4}$$

$$s(k) := \rho||A^T B(\mathbf{z}(k) - \mathbf{z}(k-1))|| \tag{B.5}$$

define the respective primal and dual feasibility residuals [14], a common stopping criterion for the ADMM is thus when at an iteration k these values are smaller than an acceptable tolerance.

Appendix C: UPDATES OF SOCP ADMM ALGORITHM

C.1 Equivalent problem

The problem to solve via ADMM will be of the following form:

$$\min_{\substack{\mathbf{P},\hat{\mathbf{P}},\tilde{\mathbf{P}},\\ \mathbf{Q},\hat{\mathbf{Q}},\tilde{\mathbf{Q}},\\ \mathbf{v},\hat{\mathbf{v}},\tilde{\mathbf{v}}\\ \tilde{\mathbf{p}}_{\mathbf{c}},\mathbf{p}_{\mathbf{c}},\mathbf{q}_w,\tilde{\mathbf{q}}_w\\ \mathbf{P_{0+}},\mathbf{P_{0-}},,\tilde{\mathbf{P}}_{\mathbf{0+}},\tilde{\mathbf{P}}_{0-}}} \quad \sum_{i\in\mathcal{N}} K_{u_i}(\tilde{p}_{c_i}-p_{c_i}^{\max})^2+\sum_{m=1}^{M}K_0(\pi^m)(P_{0+}^m)^2+K_{\text{Loss}}\sum_{i\in\mathcal{N}\backslash\{0\}}\sum_{m=1}^{M}r_i l_i^m \tag{C.1a}$$

subject to:

Coupling Constraints:

$$\text{for } i\in\mathcal{N}\backslash\{0\}: \qquad P_i^m=\tilde{P}_i^m \quad Q_i^m=\tilde{Q}_i^m \quad l_i^m=\tilde{l}_i^m \quad v_i^m=\tilde{v}_i^m \quad \hat{v}_j^m=\tilde{v}_{A_j}^m \tag{C.1b}$$

$$\text{for } i\in\mathcal{N}: \qquad \hat{P}_j^m=\tilde{P}_{j\in\mathcal{C}_i} \quad \hat{Q}_j^m=\tilde{Q}_{j\in\mathcal{C}_i} \quad \hat{l}_j^m=\tilde{l}_{j\in\mathcal{C}_i} \quad p_{c_i}^m=\tilde{p}_{c_i} \quad q_{w_i}^m=\tilde{q}_{w_i}^m \tag{C.1c}$$

$$\text{for root:} \qquad P_{0+}^m=\tilde{P}_{0+}^m \qquad P_{0-}^m=\tilde{P}_{0-}^m \tag{C.1d}$$

Individual Equality Constraints:

$$P_i^m=\sum_{j\in\mathcal{C}_i}(\hat{P}_j^m+r_j\hat{l}_j^m)+p_{c_i}^m-w_i^m \tag{C.1e}$$

$$Q_i^m=\sum_{j\in\mathcal{C}_i}(\hat{Q}_j^m+x_j\hat{l}_j^m)+\sqrt{\frac{1}{\text{PF}_i^2}-1}p_{c_i}^m-q_{w_i}^m \tag{C.1f}$$

$$\text{for } i\in\mathcal{N}\backslash\{0\}: \quad \hat{v}_i=v_i^m+2(r_iP_i^m+x_iQ_i^m)+(r_i^2+x_i^2)l_i^m \tag{C.1g}$$

$$\text{for root:} \quad P_0^m=P_{0+}^m-P_{0-}^m \tag{C.1h}$$

Individual Inequality Constraints

$$\text{for } i\in\mathcal{N}\backslash\{0\}: (\tilde{P}_j^m)^2+(\tilde{Q}_j^m)^2\leq(\tilde{v}_j^m)(\tilde{l}_j^m) \tag{C.1i}$$

$$(1-\epsilon)^2 V + 0^2 \leq \tilde{v}_i^m \leq (1+\epsilon)^2 v_0^2 \tag{C.1j}$$

$$\text{for } i \in \mathcal{N} : p_{c_i}^{\min} \leq \tilde{p}_{c_i} \leq p_{c_i}^{\max} \tag{C.1k}$$

$$-\sqrt{s_{w_i}^2 - (w_i^m)^2} \leq \tilde{q}_{w_i}^m \leq \sqrt{s_{w_i}^2 - (w_i^m)^2} \tag{C.1l}$$

$$\text{for root: } \tilde{P}_{0+}^m \geq 0, \tilde{P}_{0-}^m \geq 0 \tag{C.1m}$$

Table C.1: Lagrange Multipliers

Equality Constraint	Lagrange Multiplier
$P_i^m = \tilde{P}_i^m$	λ_i^m
$Q_i^m = \tilde{Q}_i^m$	μ_i^m
$l_i^m = \tilde{l}_i^m$	γ_i^m
$v_i^m = \tilde{v}_i^m$	ω_i^m
$\hat{v}_j^m = \tilde{v}_{A_j}^m$	$\hat{\omega}_j^m$
$\hat{P}_j^m = \tilde{P}_{j\in\mathcal{C}_i}$	$\hat{\lambda}_j^m$
$\hat{Q}_j^m = \tilde{Q}_{j\in\mathcal{C}_i}$	$\hat{\mu}_j^m$
$\hat{l}_j^m = \tilde{l}_{j\in\mathcal{C}_i}$	$\hat{\gamma}_j^m$
$p_{c_i}^m = \tilde{p}_{c_i}$	η_i^m
$q_{w_i}^m = \tilde{q}_{w_i}^m$	θ_i^m
$P_{0+}^m = \tilde{P}_{0+} i^m$	ζ_+^m
$P_{0-}^m = \tilde{P}_{0-} i^m$	ζ_-^m

C.2 Augmented Lagrangian

$$\begin{aligned}
L_\rho(\mathbf{X},\mathbf{Z},\mathbf{Y}) = &\sum_{i\in\mathcal{N}} K_{u_i}(\tilde{p}_{c_i} - p_{c_i}^{\max})^2 + \sum_{m=1}^{M} K_0 \pi^m (P_{0+}^m)^2 + \sum_{i\in\mathcal{N}_+}\sum_{m=1}^{M} \pi^m r_i l_i^m \\
&+ \sum_{i\in\mathcal{N}_+}\sum_{m=1}^{M} \lambda_i^m (P_i^m - \tilde{P}_i^m) + \sum_{i\in\mathcal{N}}\sum_{m=1}^{M}\sum_{j\in\mathcal{C}_i} \hat{\lambda}_j^m (\hat{P}_j^m - \tilde{P}_j^m) + \sum_{i\in\mathcal{N}_+}\sum_{m=1}^{M} \mu_i^m (Q_i^m - \tilde{Q}_i^m) \\
&+ \sum_{i\in\mathcal{N}}\sum_{m=1}^{M}\sum_{j\in\mathcal{C}_i} \hat{\mu}_j^m (\hat{Q}_j^m - \tilde{Q}_j^m) + \sum_{i\in\mathcal{N}_+}\sum_{m=1}^{M} \gamma_i^m (l_i^m - \tilde{l}_i^m) + \sum_{i\in\mathcal{N}}\sum_{m=1}^{M}\sum_{j\in\mathcal{C}_i} \hat{\gamma_j}^m (\hat{l}_j^m - \tilde{l}_j^m) \\
&+ \sum_{i\in\mathcal{N}_+}\sum_{m=1}^{M} \omega_i^m (v_i^m - \tilde{v}_i^m) + \sum_{i\in\mathcal{N}_+}\sum_{m=1}^{M} \hat{\omega}_j^m (\hat{v}_j^m - \tilde{v}_j^m) + \sum_{i\in\mathcal{N}}\sum_{m=1}^{M} \eta_i^m (p_{c_i}^m - \tilde{p}_{c_i})
\end{aligned}$$

Table C.2: Variables

	Nodes involved	Variables
X_0^m	Root and its children $j \in \mathcal{C}_0$	$\{P_0^m, Q_0^m, P_{0+}^m, P_{0-}^m, \hat{P}_j^m, \hat{Q}_j^m, \hat{l}_j^m, p_{c_0}^m, q_{w_0}^m\}$
X_i^m	Neither root nor leaf and the children $j \in \mathcal{C}_i$	$\{P_i^m, Q_i^m, v_i^m, l_i^m, \hat{P}_j^m, \hat{Q}_j^m, \hat{v}_i^m, p_{c_i}^m, q_{w_i}^m\}$
X_i^m	Leaf	$\{P_i^m, Q_i^m, v_i^m, l_i^m, \hat{v}_i^m, p_{c_i}^m, q_{w_i}^m\}$
Z_0^m	Root	$\{\tilde{P}_{0+}^m, \tilde{P}_{0-}^m, \tilde{q}_{w_0}^m\}$
Z_0	Root	$\{\{Z_0^m\}_{m=1}^M, \tilde{p}_{c_0}\}$
Z_i^m	Not root	$\{\tilde{P}_i^m, \tilde{Q}_i^m, \tilde{v}_i^m, \tilde{l}_i^m, \tilde{q}_{w_i}^m\}$
Z_i	Not root	$\{\{Z_i^m\}_{m=1}^M, \tilde{p}_{c_i}\}$

$$
\begin{aligned}
&+ \sum_{i\in\mathcal{N}}\sum_{m=1}^{M} \theta_i^m (q_{w_i}^m - \tilde{q}_{w_i}^m) + \sum_{m=1}^{M} \zeta_+^m (P_{0+}^m - \tilde{P}_{0+}^m) + \sum_{m=1}^{M} \zeta_-^m (P_{0-}^m - \tilde{P}_{0-}^m) \\
&+ \frac{\rho}{2}\Bigg[\sum_{i\in\mathcal{N}_+}\sum_{m=1}^{M} (P_i^m - \tilde{P}_i^m)^2 + \sum_{i\in\mathcal{N}}\sum_{m=1}^{M}\sum_{j\in\mathcal{C}_i} (\hat{P}_j^m - \tilde{P}_j^m)^2 + \sum_{i\in\mathcal{N}_+}\sum_{m=1}^{M} (Q_i^m - \tilde{Q}_i^m)^2 \\
&+ \sum_{i\in\mathcal{N}}\sum_{m=1}^{M}\sum_{j\in\mathcal{C}_i} (\hat{Q}_j^m - \tilde{Q}_j^m)^2 + \sum_{i\in\mathcal{N}_+}\sum_{m=1}^{M} (l_i^m - \tilde{l}_i^m)^2 + \sum_{i\in\mathcal{N}}\sum_{m=1}^{M}\sum_{j\in\mathcal{C}_i} (\hat{l}_j^m - \tilde{l}_j^m)^2 \\
&+ \sum_{i\in\mathcal{N}_+}\sum_{m=1}^{M} (v_i^m - \tilde{v}_i^m)^2 + \sum_{i\in\mathcal{N}_+}\sum_{m=1}^{M} (\hat{v}_j^m - \tilde{v}_j^m)^2 + \sum_{i\in\mathcal{N}}\sum_{m=1}^{M} (p_{c_i}^m - \tilde{p}_{c_i})^2 \\
&+ \sum_{i\in\mathcal{N}}\sum_{m=1}^{M} (q_{w_i}^m - \tilde{q}_{w_i}^m)^2 + \sum_{m=1}^{M} (P_{0+}^m - \tilde{P}_{0+}^m)^2 + \sum_{m=1}^{M} (P_{0-}^m - \tilde{P}_{0-}^m)^2 \Bigg]
\end{aligned} \tag{C.2}
$$

C.3 Updates

We will divide the nodes into three subsets $\{\text{root}, \text{leaf}, \text{other}\}$ and for each of these cases we will write the updates. Each step of the ADMM will consist of minimizing the augmented Lagrangian with respect to either X or Z and updating the Lagrange parameters.

C.3.1 X_0^m-update

For the root in scenario m, the X-update will be broken down to the following quadratic program:

$$
\min_{X_0^m} K_0 \pi^m (P_{0+}^m)^2 + \sum_{j\in\mathcal{C}_\rangle} \hat{\lambda}_j^m (\hat{P}_j^m - \tilde{P}_j^m) + \sum_{j\in\mathcal{C}_\prime} \hat{\mu}_j^m (\hat{Q}_j^m - \tilde{Q}_j^m) + \sum_{j\in\mathcal{C}_\prime} \hat{\gamma}_j^m (\hat{l}_j^m - \tilde{l}_j^m)
$$

$$+ \eta_0^m(p_{c_0}^m - \tilde{p}_{c_0}^m) + \theta_0^m(q_{w_0} - \tilde{q}_{w_i}^m) + \zeta_+^m(P_{0+}^m - \tilde{P}_{0+}^m) + \zeta_-^m(P_{0-}^m - \tilde{P}_{0-}^m)$$
$$+ \frac{\rho}{2}\left[\sum_{j\in\mathcal{C}\prime}(\hat{P}_j^m - \tilde{P}_j^m)^2 + \sum_{j\in\mathcal{C}\prime}(\hat{Q}_j^m - \tilde{Q}_j^m)^2 + \sum_{j\in\mathcal{C}\prime}(\hat{l}_j^m - \tilde{l}_j^m)^2\right.$$
$$\left. + (p_{c_0}^m - \tilde{p}_{c_0}^m)^2 + (q_{w_i} - \tilde{q}_{w_0}^m)^2 + (P_{0+}^m - \tilde{P}_{0+}^m)^2 + (P_{0-}^m - \tilde{P}_{0-}^m)^2\right] \quad \text{(C.3a)}$$

subject to:

$$P_0^m = P_{0+}^m - P_{0-}^m \quad \text{(C.3b)}$$
$$P_0^m = \sum_{j\in\mathcal{C}_0}(\hat{P}_j^m + r_j\hat{l}_j^m) + p_{c_i}^m - p_{g_i}^m \quad \text{(C.3c)}$$
$$Q_0^m = \sum_{j\in\mathcal{C}_0}(\hat{Q}_j^m + x_j\hat{l}_j^m) + \sqrt{\frac{1}{\mathrm{PF}_i^2} - 1}p_{c_i}^m - q_{w_0}^m \quad \text{(C.3d)}$$

This problem is a QP of the form

$$\frac{1}{2}x^TAx + b^Tx \quad \text{(C.4a)}$$
$$\text{s.t. : } Cx = d \quad \text{(C.4b)}$$

Where $A = 2$
$$\begin{bmatrix} \overbrace{\frac{\rho}{2} + K_0\pi^m}^{P_{0+}^m} & \overbrace{0}^{P_{0-}^m} & \overbrace{0}^{\hat{P}_j^m} & \overbrace{0}^{\hat{Q}_j^m} & \overbrace{0}^{\hat{l}_j^m} & \overbrace{0}^{p_{c_0}^m} & \overbrace{0}^{q_{w_0}^m} \\ 0 & \frac{\rho}{2} & 0 & 0 & 0 & 0 & 0 \\ 0 & 0 & \frac{\rho}{2} & 0 & 0 & 0 & 0 \\ 0 & 0 & 0 & \frac{\rho}{2} & 0 & 0 & 0 \\ 0 & 0 & 0 & 0 & \frac{\rho}{2} & 0 & 0 \\ 0 & 0 & 0 & 0 & 0 & \frac{\rho}{2} & 0 \\ 0 & 0 & 0 & 0 & 0 & 0 & \frac{\rho}{2} \end{bmatrix}_{(4+3\times|\mathcal{C}_0|)\times(4+3\times|\mathcal{C}_0|)}.$$

$$b = \begin{bmatrix} \zeta_+^m - \rho\tilde{P}_{0+}^m \\ \zeta_-^m - \rho\tilde{P}_{0-}^m \\ \hat{\lambda}_j^m - \rho\tilde{P}_j^m \\ \hat{\mu}_j^m - \rho\tilde{Q}_j^m \\ \hat{\gamma}_j^m - \rho\tilde{l}_j^m \\ \eta_0^m - \rho\tilde{p}_{c_0} \\ \theta_0^m - \rho\tilde{q}_{w_0}^m \end{bmatrix}_{(4+3\times|\mathcal{C}_0|)\times 1} \qquad \text{for } j \in \mathcal{C}_0.$$

$$C = [\overbrace{1}^{P_{0+}^m} \overbrace{-1}^{P_{0-}^m} \overbrace{-1}^{\hat{P}_j^m} \overbrace{0}^{\hat{Q}_j^m} \overbrace{-r_j}^{\hat{l}_j^m} \overbrace{-1}^{p_{c_0}^m} \overbrace{0}^{q_{w_0}^m}] \text{ and } d = [-p_{w_0}^m]$$

This quadratic problem has a closed form solution developed in Appendix D.

C.3.2 X_i^m-update

For the nodes that are not root or leaf in scenario m, the X-update will be broken down to the following quadratic program:

$$\min_{X_i^m} \pi^m r_i l_i^m + \lambda_i^m(P_i^m - \tilde{P}_i^m) + \sum_{j\in\mathcal{C}_\rangle} \hat{\lambda}_j^m(\hat{P}_j^m - \tilde{P}_j^m) + \mu_i^m(Q_i^m - \tilde{Q}_i^m) + \sum_{j\in\mathcal{C}_\prime} \hat{\mu}_j^m(\hat{Q}_j^m - \tilde{Q}_j^m)$$
$$+ \gamma_i^m(l_i^m - \tilde{l}_i^m) + \sum_{j\in\mathcal{C}_\prime} \hat{\gamma}_j^m(\hat{l}_j^m - \tilde{l}_j^m) + \omega_i^m(v_i^m - \tilde{v}_i^m) + \hat{\omega}_i^m(\hat{v}_i^m - \tilde{v}_i^m) + \eta_i^m(p_{c_i}^m - \tilde{p}_{c_i}^m) + \theta_i^m(q_{w_i} - \tilde{q}_{w_i}^m)$$
$$+ \frac{\rho}{2}\Bigg[(P_i^m - \tilde{P}_i^m)^2 + \sum_{j\in\mathcal{C}_\prime}(\hat{P}_j^m - \tilde{P}_j^m)^2 + (Q_i^m - \tilde{Q}_i^m) + \sum_{j\in\mathcal{C}_\prime}(\hat{Q}_j^m - \tilde{Q}_j^m)^2 + (l_i^m - \tilde{l}_i^m)^2$$
$$+ \sum_{j\in\mathcal{C}_\prime}(\hat{l}_j^m - \tilde{l}_j^m)^2 + (v_i^m - \tilde{v}_i^m)^2 + (\tilde{v}_i^m - \tilde{v}_i^m)^2 + (p_{c_i}^m - \tilde{p}_{c_i}^m)^2 + (q_{w_i}^m - \tilde{q}_{w_i}^m)^2\Bigg] \quad \text{(C.5a)}$$

subject to:

$$P_i^m = \sum_{j\in\mathcal{C}_i}(\hat{P}_j^m + r_j\hat{l}_j^m) + p_{c_i}^m - p_{g_i}^m \quad \text{(C.5b)}$$

$$Q_i^m = \sum_{j\in\mathcal{C}_i}(\hat{Q}_j^m + x_j\hat{l}_j^m) + \sqrt{\frac{1}{\mathrm{PF}_i^2} - 1}p_{c_i}^m - q_{w_i}^m \quad \text{(C.5c)}$$

$$\hat{v}_i^m = v_i^m + 2(r_i P_i^m + x_i Q_i^m) + (r_i^2 + x_i^2) l_i^m \tag{C.5d}$$

This problem is a QP of the form

$$\frac{1}{2} x^T A x + b^T x \tag{C.6a}$$

$$\text{s.t. : } Cx = d \tag{C.6b}$$

$$A = 2 \begin{bmatrix} \overbrace{\frac{\rho}{2}}^{P_i^m} & \overbrace{0}^{Q_i^m} & \overbrace{0}^{v_i^m} & \overbrace{0}^{l_i^m} & \overbrace{0}^{\hat{P}_j^m} & \overbrace{0}^{\hat{Q}_j^m} & \overbrace{0}^{\hat{l}_j^m} & \overbrace{0}^{\hat{v}_i^m} & \overbrace{0}^{p_{c_0}^m} & \overbrace{0}^{q_{w_0}^m} \\ 0 & \frac{\rho}{2} & 0 & 0 & 0 & 0 & 0 & 0 & 0 & 0 \\ 0 & 0 & \frac{\rho}{2} & 0 & 0 & 0 & 0 & 0 & 0 & 0 \\ 0 & 0 & 0 & \frac{\rho}{2} & 0 & 0 & 0 & 0 & 0 & 0 \\ 0 & 0 & 0 & 0 & \frac{\rho}{2} & 0 & 0 & 0 & 0 & 0 \\ 0 & 0 & 0 & 0 & 0 & \frac{\rho}{2} & 0 & 0 & 0 & 0 \\ 0 & 0 & 0 & 0 & 0 & 0 & \frac{\rho}{2} & 0 & 0 & 0 \\ 0 & 0 & 0 & 0 & 0 & 0 & 0 & \frac{\rho}{2} & 0 & 0 \\ 0 & 0 & 0 & 0 & 0 & 0 & 0 & 0 & \frac{\rho}{2} & 0 \\ 0 & 0 & 0 & 0 & 0 & 0 & 0 & 0 & 0 & \frac{\rho}{2} \end{bmatrix}_{(7+3\times|\mathcal{C}_0|)\times(7+3\times|\mathcal{C}_0|)}.$$

$$b = \begin{bmatrix} \gamma_i^m - \rho\tilde{P}_i^m \\ \mu_i^m - \rho\tilde{Q}_i^m \\ \omega_i^m - \rho\tilde{v}_i^m \\ \gamma_i^m - \rho\tilde{l}_i^m + \pi^m r_i \\ \hat{\lambda}_j^m - \rho\tilde{P}_j^m \\ \hat{\mu}_j^m - \rho\tilde{Q}_j^m \\ \hat{\gamma}_j^m - \rho\tilde{l}_j^m \\ \hat{\omega}_i^m - \rho\tilde{v}_{A_i} \\ \eta_i^m - \rho\tilde{p}_{c_i} \\ \theta_i^m - \rho\tilde{q}_{w_i}^m \end{bmatrix}_{(7+3\times|\mathcal{C}_i|)\times 1} \quad \text{for } j \in \mathcal{C}_i.$$

$$C = \begin{bmatrix} \overbrace{1}^{P_i^m} & \overbrace{0}^{Q_i^m} & \overbrace{0}^{v_i^m} & \overbrace{0}^{l_i^m} & \overbrace{-1}^{\hat{P}_j^m} & \overbrace{0}^{\hat{Q}_j^m} & \overbrace{-r_j}^{\hat{l}_j^m} & \overbrace{0}^{\hat{v}_i^m} & \overbrace{-1}^{p_{c_i}^m} & \overbrace{0}^{q_{w_i}^m} \\ 0 & 1 & 0 & 0 & 0 & -1 & -x_j & 0 & -\sqrt{\frac{1}{\mathrm{PF}_i^2} - 1} & 1 \\ 2r_i & 2x_i & 1 & (r_i^2 + x_i^2) & 0 & 0 & 0 & 1 & 0 & 0 \end{bmatrix}_{3\times(7+3\times|\mathcal{C}_i|)}$$

and $d = \begin{bmatrix} -p_{w_i}^m \\ 0 \\ 0 \end{bmatrix}$

Note that in the case where $A_i = 1$ then the term for $\hat{v}_i^m$ in the third row of C disappears and d will change to: $d = \begin{bmatrix} -p_{w_i}^m \\ 0 \\ -V_0^2 \end{bmatrix}$

C.3.3 X_i^m-update leaf

For the nodes that are not root or leaf in scenario m, the X-update will be broken down to the following quadratic program:

$$\min_{X_i^m} \pi^m r_i l_i^m + \lambda_i^m(P_i^m - \tilde{P}_i^m) + \mu_i^m(Q_i^m - \tilde{Q}_i^m) + \gamma_i^m(l_i^m - \tilde{l}_i^m) + \omega_i^m(v_i^m - \tilde{v}_i^m) + \hat{\omega}_i^m(\hat{v}_i^m - \tilde{v}_i^m)$$

$$+ \eta_i^m(p_{c_i}^m - \tilde{p}_{c_i}^m) + \theta_i^m(q_{w_i} - \tilde{q}_{w_i}^m) + \frac{\rho}{2}\left[(P_i^m - \tilde{P}_i^m)^2 + (Q_i^m - \tilde{Q}_i^m) + (l_i^m - \tilde{l}_i^m)^2\right.$$
$$\left.+(v_i^m - \tilde{v}_i^m)^2 + (\tilde{v}_i^m - \tilde{v}_i^m)^2 + (p_{c_i}^m - \tilde{p}_{c_i}^m)^2 + (q_{w_i}^m - \tilde{q}_{w_i}^m)^2\right] \quad \text{(C.7a)}$$

subject to:

$$P_i^m = p_{c_i}^m - p_{g_i}^m \quad \text{(C.7b)}$$

$$Q_i^m = \sqrt{\frac{1}{\mathrm{PF}_i^2} - 1}p_{c_i}^m - q_{w_i}^m \quad \text{(C.7c)}$$

$$\hat{v}_i^m = v_i^m + 2(r_i P_i^m + x_i Q_i^m) + (r_i^2 + x_i^2)l_i^m \quad \text{(C.7d)}$$

This problem is a QP of the form

$$\frac{1}{2}x^T Ax + b^T x \quad \text{(C.8a)}$$

$$\text{s.t. : } Cx = d \quad \text{(C.8b)}$$

$$A = 2\begin{bmatrix} \overbrace{\frac{\rho}{2}}^{P_i^m} & \overbrace{0}^{Q_i^m} & \overbrace{0}^{v_i^m} & \overbrace{0}^{l_i^m} & \overbrace{0}^{\hat{v}_i^m} & \overbrace{0}^{p_{c_0}^m} & \overbrace{0}^{q_{w_0}^m} \\ 0 & \frac{\rho}{2} & 0 & 0 & 0 & 0 & 0 \\ 0 & 0 & \frac{\rho}{2} & 0 & 0 & 0 & 0 \\ 0 & 0 & 0 & \frac{\rho}{2} & 0 & 0 & 0 \\ 0 & 0 & 0 & 0 & \frac{\rho}{2} & 0 & 0 \\ 0 & 0 & 0 & 0 & 0 & \frac{\rho}{2} & 0 \\ 0 & 0 & 0 & 0 & 0 & 0 & \frac{\rho}{2} \end{bmatrix}_{7\times 7}.$$

$$b = \begin{bmatrix} \lambda_i^m - \rho\tilde{P}_i^m \\ \mu_i^m - \rho\tilde{Q}_i^m \\ \omega_i^m - \rho\tilde{v}_i^m \\ \gamma_i^m - \rho\tilde{l}_i^m + \pi^m r_i \\ \eta_i^m - \rho\tilde{p}_{c_i} \\ \theta_i^m - \rho\tilde{q}_{w_i}^m \end{bmatrix}_{7\times 1}$$

$$C = \begin{bmatrix} \overbrace{1}^{P_i^m} & \overbrace{0}^{Q_i^m} & \overbrace{0}^{v_i^m} & \overbrace{0}^{l_i^m} & \overbrace{-1}^{\hat{P}_j^m} & \overbrace{0}^{\hat{Q}_j^m} & \overbrace{-r_j}^{\hat{l}_j^m} & \overbrace{0}^{\hat{v}_i^m} & \overbrace{-1}^{p_{c_i}^m} & \overbrace{0}^{q_{w_i}^m} \\ 0 & 1 & 0 & 0 & 0 & -1 & -x_j & 0 & -\sqrt{\frac{1}{\mathrm{PF}_i^2} - 1} & 1 \\ 2r_i & 2x_i & 1 & (r_i^2 + x_i^2) & 0 & 0 & 0 & 1 & 0 & 0 \end{bmatrix}_{3\times(7+3\times|\mathcal{C}_i|)}$$

and $d = \begin{bmatrix} -p_{w_i}^m \\ 0 \\ 0 \end{bmatrix}$

C.3.4 Z_0^m-update

For $\tilde{p}_{c_0}$ the Lagrangian breaks down to:

$$L = k_{u0}(\tilde{p}_{c_0} - p_{c_0}^{\max})^2 + \sum_{m=1}^{M} \eta_0^m (p_{c_0}^m - \tilde{p}_{c_0}) + \frac{\rho}{2} \sum_{m=1}^{M} (p_{c_i}^m - \tilde{p}_{c_i})^2 \tag{C.9}$$

Taking the derivative and setting it to zero yields:

$$\frac{\partial L}{\partial \tilde{p}_{c_0}} = 0$$

$$\Rightarrow \tilde{p}_{c_0}^* = \frac{2K_0 p_c^{\max} + \sum_{m=1}^{M} \left[\eta_0^m + \rho p_{c_0}^m\right]}{2K_0 + \rho M} \tag{C.10}$$

Since p_{c_0} has to be within specific boundaries:

$$\tilde{p}_{c_0}(k+1) = \max\left\{p_{c_0}^{\min}, \min\{\tilde{p}_{c_0}^*, p_{c_0}^{\max}\}\right\} \tag{C.11}$$

For $\tilde{P}^m_{0+}$:

$$L = \zeta^m_+(P^m_{0+} - \tilde{P}^m_{0+}) + \frac{\rho}{2}(P^m_{0+} - \tilde{P}^m_{0+})^2 \tag{C.12}$$

Following the same logic:

$$\frac{\partial L}{\partial \tilde{P}_{0+}} = 0 \Rightarrow \tilde{P}^{m*}_{0+} = \frac{\zeta^m_+ + \rho P^m_{0+}}{\rho} \tag{C.13}$$

Since P^m_{0+} has to be greater than zero :

$$\tilde{P}^m_{0+}(k+1) = \max\{0, \tilde{P}^{m*}_{0+}\} \tag{C.14}$$

Similarly for $\tilde{P}^m_{0-}$:

$$\tilde{P}^{m*}_{0-} = \frac{\zeta^m_- + \rho P^m_{0-}}{\rho} \tag{C.15}$$

$$\tilde{P}^m_{0-}(k+1) = \max\{0, \tilde{P}^{m*}_{0-}\} \tag{C.16}$$

For $\tilde{q}^m_{w_0}$ the Lagrangian becomes:

$$L = \theta^m_i(q^m_{w_0} - \tilde{q}^m_{w_i}) + \frac{\rho}{2}(q^m_{w_i} - \tilde{q}^m_{w_i})^2 \tag{C.17}$$

Hence:

$$\frac{\partial L}{\partial \tilde{q}^m_{w_0}} = 0 \Rightarrow \tilde{q}^{m*}_{w_0} = \frac{\theta^m_i + \rho q^m_{w_i}}{\rho} \tag{C.18}$$

To conform to the bounds:

$$q^m_{w_0}(k+1) = \max\left\{q^{\min}_w, \min\{\tilde{q}^{m*}_{w_0}, q^{\max}_{w_0}\}\right\} \tag{C.19}$$

C.3.5 Z_i-update

For $\tilde{p}_{c_i}$ the Lagrangian breaks down to:

$$L = K_{u_i}(\tilde{p}_{c_i} - p_{c_i}^{\max})^2 + \sum_{m=1}^{M} \eta_i^m (p_{c_i}^m - \tilde{p}_{c_i}) + \frac{\rho}{2} \sum_{m=1}^{M} (p_{c_i}^m - \tilde{p}_{c_i})^2 \tag{C.20}$$

Taking the derivative and setting it to zero yields:

$$\begin{aligned} \frac{\partial L}{\partial \tilde{p}_{c_0}} &= 0 \\ \Rightarrow \tilde{p}_{c_i}^* &= \frac{2K_{u_i} p_{c_i}^{\max} + \sum\limits_{m=1}^{M} \left[\eta_i^m + \rho p_{c_i}^m\right]}{2K_{u_i} + \rho M} \end{aligned} \tag{C.21}$$

Since p_{c_i} has to be within specific boundaries:

$$\tilde{p}_{c_i}(k+1) = \max\left\{p_{c_i}^{\min}, \min\{\tilde{p}_{c_i}^*, p_{c_i}^{\max}\}\right\} \tag{C.22}$$

For $\tilde{q}_{w_i}^m$ the Lagrangian becomes:

$$L = \theta_i^m (q_{w_i}^m - \tilde{q}_{w_i}^m) + \frac{\rho}{2} (q_{w_i}^m - \tilde{q}_{w_i}^m)^2 \tag{C.23}$$

Hence:

$$\frac{\partial L}{\partial \tilde{q}_{w_i}^m} = 0 \Rightarrow \tilde{q}_{w_i}^{m*} = \frac{\theta_i^m + \rho q_{w_i}^m}{\rho} \tag{C.24}$$

To conform to the bounds:

$$q_{w_i}^m(k+1) = \max\left\{q_w^{\min}, \min\{\tilde{q}_{w_i}^{m*}, q_{w_i}^{\max}\}\right\} \tag{C.25}$$

$\tilde{P}_i^m, \tilde{Q}_i^m, \tilde{v}_i^m, \tilde{l}_i^m$**-update:**

$$\begin{aligned} L = \min \big\{ & \lambda_i^m (P_i^m 0 \tilde{P}_i^m) + \hat{\lambda}_i^m (\hat{P}_i^m - \tilde{P}_i^m) + \mu_i^m (Q_i^m - \tilde{Q}_i^m) + \hat{\mu}_i^m (\hat{Q}_i^m - \tilde{Q}_i^m) \\ & + \gamma_i^m (l_i^m - \tilde{l}_i^m) + \hat{\gamma}_i^m (\hat{l}_i^m - \tilde{l}_i^m) + \omega_i^m (v_i^m - \tilde{v}_i^m) + \sum_{j \in \mathcal{C}_i} \hat{\omega}_j^m (\hat{v}_j^m - \tilde{v}_i^m) \\ & + \frac{\rho}{2} \left[(P_i^m - \tilde{P}_i^m)^2 + (\hat{P}_i^m - \tilde{P}_i^m)^2 + (Q_i^m - \tilde{Q}_i^m)^2 + (\hat{Q}_i^m - \tilde{Q}_i^m) \right. \\ & \left. + (l_i^m - \tilde{l}_i^m)^2 + (\hat{l}_i^m - \tilde{l}_i^m)^2 + (v_i^m - \tilde{v}_i^m)^2 + \sum_{j \in \mathcal{C}_i} (\hat{v}_j - \tilde{v}_i^m)^2 \right] \big\} \end{aligned} \tag{C.26a}$$

subject to:

$$(1-\epsilon)^2 V_0^2 \leq \tilde{v}_i^m \leq (1+\epsilon)^2 V_0^2 \tag{C.26b}$$

$$(\tilde{P}_i^m)^2 + (\tilde{Q}_i^m)^2 \leq \tilde{v}_i^m \tilde{l}_i^m, \tilde{v}_i^m \geq 0, \tilde{l}_i^m \geq 0 \tag{C.26c}$$

This problem has a closed form solution which is derived in Appendix E.

C.3.6 Z_i-update leaf

For $\tilde{p}_{c_i}$ the Lagrangian breaks down to:

$$L = K_{u_i} (\tilde{p}_{c_i} - p_{c_i}^{\max})^2 + \sum_{m=1}^{M} \eta_i^m (p_{c_i}^m - \tilde{p}_{c_i}) + \frac{\rho}{2} \sum_{m=1}^{M} (p_{c_i}^m - \tilde{p}_{c_i})^2 \tag{C.27}$$

Taking the derivative and setting it to zero yields:

$$\begin{aligned} \frac{\partial L}{\partial \tilde{p}_{c_0}} &= 0 \\ \Rightarrow \tilde{p}_{c_i}^* &= \frac{2K_{u_i} p_{c_i}^{\max} + \sum_{m=1}^{M} \left[\eta_i^m + \rho p_{c_i}^m \right]}{2K_{u_i} + \rho M} \end{aligned} \tag{C.28}$$

Since p_{c_i} has to be within specific boundaries:

$$\tilde{p}_{c_i}(k+1) = \max\left\{p_{c_i}^{\min}, \min\{\tilde{p}_{c_i}^{*}, p_{c_i}^{\max}\}\right\} \tag{C.29}$$

For $\tilde{q}_{w_i}^m$ the Lagrangian becomes:

$$L = \theta_i^m(q_{w_i}^m - \tilde{q}_{w_i}^m) + \frac{\rho}{2}(q_{w_i}^m - \tilde{q}_{w_i}^m)^2 \tag{C.30}$$

Hence:

$$\frac{\partial L}{\partial \tilde{q}_{w_i}^m} = 0 \Rightarrow \tilde{q}_{w_i}^{m*} = \frac{\theta_i^m + \rho q_{w_i}^m}{\rho} \tag{C.31}$$

To conform to the bounds:

$$q_{w_i}^m(k+1) = \max\left\{q_w^{\min}, \min\{\tilde{q}_{w_i}^{m*}, q_{w_i}^{\max}\}\right\} \tag{C.32}$$

$\tilde{P}_i^m, \tilde{Q}_i^m, \tilde{v}_i^m, \tilde{l}_i^m$**- leaf update:**

$$\begin{aligned} L = \min\big\{&\lambda_i^m(P_i^m 0\tilde{P}_i^m) + \hat{\lambda}_i^m(\hat{P}_i^m - \tilde{P}_i^m) + \mu_i^m(Q_i^m - \tilde{Q}_i^m) + \hat{\mu}_i^m(\hat{Q}_i^m - \tilde{Q}_i^m) \\ &+ \gamma_i^m(l_i^m - \tilde{l}_i^m) + \hat{\gamma}_i^m(\hat{l}_i^m - \tilde{l}_i^m) + \omega_i^m(v_i^m - \tilde{v}_i^m) + \\ &+ \frac{\rho}{2}\left[(P_i^m - \tilde{P}_i^m)^2 + (\hat{P}_i^m - \tilde{P}_i^m)^2 + (Q_i^m - \tilde{Q}_i^m)^2 + (\hat{Q}_i^m - \tilde{Q}_i^m)\right. \\ &\left.+(l_i^m - \tilde{l}_i^m)^2 + (\hat{l}_i^m - \tilde{l}_i^m)^2 + (v_i^m - \tilde{v}_i^m)^2\right]\big\} \end{aligned} \tag{C.33a}$$

subject to:

$$(1-\epsilon)^2 V_0^2 \leq \tilde{v}_i^m \leq (1+\epsilon)^2 V_0^2 \tag{C.33b}$$

$$(\tilde{P}_i^m)^2 + (\tilde{Q}_i^m)^2 \leq \tilde{v}_i^m \tilde{l}_i^m, \tilde{v}_i^m \geq 0, \tilde{l}_i^m \geq 0 \tag{C.33c}$$

This problem has similar form to (C.26) and has a closed form solution.

Appendix D: CLOSED FORM SOLUTION OF EQUALITY CONSTRAINED QP IN X-UPDATE

$$\frac{1}{2}x^T Ax + b^T x \tag{D.1}$$

$$\text{s.t. : } Cx = d \tag{D.2}$$

The Lagrangian is :

$$L(x, \lambda) = \frac{1}{2}x^T Ax + b^T x + \lambda^T (Cx - d) \tag{D.3}$$

Setting the derivative to zero for optimum x yields:

$$\frac{\partial L}{\partial x} = Ax + b + C^T \lambda = \mathbf{0} \tag{D.4}$$

hence:

$$x^* = A^{-1}(-b - C^T \lambda) \tag{D.5}$$

Since $Cx = d$:

$$Cx^* = CA^{-1}(-b - C^T \lambda) = d \tag{D.6}$$

$$\Rightarrow CA^{-1}(-b) - CA^{-1}C^T \lambda = d \tag{D.7}$$

$$\Rightarrow \lambda = -(CA^{-1}C^T)^{-1}(d + CA^{-1}b) \tag{D.8}$$

Replacing derived λ from (D.6) in (D.5) yields the optimum x^*:

$$x^* = A^{-1}(-b + C^T((CA^{-1}C^T)^{-1}(d + CA^{-1}b))) \tag{D.9}$$

Appendix E: CLOSED FORM SOLUTION OF SOCP CONSTRAINT IN Z-UPDATE

$$
\begin{aligned}
L = \min \big\{ & \lambda_i^m (P_i^m 0 \tilde{P}_i^m) + \hat{\lambda}_i^m (\hat{P}_i^m - \tilde{P}_i^m) + \mu_i^m (Q_i^m - \tilde{Q}_i^m) + \hat{\mu}_i^m (\hat{Q}_i^m - \tilde{Q}_i^m) \\
& + \gamma_i^m (l_i^m - \tilde{l}_i^m) + \hat{\gamma}_i^m (\hat{l}_i^m - \tilde{l}_i^m) + \omega_i^m (v_i^m - \tilde{v}_i^m) + \sum_{j \in \mathcal{C}_i} \hat{\omega}_j^m (\hat{v}_j^m - \tilde{v}_i^m) \\
& + \frac{\rho}{2} \left[(P_i^m - \tilde{P}_i^m)^2 + (\hat{P}_i^m - \tilde{P}_i^m)^2 + (Q_i^m - \tilde{Q}_i^m)^2 + (\hat{Q}_i^m - \tilde{Q}_i^m) \right. \\
& \left. + (l_i^m - \tilde{l}_i^m)^2 + (\hat{l}_i^m - \tilde{l}_i^m)^2 + (v_i^m - \tilde{v}_i^m)^2 + \sum_{j \in \mathcal{C}_i} (\hat{v}_j - \tilde{v}_i^m)^2 \right] \big\}
\end{aligned} \tag{E.1a}
$$

subject to:

$$
(1-\epsilon)^2 V_0^2 \leq \tilde{v}_i^m \leq (1+\epsilon)^2 V_0^2 \tag{E.1b}
$$

$$
(\tilde{P}_i^m)^2 + (\tilde{Q}_i^m)^2 \leq \tilde{v}_i^m \tilde{l}_i^m, \tilde{v}_i^m \geq 0, \tilde{l}_i^m \geq 0 \tag{E.1c}
$$

Define new variable: $\tilde{v}_i^{m'} = \sqrt{\frac{|\mathcal{C}_i|+1}{2}} \tilde{v}_i^m$. The problem becomes of the form:

$$
\min_{y_1, y_2, y_3, y_4} \sum_{i=1}^{4} (y_i^2 + c_i y_i) \tag{E.2a}
$$

subject to :

$$
y_1^2 + y_2^2 \leq k^2 y_3 y_4 \tag{E.2b}
$$

$$
y_3 \in [y_3^{\min}, y_3^{\max}] \tag{E.2c}
$$

$$
y_3 > 0 \tag{E.2d}
$$

where $y_1 = \tilde{P}_i^m$, $y_2 = \tilde{Q}_i^m$, $y_3 = \tilde{v}_i^{m'}$ and $y_4 = \tilde{l}_i^m$:

$$
k^2 = \sqrt{\frac{2}{|\mathcal{C}_i| + 1}} \tag{E.3}
$$

$$c_1 = -\frac{1}{\rho}(\lambda_i^m + \hat{\lambda}_i^m) - P_i^m - \hat{P}_i^m \tag{E.4}$$

$$c_2 = \frac{1}{\rho}(\mu_i^m + \hat{\mu}_i^m) - Q_i^m - \hat{Q}_i^m \tag{E.5}$$

$$c_3 = -\omega_i^m \sqrt{\frac{2}{|\mathcal{C}_i| + 1}} - \sum_{j \in \mathcal{C}_i} \hat{\omega}_j \sqrt{\frac{2}{|\mathcal{C}_i| + 1}} - \sum_{j \in \mathcal{C}_i} \hat{v}_j \sqrt{\frac{2}{|\mathcal{C}_i| + 1}} - \sqrt{\frac{2}{|\mathcal{C}_i| + 1}} v_i^m \tag{E.6}$$

$$c_4 = -\frac{1}{\rho}(\gamma_i^m + \hat{\gamma}_i^m) - l_i^m - \hat{l}_i^m \tag{E.7}$$

This problem has can be solved in closed form using the results in [14].

Appendix F: PROBLEM FORMULATION AND THE ADMM ALGORITHM FOR THE SIMULATIONS ON SINGLE-FEEDER NETWORK WITH `LINDISTFLOW` APPROXIMATION

F.1 Equivalent problem

The equivalent problem amenable for the ADMM, leveraging the model where power flows are considered to be flowing out of a node is explained here (see Section 3.2). The optimization problem to be solved via the ADMM is as follows, where all listed constraints hold for $m \in \{1, ..., M\}$.

$$\min_{\mathbf{x},\mathbf{z}} \sum_{i=1}^{N} \left[K_{u_i}(\widetilde{p}_{c_i} - p_{c_i}^{\max})^2\right] + \sum_{m=1}^{M} \pi^m K_0 (P_{0+}^m)^2 + \sum_{i=0}^{N-1} \sum_{m=1}^{M} \pi^m r_i \frac{(P_i^m)^2 + (Q_i^m)^2}{V_0^2} \tag{F.1a}$$

subj. to

Coupling Constraints:

$$\widetilde{P}_i^m = P_i^m,\ \widetilde{P}_i^m = \hat{P}_i^m,\ \widetilde{Q}_i^j = Q_i^j,\ \widetilde{Q}_i^j = \hat{Q}_i^j\ (i \in \{0, ..., N-1\}) \tag{F.1b}$$

$$\widetilde{v}_i^m = v_i^m,\ \widetilde{v}_i^j = \hat{v}_i^m,\ \widetilde{p}_{c_i} = p_{c_i}^m,\ \widetilde{q}_{w_i}^m = q_{w_i}^m\ (i \in \{1, ..., N\}) \tag{F.1c}$$

$$\widetilde{P}_{0+}^m = P_{0+}^m, \widetilde{P}_{0-}^m = P_{0-}^m \tag{F.1d}$$

Individual Constraints:

$$\hat{v}_{i+1}^m = v_i^m - \frac{r_i P_i^m + x_i Q_i^m}{1000 V_0^2} \quad (i \in \{0, ..., N-1\}) \tag{F.1e}$$

$$\hat{P}_{i-1}^m = P_i^m + p_{c_i}^m - w_i^m \quad (i \in \{1, ..., N\}) \tag{F.1f}$$

$$\hat{Q}_{i-1}^m = Q_i^m + \sqrt{\frac{1}{\mathrm{PF}_i^2} - 1} p_{c_i}^m - q_{w_i}^m \quad (i \in \{1, ..., N\}) \tag{F.1g}$$

$$p_{c_i}^{\min} \leq \widetilde{p}_{c_i} \leq p_{c_i}^{\max} \quad (i \in \{1, ..., N\}) \tag{F.1h}$$

$$-\sqrt{s_{w_i}^2 - (w_i^m)^2} \leq \widetilde{q}_{w_i}^m \leq \sqrt{s_{w_i}^2 - (w_i^m)^2} (i \in \{1, ..., N\}) \tag{F.1i}$$

$$1 - \epsilon \leq \widetilde{v}_i^m \leq 1 + \epsilon \quad (i \in \{1, ..., N\}) \tag{F.1j}$$

$$P_0^m = P_{0+}^m - P_{0-}^m \tag{F.1k}$$

$$\widetilde{P}_{0+}^m \geq 0, \widetilde{P}_{0-}^m \geq 0, P_N^m = 0, Q_N^m = 0, v_0^m = 1 \tag{F.1l}$$

The optimization variables $\mathbf{x} := \{\mathbf{x}_0, \mathbf{x}_1, ..., \mathbf{x}_N\}$ and $\mathbf{z} := \{\mathbf{z}_0, \mathbf{z}_1, ..., \mathbf{z}_N\}$ of the previous problem are defined in (F.2). In the following lists, the boldface variables on the right-hand sides represent vectors of length J collecting the corresponding values of that variable in all scenarios.

$$\mathbf{x}_0 := \{\mathbf{P}_0, \mathbf{Q}_0, \mathbf{v}_0, \mathbf{P}_{0+}, \mathbf{P}_{0-}\} \tag{F.2a}$$

$$\mathbf{x}_N := \left\{\mathbf{P}_N, \mathbf{Q}_N, \mathbf{v}_N, \mathbf{p}_{c_N}, \mathbf{q}_{w_N}, \hat{\mathbf{P}}_{N-1}, \hat{\mathbf{Q}}_{N-1}\right\} \tag{F.2b}$$

$$\mathbf{z}_0 := \left\{\widetilde{\mathbf{P}}_0, \widetilde{\mathbf{Q}}_0, \widetilde{\mathbf{v}}_0, \widetilde{\mathbf{P}}_{0+}, \widetilde{\mathbf{Q}}_{0+}\right\} \tag{F.2c}$$

$$\mathbf{z}_N = \{\widetilde{\mathbf{v}}_N, \widetilde{p}_{c_N}, \widetilde{\mathbf{q}}_{w_N}\} \tag{F.2d}$$

and for $i \in \{1, 2, ..., N-1\}$,

$$\mathbf{x}_i := \left\{\mathbf{P}_i, \mathbf{Q}_i, \mathbf{v}_i, \mathbf{p}_{c_i}, \mathbf{q}_{w_i}, \hat{\mathbf{P}}_{i-1}, \hat{\mathbf{Q}}_{i-1}, \hat{\mathbf{v}}_{i+1}\right\} \tag{F.2e}$$

$$\mathbf{z}_i := \left\{\widetilde{\mathbf{P}}_i, \widetilde{\mathbf{Q}}_i, \widetilde{\mathbf{v}}_i, \widetilde{p}_{c_i}, \widetilde{\mathbf{q}}_{w_i}\right\}. \tag{F.2f}$$

F.2 Augmented Lagrangian

$$\sum_{i=1}^{N} \left[K_{u_i}(\widetilde{p}_{c_i} - p_{c_i}^{Max})^2\right] + \sum_{m=1}^{M} K_0 (P_{0+}^m)^2 + \sum_{i=0}^{N-1} \sum_{m=1}^{M} \pi^m r_i \frac{(P_i^m)^2 + (Q_i^m)^2}{V_0^2}$$

Table F.1: Given Variables and Description

Variables	Description
$\widetilde{P}_i$	i=0,...,N-1
P_i^m	$i = 0, ..., N$
$\hat{P}_i^m$	$i = 0, ..., N-1$
$\widetilde{v}_i^m$	$i = 1, ..., N$
v_i^m	$i = 1, 2, ..., N$
$\hat{v}_i^m$	$i = 1, ..., N$

Table F.2: Coupling Constraints & Associated Lagrange Parameters

Constraints	Lagrange Parameters	Range
$\widetilde{P}_i = P_i^m$	λ_i^m	$i = 0, ..., N-1$
$\hat{P}_i^m = \widetilde{P}_i$	$\hat{\lambda}_{i+1}^m$	$i = 0, ..., N-1$
$\widetilde{v}_i^m = v_i^m$	ω_i^m	$i = 1, ..., N$
$\widetilde{v}_i^m = \hat{v}_i^m$	$\hat{\omega}_{i-1}^m$	$i = 1, 2, ..., N$

$$
\begin{aligned}
&+ \sum_{i=0}^{N-1} \sum_{m=1}^{M} \Big[\lambda_i^m (\widetilde{P}_i^m - P_i^m) + \hat{\lambda}_{i+1}^m (\widetilde{P}_i^m - \hat{P}_i^m) + \mu_i^m (\widetilde{Q}_i^m - Q_i^m) + \hat{\mu}_{i+1}^m (\widetilde{Q}_i^m - \hat{Q}_i^m) \Big] \\
&\quad + \sum_{i=1}^{N} \sum_{m=1}^{M} \left[\omega_i^m (\widetilde{v}_i^m - v_i^m) + \hat{\omega}_{i-1}^m (\widetilde{v}_i^m - \hat{v}_i^m) + \eta_i^m (\widetilde{p}_{c_i} - p_{c_i}^m) + \theta_i^m (\widetilde{q}_{w_i}^m - q_{w_i}^m) \right] \\
&\quad + \sum_{m=1}^{M} \zeta_+^m (\widetilde{P}_{0+}^m - P_{0+}^m) + \zeta_-^m (\widetilde{P}_{0-}^m - P_{0-}^m) + \frac{\rho}{2} \sum_{m=1}^{M} (\widetilde{P}_{0+}^m - P_{0+}^m)^2 + (\widetilde{P}_{0-}^m - P_{0-}^m)^2 \\
&\quad + \frac{\rho}{2} \sum_{i=0}^{N-1} \sum_{m=1}^{M} \Big[(\widetilde{P}_i^m - P_i^m)^2 + (\widetilde{P}_i^m - \hat{P}_i^m)^2 + (\widetilde{Q}_i^m - Q_i^m)^2 + (\widetilde{Q}_i^m - \hat{Q}_i^m)^2 \Big] \\
&\quad\quad + \frac{\rho}{2} \sum_{i=1}^{N} \sum_{m=1}^{M} \left[(\widetilde{v}_i^m - v_i^m)^2 + (\widetilde{v}_i^m - \hat{v}_i^m)^2 + (\widetilde{p}_{c_i}^m - Q_i^m)^2 + (\widetilde{q}_{w_i}^m - \hat{q}_{w_i}^m)^2 \right] \quad \text{(F.3)}
\end{aligned}
$$

F.3 x-update

F.3.1 $i = 1, 2, ..., N-1$

The x-update for $i = 1, ..., N-1$ is as follows:

(Parentheses denotes iteration number)

$$x_i^m(k+1) = \text{argmin}\{\pi^m r_i \frac{(P_i^m)^2 + (Q_i^m)^2}{V_0^2} + \lambda_i^m(k)(\widetilde{P}_i^m(k) - P_i^m) + \hat{\lambda}_i^m(k)(\widetilde{P}_{i-1}^m(k) - \hat{P}_{i-1}^m)$$
$$+\mu_i^m(k)(\widetilde{Q}_i^m(k) - Q_i^m) + \hat{\mu}_i^m(k)(\widetilde{Q}_{i-1}^m(k) - \hat{Q}_{i-1}^m) + \omega_i^m(k)(\widetilde{v}_i^m(k) - v_i^m) + \hat{\omega}_i^m(k)(\widetilde{v}_{i+1}^m(k) - \hat{v}_{i+1}^m)$$
$$+\eta_i^m(k)(\widetilde{p}_{c_i}(k) - p_{c_i}^m) + \theta_i^m(k)(\widetilde{q}_{g_i}^m(k) - q_{w_i}^m) + \frac{\rho}{2}[(\widetilde{P}_i^m(k) - P_i^m)^2 + (\widetilde{P}_{i-1}^m(k) - \hat{P}_{i-1}^m)^2 + (\widetilde{Q}_i^m(k) - Q_i^m)^2$$
$$+ (\widetilde{Q}_{i-1}^m(k) - \hat{Q}_{i-1}^m)^2 + (\widetilde{v}_i^m(k) - v_i^m)^2 + (\widetilde{v}_{i+1}^m(k) - \hat{v}_{i+1}^m)^2 + (\widetilde{p}_{c_i}(k) - p_{c_i}^m)^2 + (\widetilde{q}_{g_i}^m(k) - q_{w_i}^m)^2]\} \tag{F.4}$$

where $x_i^m(k+1) = [P_i^m, \hat{P}_{i-1}^m, Q_i^m, \hat{Q}_{i-1}^m, v_i^m, \hat{v}_{i+1}^m, p_{c_i}^m, q_{w_i}^m]^T$ subject to

$$-\hat{P}_{i-1}^m + P_i^m + p_{c_i}^m - w_i^m = 0 \tag{F.5}$$

$$-\hat{Q}_{i-1}^m + Q_i^m + \sqrt{\frac{1}{\text{PF}_i^2} - 1} p_{c_i}^m - q_{w_i}^m = 0 \tag{F.6}$$

$$-\hat{v}_{i+1}^m + v_i^m - \frac{r_i}{1000V_0^2} P_i^m - \frac{x_i}{1000V_0^2} Q_i^m = 0 \tag{F.7}$$

These equations form a quadratic convex program which can be solved in closed form. In order to solve this problem in closed form, first we have to bring the equations to the following format [24]

$$\text{argmin}\{\frac{1}{2} x^T A x + b^T x\} \tag{F.8}$$

$$\text{subject to} : Cx = d \tag{F.9}$$

Then we can solve for the optimal by calculating Gaussian elimination of KKT matrix:

$$\begin{bmatrix} A & C^T \\ C & 0 \end{bmatrix} \begin{bmatrix} x^* \\ y^* \end{bmatrix} = \begin{bmatrix} -b \\ d \end{bmatrix} \tag{F.10}$$

Next we calculate the entries for matrices A and C, and vectors b and d. Assuming that $x = [P_i^m, \hat{P}_{i-1}^m, Q_i^m, \hat{Q}_{i-1}^m, v_i^m, \hat{v}_{i+1}^m, p_{c_i}^m, q_{w_i}^m]^T$

$$A = 2\begin{bmatrix} \frac{\rho}{2}+\frac{\pi^m r_i}{V_0^2} & 0 & 0 & 0 & 0 & 0 & 0 & 0 \\ 0 & \frac{\rho}{2} & 0 & 0 & 0 & 0 & 0 & 0 \\ 0 & 0 & \frac{\rho}{2}+\frac{\pi^m r_i}{V_0^2} & 0 & 0 & 0 & 0 & 0 \\ 0 & 0 & 0 & \frac{\rho}{2} & 0 & 0 & 0 & 0 \\ 0 & 0 & 0 & 0 & \frac{\rho}{2} & 0 & 0 & 0 \\ 0 & 0 & 0 & 0 & 0 & \frac{\rho}{2} & 0 & 0 \\ 0 & 0 & 0 & 0 & 0 & 0 & \frac{\rho}{2} & 0 \\ 0 & 0 & 0 & 0 & 0 & 0 & 0 & \frac{\rho}{2} \end{bmatrix}$$

$$b = \begin{bmatrix} -\lambda_i^m(k) - \rho\widetilde{P}_i^m(k) \\ -\hat{\lambda}_i^m(k) - \rho\widetilde{P}_{i-1}^m(k) \\ -\mu_i^m(k) - \rho\widetilde{Q}_i^m(k) \\ -\hat{\mu}_i^m(k) - \rho\widetilde{Q}_{i-1}^m(k) \\ -\omega_i^m(k) - \rho\widetilde{v}_i^m(k) \\ -\hat{\omega}_i^m(k) - \rho\widetilde{v}_{i+1}^m(k) \\ -\eta_i^m(k) - \rho\widetilde{p}_{c_i}(k) \\ -\theta_i^m(k) - \rho\widetilde{q}_{g_i}^m(k) \end{bmatrix}$$

$$C = \begin{bmatrix} 1 & -1 & 0 & 0 & 0 & 0 & 1 & 0 \\ 0 & 0 & 1 & -1 & 0 & 0 & \sqrt{\frac{1}{\mathrm{PF}_i^2}-1} & -1 \\ -\frac{r_i}{1000V_0^2} & 0 & -\frac{x_i}{1000V_0^2} & 0 & 1 & -1 & 0 & 0 \end{bmatrix}$$

$$d = \begin{bmatrix} w_i^m \\ 0 \\ 0 \end{bmatrix}$$

F.3.2 $i = 0$

$$x_0^m(k+1) = \text{argmin}\{\pi^m r_0 \frac{(P_0^m)^2 + (Q_0^m)^2}{V_0^2} + \pi^m K_0 (P_{0+}^m)^2 + \lambda_0^m(k)(\widetilde{P}_0^m(k) - P_0^m)$$
$$+ \mu_0^m(k)(\widetilde{Q}_0^m(k) - Q_0^m) + \zeta_+^m(\widetilde{P}_{0+}^m(k) - P_{0+}^m) + \zeta_-^m(k)(\widetilde{P}_{0-}^m(k) - P_{0-}^m) + \hat{\omega}_0^m(k)(\widetilde{v}_1^m(k) - \hat{v}_1^m)$$
$$+ \frac{\rho}{2}[(\widetilde{P}_0^m(k) - P_0^m)^2 + (\widetilde{Q}_0^m(k) - Q_0^m)^2 + (\widetilde{P}_{0+}^m(k) - P_{0+}^m)^2 + (\widetilde{P}_{0-}^m(k) - P_{0-}^m)^2 + (\widetilde{v}_1^m(k) - \hat{v}_1^m)^2]\} \tag{F.11}$$

we assume that $\text{Cost}(P_{0+}^m) = K_0(P_{0+}^m)^2$

where $x_0^m(k+1) = [P_0^m, Q_0^m, \hat{v}_1^m, P_{0+}^m, P_{0-}^m]^T$ subject to

$$-\hat{v}_1^m + 1 - \frac{r_0}{1000V_0^2} P_0^m - \frac{x_0}{1000V_0^2} Q_0^m = 0 \tag{F.12}$$

$$P_0^m = P_{0+}^m - P_{0-}^m \tag{F.13}$$

(F.14)

$$A = 2 \begin{bmatrix} \frac{\rho}{2} + \frac{\pi^m r_0}{V_0^2} & 0 & 0 & 0 & 0 \\ 0 & \frac{\rho}{2} + \frac{\pi^m r_i}{V_0^2} & 0 & 0 & 0 \\ 0 & 0 & \frac{\rho}{2} & 0 & 0 \\ 0 & 0 & 0 & \frac{\rho}{2} + \pi^m K_0 & 0 \\ 0 & 0 & 0 & 0 & \frac{\rho}{2} \end{bmatrix}$$

$$b = \begin{bmatrix} -\lambda_0^m(k) - \rho\widetilde{P}_0^m(k) \\ -\mu_0^m(k) - \rho\widetilde{Q}_0^m(k) \\ -\hat{\omega}_0^m(k) - \rho\widetilde{v}_1^m(k) \\ -\zeta_+^m(k) - \rho\widetilde{P}_{0+}^m(k) \\ -\zeta_-^m(k) - \rho\widetilde{P}_{0-}^m(k) \end{bmatrix}$$

$$C = \begin{bmatrix} -\frac{r_0}{1000V_0^2} & -\frac{x_0}{1000V_0^2} & -1 & 0 & 0 \\ 1 & 0 & 0 & -1 & 1 \end{bmatrix}$$

$$d = \begin{bmatrix} -1 \\ 0 \end{bmatrix}$$

F.3.3 $i = N$

$$x_N^m(k+1) = \text{argmin}\{\hat{\lambda}_N^m(k)(\widetilde{P}_{N-1}^m(k) - \hat{P}_{N-1}^m) + \hat{\mu}_N^m(k)(\widetilde{Q}_{N-1}^m(k) - \hat{Q}_{N-1}^m) + \omega_N^m(k)(\widetilde{v}_N^m(k) - v_N^m)$$
$$+ \eta_N^m(k)(\widetilde{p}_{c_N}(k) - p_{c_N}^m) + \theta_N^m(k)(\widetilde{q}_{g_N}^m(k) - q_{w_N}^m) + \frac{\rho}{2}[(\widetilde{P}_{N-1}^m(k) - \hat{P}_{N-1}^m)^2 + (\widetilde{Q}_{N-1}^m(k) - \hat{Q}_{N-1}^m)^2$$
$$+ (\widetilde{v}_N^m(k) - v_N^m)^2 + (\widetilde{p}_{c_N}(k) - p_{c_N}^m)^2 + (\widetilde{q}_{w_N}^m(k) - q_{w_N}^m)^2]\} \quad \text{(F.15)}$$

where $x_N^m(k+1) = [\hat{P}_{N-1}^m, \hat{Q}_{N-1}^m, v_N^m, p_{c_N}^m, q_{w_N}^m]^T$ subject to

$$-\hat{P}_{N-1}^m + p_{c_N}^m - w_N^m = 0 \quad \text{(F.16)}$$

$$-\hat{Q}_{N-1}^m + \sqrt{\frac{1}{\text{PF}_N^2} - 1}p_{c_N}^m - q_{w_N}^m = 0 \quad \text{(F.17)}$$

$$A = 2\begin{bmatrix} \frac{\rho}{2} & 0 & 0 & 0 & 0 \\ 0 & \frac{\rho}{2} & 0 & 0 & 0 \\ 0 & 0 & \frac{\rho}{2} & 0 & 0 \\ 0 & 0 & 0 & \frac{\rho}{2} & 0 \\ 0 & 0 & 0 & 0 & \frac{\rho}{2} \\ \\ \end{bmatrix}$$

$$b = \begin{bmatrix} -\hat{\lambda}_N^m(k) - \rho\widetilde{P}_{N-1}^m(k) \\ -\hat{\mu}_N^m(k) - \rho\widetilde{Q}_{N-1}^m(k) \\ -\omega_N^m(k) - \rho\widetilde{v}_N^m(k) \\ -\eta_N^m(k) - \rho\widetilde{p}_{c_N}^m(k) \\ -\theta_N^m(k) - \rho\widetilde{q}_{g_N}^m(k) \end{bmatrix}$$

$$C = \begin{bmatrix} -1 & 0 & 0 & 1 & 0 \\ 0 & -1 & 0 & \sqrt{\frac{1}{\mathrm{PF}_N^2} - 1} & -1 \end{bmatrix}$$

$$d = \begin{bmatrix} w_N^m \\ 0 \end{bmatrix}$$

F.4 z-update

First we will assume that $u_i(\widetilde{p}_{c_i}) = -K_{u_i}(\widetilde{p}_{c_i} - p_{c_i}^{\max})^2$ therefore we can minimize the Lagrangian.

F.4.1 $i = 1, 2, ..., N-1$

$$z_i(k+1) = \operatorname{argmin}\{K_{u_i}(\widetilde{p}_{c_i} - p_{c_i}^{\max})^2 + \sum_{m=1}^{M}[\lambda_i^m(k)(\widetilde{P}_i^m - P_i^m(k+1)) + \hat{\lambda}_i^m(k)(\widetilde{P}_i^m - \hat{P}_i^m(k+1))$$

$$+\mu_i^m(k)(\widetilde{Q}_i^m - Q_i^m(k+1)) + \hat{\mu}_i^m(k)(\widetilde{Q}_i^m - \hat{Q}_i^m(k+1)) + \omega_i^m(k)(\widetilde{v}_i^m - v_i^m(k+1)) + \hat{\omega}_i^m(k)(\widetilde{v}_i^m - \hat{v}_i^m(k+1))$$

$$+\eta_i^m(k)(\widetilde{p}_{c_i} - p_{c_i}^m(k+1)) + \theta_i^m(\widetilde{q}_{w_i}^m - q_{w_i}^m(k)) + \frac{\rho}{2}[(\widetilde{P}_i^m - P_i^m(k+1))^2 + (\widetilde{P}_i^m - \hat{P}_i^m(k+1))^2 + (\widetilde{Q}_i^m - Q_i^m(k+1))^2$$

$$+(\widetilde{Q}_i^m-\hat{Q}_i^m(k+1))^2+(\widetilde{v}_i^m-v_i^m(k+1))^2+(\widetilde{v}_i^m(k)-\hat{v}_i^m(k+1))^2+(\widetilde{p}_{c_i}-p_{c_i}^m(k+1))^2+(\widetilde{q}_{w_i}^m-q_{w_i}^m(k+1))^2]]\} \tag{F.18}$$

where $z_i(k+1) = [\widetilde{\mathbf{P}}_i, \widetilde{\mathbf{Q}}_i, \widetilde{p}_{c_i}, \widetilde{\mathbf{v}}_i, \widetilde{\mathbf{q}}_{w_i}]^T$

and where $\widetilde{\mathbf{P}}_i, \widetilde{\mathbf{Q}}_i, \widetilde{\mathbf{v}}_i, \widetilde{\mathbf{q}}_{w_i}$ are vectors collecting all the samples. subject to

$$p_{c_i}^{\min} \leq \widetilde{p}_{c_i} \leq p_{c_i}^{\max} \tag{F.19}$$

$$-\sqrt{s_{w_i}^2 - (w_i^m)^2} \leq \widetilde{q}_{w_i}^m \leq \sqrt{s_{w_i}^2 - (w_i^m)^2} \tag{F.20}$$

$$1-\epsilon \leq \widetilde{v}_i^m \leq 1+\epsilon \tag{F.21}$$

In this case, problem can divide to 5 box-constraint scalar quadratic optimization problems that can be solved in closed form.

z-update for $\widetilde{P}_i^m$

The problem is unconstrained as follows:

$$\begin{aligned}\widetilde{P}_i^m(k+1) = \operatorname{argmin}\{&\lambda_i^m(k)(\widetilde{P}_i^m - P_i^m(k+1)) + \hat{\lambda}_{i+1}^m(k)(\widetilde{P}_i^m - \hat{P}_i^m(k+1)) \\ &+ \frac{\rho}{2}[(\widetilde{P}_i^m - P_i^m(k+1))^2 + (\widetilde{P}_i^m - \hat{P}_i^m(k+1))^2]\}\end{aligned} \tag{F.22}$$

which is equivalent to:

$$\widetilde{P}_i^m(k+1) = \frac{-\lambda_i^m(k) - \hat{\lambda}_{i+1}^m(k) + \rho(P_i^m(k+1) + \hat{P}_i^m(k+1)}{2\rho} \tag{F.23}$$

z-update for $\widetilde{Q}_i^m$

$$\widetilde{Q}_i^m(k+1) = \frac{-\mu_i^m(k) - \hat{\mu}_{i+1}^m(k) + \rho(Q_i^m(k+1) + \hat{Q}_i^m(k+1)}{2\rho} \tag{F.24}$$

z-update for $\widetilde{p}_{c_i}$

The problem breaks down to

$$\widetilde{p}_{c_i}(k+1) = \text{argmin}\{K_{u_i}(\widetilde{p}_{c_i} - p_{c_i}^{\max})^2 + \sum_{m=1}^{M}\left[\eta_i^m(k)(\widetilde{p}_{c_i} - p_{c_i}^m(k+1)) + \frac{\rho}{2}(\widetilde{p}_{c_i} - p_{c_i}^m(k+1))^2\right]\} \tag{F.25}$$

subject to

$$p_{c_i}^{\min} \leq \widetilde{p}_{c_i} \leq p_{c_i}^{\max} \tag{F.26}$$

which is a box constrained scalar optimization problem and the solution is as follows: The derivative of the objective is:

$$f' = (2K_{u_i} + \rho M)\widetilde{p}_{c_i} - 2K_{u_i}p_{c_i}^{\max} + \sum_{j=1}^{M}\left[\eta_i^m(k) - \rho p_{c_i}^m(k+1)\right] \tag{F.27}$$

Therefore the inverse function of the derivative evaluated at its zero would be:

$$\frac{2K_{u_i}p_{c_i}^{\max} - \sum_{m=1}^{M}\left[\eta_i^m(k) + \rho p_{c_i}^m(k+1)\right]}{2K_{u_i} + \rho M} \tag{F.28}$$

and now we can explicitly say the update is going to be:

$$\widetilde{p}_{c_i}(k+1) = \max\left[p_{c_i}^{\min}, \min\left(\frac{2K_{u_i}p_{c_i}^{\max} - \sum_{m=1}^{M}\left[\eta_i^m(k) - \rho p_{c_i}^m(k+1)\right]}{2K_{u_i} + \rho M}, p_{c_i}^{\max}\right)\right] \tag{F.29}$$

z-update for $\widetilde{v}_i^m$

$$\widetilde{v}_i^m(k+1) = \text{argmin}(\omega_i^m(k)(\widetilde{v}_i^m - v_i^m(k+1)) + \hat{\omega}_{i-1}^m(k)(\widetilde{v}_i^m - \hat{v}_i^m(k+1)) + \frac{\rho}{2}(\widetilde{v}_i^m(k) - v_i^m(k+1))^2 + \frac{\rho}{2}(\widetilde{v}_i^m(k) - \hat{v}_i^m(k+1))^2) \quad \text{(F.30)}$$

subject to

$$1 - \epsilon \leq \widetilde{v}_i^m \leq 1 + \epsilon \quad \text{(F.31)}$$

and

$$\widetilde{v}_i^m(k+1) = \max\left[1-\epsilon, \min\left(\frac{-\omega_i^m(k) - \hat{\omega}_{i-1}^m(k) + \rho(v_i^m(k+1) + \hat{(v)}_i^m(k+1))}{2\rho}, 1+\epsilon\right)\right] \quad \text{(F.32)}$$

z-update for $\widetilde{q}_{g_i}^m$

$$\widetilde{q}_{g_i}^m(k+1) = \text{argmin}(\theta_i^m(\widetilde{q}_{g_i}^m - q_{w_i}^m(k)) + \frac{\rho}{2}(\widetilde{q}_{g_i}^m - q_{w_i}^m(k+1))^2) \quad \text{(F.33)}$$

subject to

$$-\sqrt{s_{w_i}^2 - (w_i^m)^2} \leq \widetilde{q}_{w_i}^m \leq \sqrt{s_{w_i}^2 - (w_i^m)^2} \quad \text{(F.34)}$$

and we will find:

$$\widetilde{q}_{w_i}^m(k+1) = \max\left[-\sqrt{s_{w_i}^2 - (w_i^m)^2}, \min\left(\frac{-\theta_i^m(k) + \rho q_{w_i}^m(k+1)}{\rho}, \sqrt{s_{w_i}^2 - (w_i^m)^2}\right)\right] \quad \text{(F.35)}$$

F.4.2 $i = 0$

$$z_0^m(k+1) = \text{argmin}\{\lambda_0^m(k)(\widetilde{P}_0^m - P_0^m(k+1)) + \hat{\lambda}_1^m(k)(\widetilde{P}_0^m - \hat{P}_0^m(k+1)) + \mu_0^m(k)(\widetilde{Q}_0^m - Q_0^m(k+1))$$
$$+ \hat{\mu}_1^m(k)(\widetilde{Q}_0^m - \hat{Q}_0^m(k+1)) + \zeta_+^m(k)(\widetilde{P}_{0+}^m - P_{0+}^m(k+1)) + \zeta_-^m(k)(\widetilde{P}_{0-}^m - P_{0-}^m(k+1))$$
$$+ \frac{\rho}{2}[(\widetilde{P}_0^m - P_0^m(k+1))^2 + (\widetilde{P}_0^m - \hat{P}_0^m(k+1))^2$$
$$+ (\widetilde{Q}_0^m - Q_0^m(k+1))^2 + (\widetilde{Q}_0^m - \hat{Q}_0^m(k+1))^2 + (\widetilde{P}_{0+}^m - P_{0+}^m(k+1))^2 + (\widetilde{P}_{0-}^m - P_{0-}^m(k+1))^2]\} \tag{F.36}$$

where $z_0^m(k+1) = [\widetilde{P}_0^m, \widetilde{Q}_0^m, \widetilde{P}_{0+}^m, \widetilde{P}_{0-}^m]^T$

solving for $\widetilde{P}_0^m$

$$\widetilde{P}_0^m(k+1) = \text{argmin}\{\lambda_0^m(k)(\widetilde{P}_0^m - P_0^m(k+1)) + \hat{\lambda}_1^m(k)(\widetilde{P}_0^m - \hat{P}_0^m(k+1))$$
$$+ \frac{\rho}{2}(\widetilde{P}_0^m - P_0^m(k+1))^2 + \frac{\rho}{2}(\widetilde{P}_0^m - \hat{P}_0^m(k+1))^2\} \tag{F.37}$$

which is unconstrained and is solve as follows:

$$\widetilde{P}_0^m(k+1) = \frac{-\lambda_0^m(k) - \hat{\lambda}_1^m(k) + \rho(P_0^m(k+1) + \hat{P}_0^m(k+1))}{2\rho} \tag{F.38}$$

solving for $\widetilde{Q}_0^m$

$$\widetilde{Q}_0^m(k+1) = \frac{-\mu_0^m(k) - \hat{\mu}_1^m(k) + \rho(Q_0^m(k+1) + \hat{Q}_0^m(k+1))}{2\rho} \tag{F.39}$$

solving for $\widetilde{P}^m_{0+}$

The objective for $\widetilde{P}^m_{0+}$ is

$$\widetilde{P}^m_{0+}(k+1) = \text{argmin}\{\zeta^m_+(k)(\widetilde{P}^m_{0+} - P^m_{0+}(k+1)) + \frac{\rho}{2}(\widetilde{P}^m_{0+} - P^m_{0+}(k+1))^2\} \tag{F.40}$$

with constraint $\widetilde{P}^m_{0+} \geq 0$

This can be solved in closed form by:

$$\widetilde{P}^m_{0+}(k+1) = \max\left(\frac{\rho P^m_{0+}(k+1) - \zeta^m_+(k)}{\rho}, 0\right) \tag{F.41}$$

solving for $\widetilde{P}^m_{0-}$

Similarly ,

$$\widetilde{P}^m_{0-}(k+1) = \max\left(\frac{\rho P^m_{0-}(k+1) - \zeta^m_-(k)}{\rho}, 0\right) \tag{F.42}$$

F.4.3 $i = N$

$$\begin{aligned} z^m_N(k+1) = \text{argmin}\{&\omega^m_N(k)(\widetilde{v}^m_N - v^m_N(k+1)) + \hat{\omega}^m_{N-1}(k)(\widetilde{v}^m_N - \hat{v}^m_N(k+1)) \\ &+ \theta^m_N(\widetilde{q}^m_{w_N} - q^m_{w_N}(k)) \\ &+ \frac{\rho}{2}[(\widetilde{v}^m_N - v^m_N(k+1))^2 + (\widetilde{v}^m_N(k) - \hat{v}^m_N(k+1))^2 + (\widetilde{q}^m_{w_N} - q^m_{w_N}(k+1))^2]\} \end{aligned} \tag{F.43}$$

subject to

$$-\sqrt{s_{w_N}^2 - (w_N^m)^2} \leq \widetilde{q}_{w_N}^m \leq \sqrt{s_{w_N}^2 - (w_N^m)^2} \tag{F.44}$$

$$1 - \epsilon \leq \widetilde{v}_N^m \leq 1 + \epsilon \tag{F.45}$$

For $\widetilde{q}_{w_N}^m$

$$\widetilde{q}_{w_N}^m(k+1) = \text{argmin}\{\theta_N^m(\widetilde{q}_{w_N}^m - q_{w_N}^m(k)) + \frac{\rho}{2}(\widetilde{q}_{w_N}^m - q_{w_N}^m(k+1))^2\} \tag{F.46}$$

subject to $-\sqrt{s_{w_N}^2 - (w_N^m)^2} \leq \widetilde{q}_{w_N}^m \leq \sqrt{s_{w_N}^2 - (w_N^m)^2}$

$$\widetilde{q}_{w_N}^m(k+1) = \max\left[-\sqrt{s_{w_N}^2 - (w_N^m)^2}, \min\left(\frac{-\theta_N^m(k) + \rho q_{w_N}^m(k+1)}{\rho}, \sqrt{s_{w_N}^2 - (w_N^m)^2}\right)\right] \tag{F.47}$$

For $\widetilde{v}_N^m$

$$\widetilde{v}_N^m(k+1) = \text{argmin}\{\omega_N^m(k)(\widetilde{v}_N^m - v_N^m(k+1)) + \hat{\omega}_N^m(k)(\widetilde{v}_N^m - \hat{v}_N^m(k+1)) + \frac{\rho}{2}(\widetilde{v}_N^m - v_N^m(k+1))^2 + \frac{\rho}{2}(\widetilde{v}_N^m(k) - \hat{v}_N^m(k+1))^2\} \tag{F.48}$$

subject to $1 - \epsilon \leq \widetilde{v}_N^m \leq 1 + \epsilon$

$$\widetilde{v}_N^m(k+1) = \max\left[1 - \epsilon, \min\left(\frac{-\omega_N^m(k) - \hat{\omega}_{N-1}^m(k) + \rho(v_N^m(k+1) + \hat{v}_N^m(k+1))}{2\rho}, 1 + \epsilon\right)\right] \tag{F.49}$$

BIBLIOGRAPHY

[1] M. Bazrafshan and N. Gatsis, "Decentralized stochastic programming for real and reactive power management in distribution systems," in *Proc. IEEE SmartGrid*, (Venice, Italy), 2014.

[2] M. Bazrafshan and N. Gatsis, "Voltage regulation in electricity distribution networks using the conditional value at risk," in *Proceeding of IEEE Global Conference on Signal and Information Processing*, (Georgia, Atlanta, USA), 2014.

[3] M. E. Baran and F. F. Wu, "Optimal sizing of capacitors placed on a radial distribution feeder," *IEEE Trans. Power Delivery*, vol. 4, pp. 735–743, Jan. 1989.

[4] M. E. Baran and F. F. Wu, "Network reconfiguration in distribution systems for loss reduction and load balancing," *IEEE Trans. Power Delivery*, vol. 4, Apr. 1989.

[5] M. E. Baran and F. F. Wu, "Optimal capacitor placement on radial distribution systems," *IEEE Trans. Power Delivery*, vol. 4, pp. 725–734, Jan. 1989.

[6] K. Turitsyn, P. Šulc, S. Backhaus, and M. Chertkov, "Distributed control of reactive power flow in a radial distribution circuit with high photovoltaic penetration," in *Proc. IEEE PES General Meeting*, (Minneapolis, MN), pp. 1–6, July 2010.

[7] K. Turitsyn, P. Šulc, S. Backhaus, and M. Chertkov, "Local control of reactive power by distributed photovoltaic generators," in *Proc. 1st IEEE Int. Conf. Smart Grid Communications*, (Gaithersburg, MD), pp. 79–84, Oct. 2010.

[8] H. Yeh, D. F. Gayme, and S. H. Low, "Adaptive VAR control for distribution circuits with photovoltaic generators," *IEEE Trans. Smart Grid*, vol. 27, pp. 1656–1663, Aug. 2012.

[9] P. Šulc, S. Backhaus, and M. Chertkov, "Optimal distributed control of reactive power via the alternating direction method of multipliers." http://arxiv.org/pdf/1310.5748.pdf, Oct. 2013.

[10] M. Kraning, E. Chu, J. Lavaei, and S. Boyd, "Dynamic network energy management via proximal message passing," *Foundations and Trends in Optimization*, vol. 1, no. 2, pp. 1–54, 2013.

[11] M. Farivar, R. Neal, C. Clarke, and S. Low, "Optimal inverter VAR control in distribution systems with high PV penetration," in *Proc. IEEE PES General Meeting*, (San Diego, CA), pp. 1–7, July 2012.

[12] N. Li, L. Chen, and S. H. Low, "Demand response in radial distribution networks: Distributed algorithm," in *Proc. Asilomar Conf. Signals, Systems, and Computers*, (Pacific Grove, CA), pp. 1549–1553, Nov. 2012.

[13] N. Li, L. Gan, L. Chen, and S. H. Low, "An optimization-based demand response in radial distribution networks," in *Proc. IEEE Workshop Smart Grid Communications: Design for Performance*, (Anaheim, CA), pp. 1–6, Dec. 2012.

[14] Q. Peng and S. H. Low, "Distributed algorithm for optimal power flow on a radial network," *arxiv*, Apr. 2014.

[15] A. Lam, B. Zhang, A. Dominguez-Garcia, and D. Tse, "Optimal distributed voltage regulation in power distribution networks," *arxiv*, Apr. 2012.

[16] E. D. Anese, H. Zhu, and G. B. Giannakis, "Distributed optimal power flow for smart microgrids," *IEEE Trans. Smart Grid*, vol. 4, pp. 1464–1475, Sept. 2013.

[17] E. D. Anese, S. Dhople, B. Johnson, and G. B. Giannakis, "Decentralized optimal dispatch of photovoltaic inverters in residential distribution systems," *IEEE Trans. Energy Conversion*, 2014, submitted.

[18] A. J. Conejo, M. Carrion, and J. M. Morales, *Decision making under uncertainty in electricity markets*. New York: Springer, 2010.

[19] Y. Zhang and G. B. Giannakis, "Robust optimal power flow with wind integration using conditional value-at-risk," in *Proc. of the 4th Intl. Conf. on Smart Grid Communications*, Oct 2013.

[20] T. Summers, J. Warrington, M. Morari, and J. Lygeros, "Stochastic optimal power flow based on convex approximations of chance constraints,"

[21] R. T. Rockafellar and S. Uryasev, "Optimization of conditional value-at-risk," *Journal of Risk*, vol. 2, pp. 21–41, Spring 2000.

[22] M. Farivar, C. R. Clarke, S. H. Low, and K. M. Chandi, "Inverter VAR control for distribution systems with renewables," in *Proc. IEEE SmartGrid*, 2011.

[23] K. Turitsyn, P. Šulc, S. Backhaus, and M. Chertkov, "Options for control of reactive power by distributed photovoltaic generators," *Proceedings of the IEEE*, vol. 99, pp. 1063–1073, June 2011.

[24] S. Boyd and L. Vandenberghe, *Convex Optimization*. Cambridge University Press, 2004.

[25] E. Liu and J. Bebic, "Distribution system voltage performance for high-penetration photovoltaics," tech. rep., NREL/SR-581-42298, 2008.

[26] J. D. Bertsekas, *Parallel and Distributed Computation: Numerical Methods*. Prentice Hall, 1989.

[27] A. Shapiro, D. Dentcheva, and A. Ruszczynski, *Lectures on Stochastic Programming: Modeling and Theory*. Philadelphia, PA: SIAM, 2009.

[28] M. Grant and S. Boyd, "CVX: Matlab software for disciplined convex programming, version 2.1: Matlab software for disciplined convex programming, version 2.1." `http://cvxr.com/cvx`, mar 2014.

[29] M. Grant and S. Boyd, "Graph implementations for nonsmooth convex programs," in *Recent Advances in Learning and Control* (V. Blondel, S. Boyd, and H. Kimura, eds.), Lecture Notes in Control and Information Sciences, pp. 95–110, Springer-Verlag Limited, 2008.

[30] "The smargrid: An introduction." prepared for the U.S. Department of Energy by Litos Strategic Communication.

[31] "IEEE 1547 standard for interconnecting distributed resources with electric power systems.."

[32] S. Boyd, N. Parikh, E. Chu, B. Peleato, and J. Eckstein, "Distributed optimization and statistical learning via the alternating direction method of multipliers," *Foundations and Trends in Machine Learning*, vol. 3, no. 1, pp. 1–122, 2011.

VITA

Mohammadhafez Bazrafshan was born on July 9, 1990 in Tehran, Iran. When he was four years old, his family moved to a small city in north of Iran, called Gorgan, where he lived until graduating from high school in 2007. He moved back to Tehran in 2007 to pursue an undergraduate degree in Electrical Engineering from Iran University of Science and Technology and received his Bachelor's degree in July 2012. In August 2012, he started his graduate studies in Electrical Engineering at the University of Texas at San Antonio. His research interests span areas of optimization, smart grid and machine learning.